International Conference on Renewable Energy and Sustainability

(ICRES-19)

Visakhapatnam, Andhra Pradesh

5^{th}- 6^{th} April' 19

Institute For Engineering Research and Publication

www.iferp.in

Publisher: IFERP Explore

PREFACE

We cordially invite you to attend the ***International Conference on Renewable Energy and Sustainability (ICRES-19)*** which will be held at ***Ambica Sea Green HOTEL, Visakhapatnam*** on ***April 5th -6th, 2019***. The main objective of ***ICRES-19*** is to provide a platform for researchers, engineers, academicians as well as industrial professionals from all over the world to present their research results and development activities in relevant fields of Electrical, Electronics & Communication Engineering. This conference will provide opportunities for the delegates to exchange new ideas and experience face to face, to establish business or research relationship and to find global partners for future collaboration.

These proceedings collect the up-to-date, comprehensive and worldwide state-of-art knowledge on cutting edge development of academia as well as industries. All accepted papers were subjected to strict peer-reviewing by a panel of expert referees. The papers have been selected for these proceedings because of their quality and the relevance to the conference. We hope these proceedings will not only provide the readers a broad overview of the latest research results but also will provide the readers a valuable summary and reference in these fields.

The conference is supported by many universities, research institutes and colleges. Many professors played an important role in the successful holding of the conference, so we would like to take this opportunity to express our sincere gratitude and highest respects to them. They have worked very hard in reviewing papers and making valuable suggestions for the authors to improve their work. We also would like to express our gratitude to the external reviewers, for providing extra help in the review process, and to the authors for contributing their research result to the conference.

Since February 2019, the Organizing Committees have received more than 62 manuscript papers, and the papers cover all the aspects in Electrical, Electronics & Communication Engineering. Finally, after review, about 12 papers were included to the proceedings of ***ICRES-19***

We would like to extend our appreciation to all participants in the conference for their great contribution to the success of ***ICRES-19*** We would like to thank the keynote and individual speakers and all participating authors for their hard work and time. We also sincerely appreciate the work by the technical program committee and all reviewers, whose contributions made this conference possible. We would like to extend our thanks to all the referees for their constructive comments on all papers; especially, we would like to thank to organizing committee for their hard work.

Acknowledgement

IFERP is hosting the ***International Conference on Renewable Energy and Sustainability (ICRES-19)*** this year in month of April. The main objective of ICSPECS is to grant the amazing opportunity to learn about groundbreaking developments in modern industry, talk through difficult workplace scenarios with peers who experience the same pain points, and experience enormous growth and development as a professional. There will be no shortage of continuous networking opportunities and informational sessions. The sessions serve as an excellent opportunity to soak up information from widely respected experts. Connecting with fellow professionals and sharing the success stories of your firm is an excellent way to build relations and become known as a thought leader.

I express my hearty gratitude to all my Colleagues, staffs, Professors, reviewers and members of organizing committee for their hearty and dedicated support to make this conference successful. I am also thankful to all our delegates for their pain staking effort to travel such a long distance to attain this conference.

Ankit Rath
Chief Scientific Officer
Institute for Engineering Research and Publication (IFERP)

Keynote Speaker

Dr.C.V.GOPINATH

Principal, BITS, Visakhapatnam, India

Dr.C.V.Gopinath educated in GITAM and Andhra Universities and an expert in Solid Modeling and Reverse Engineering. On these topics he published research papers in International/National Journals/Conferences. He published books, conducted programs, delivered lectures in various National and International forums. He conducted two AICTE sponsored Staff Development Programs on CAD/CAM. His vast experience includes 16 years teaching in GITAM and Alliance Universities and 12 years as Principal of reputed institutes of AP and Odisha. He was instrumental in NBA accreditation for all the departments of JITM (Now Centurion University of Technology and Management), Paralakhemundi, Odisha and Chaitanya Engineering College, Visakhapatnam.

Currently he is with BITS Visakhapatnam as Principal

ICRES-19

International Conference on Renewable Energy and Sustainability

Visakhapatnam, Andhra Pradesh, April 5th - 6th, 2019

Organizing Committee

Dr.Prof. Manjula.S
HOD, Electronics and Communication Engineering, Samskruti College of Engg and Technology GHATKESAR Hyderabad

Dr.Sudarshan Rao K
Professor and Head, Mechanical Engineering
Shri Madhwa Vadiraja Institute of Technology & Management

Nilesh B Bahadurev
Associate Professor
Electronics and Communication Engineering
Sanjay Ghodawat University

Dr. P.M.K.Prasad
Associate Professor
Electronics and Communication Engineering
GVP College of Engineering for Women

Dr. Mohammad Arif Kamal
Associate Professor
Architecture
Aligarh Muslim University, Aligarh, INDIA

Tadanki Vijay Mun
Assistant Professor
Power & Industrial Drives
K L University, Guntur

Dr. K. Rasadurai
Professor
Electronics and Communication Engineering
Kuppam Engineering College

Dr. C. V. Gopinath
Principal, Baba Institute of Technology and Sciences(BITS), Madhurawada
VISAKHAPATNAM

Raja Sekhar. G
Associate Professor
Electrical and Electronics Engineering
K L University, Vijayawada

Dr. R. Murugesan
Associate Professor, Electrical and Electronics Engineering, Annamacharya institute of technology and science

Dr.J.Vijaya Kumar
Associate Professor
Power systems
ANITS (Autonomous), Visakhapatnam

Karumbaiah Chappanda Nanaiah
Assistant Professor, Electrical Engineering
Birla Institute of Technology of Science, Hyderabad campus

Dr. Basavaraj V Madiggond
Professor & Head
Electrical and Electronics Engineering
Hirasugar Institute of Technology, Nidasoshi

Dr A M Varaprasadh
Ex-DRDO Scientist
RCI Dr APJ Abdul Kalam Missile Complex

Dr. Puja Dash
Associate Professor, Electrical and Electronics Engineering, Gayatri Vidya Parishad College of Engineering (Autonomous)

Dr. Gajanan Anne
Associate Professor, Mechanical Engineering, Shri Madhwa Vadiraja Institute of Technology and Management (SMVITM)

Dr. Sandeep Biswal
Assistant Professor
Electrical Engineering
G. H. Raisoni University Amravati

Dr. R. N.Ponnalagu
Assistant Professor
Electrical Engineering
BITS Pilani, Hyderabad Campus

N.Veeraiah
Assistant Professor, Electronics and Communication Engineering, DVR & DHS MIC COLLEGE OF TECHNOLOGY, Kanchikacharla

Dr. Mithun Mondal
Assistant professor
Electrical and Electronics Engineering
Birla Institute of Technology & Science, Pilani

Prathyusha. Kuncha
Assistant Professor
Electronics and Communication Engineering
NRI Institute of Technology

M.Chaitanya Suman
Assistant Professor, Electronics and Communication Engineering, Vignan Nirula Institute of Technology for Women

A.Sampath Dakshina Murthy
Assistant Professor, Electronics and Communication Engineering, Vignan's Institute of Information Technology (A), Visakhapatnam

Ramisetty Uma Maheswari
Assistant Professor, Electronics and Communication Engineering, Vignan's Institute of Information Technology (A), Visakhapatnam

CONTENTS

CONTENTS

Microstructural Characterization of Calcite Mineral Precipitation in Bacteria Incorporated Concrete

[1] K Satya Sai Trimurty Naidu, [2] M V Seshagiri Rao, [3] V Srinivasa Reddy
[1] Research Scholar, Department of Civil Engineering, JNTUH CEH, Hyderabad
[2] Professor of Civil Engineering, CVR College of Engineering, Hyderabad
[3] Professor of Civil Engineering, GRIET, Hyderabad

Abstract:-- **Bacteria promote calcium carbonate precipitation in the form of calcite crystals due to its metabolic reactions. The formation of calcite ($CaCO_3$) by process of bio-mineralization can be analyzed using various characterization techniques/methods. The micro-structural observations could improve the understanding of the mechanism of self-healing phenomenon by calcifying bacteria. The present paper is focused on characterizing the mineral precipitation in concrete by Bacillus subtilis JC3 as calcite using relevant nanocharacterization techniques such as Scanning Electron Microscope (SEM), X-ray diffraction (XRD) and Thermogravimetric (TG) analyses and to validate that cracks/ or pores in bacteria incorporated concrete were sealed up by the precipitation of calcium carbonate crystals grown due to complex metabolic mechanism through nitrogen cycle by Bacillus subtilis JC3. It was confirmed from the relevant nano-characterization techniques that cracks/pores were sealed up by calcite crystals grown due to complex metabolic mechanism of nitrogen cycle by Bacillus subtilis JC3.**

Index Terms: bacterial concrete, Bacillus subtilis, SEM, XRD, TGA

1. INTRODUCTION

The objective of this research was to observe the microstructure of bacteria induced cement-sand matrix and to confirm the presence of calcite crystals using TGA, quantified by X-Ray Powder Diffraction (XRD) analysis and visualized by SEM. The above characterization studies establish the fact that the $CaCO_3$ is precipitated in the concrete by *Bacillus subtilis* JC3. Microbial calcite precipitation was visualized by SEM, quantified by X-Ray Powder Diffraction (XRD) analysis and confirmed by TG/DTG Analysis. The samples for the tests were collected, from the bacteria treated cement mortar samples and from control specimens i.e., samples without bacteria, in the form of powders and/or broken pieces.

Aerobic alkaliphilic microorganisms Bacillus subtilis strain with accession number JC3 was isolated, deposited, cultured and grown at JNTUH Bacteria Discovery Laboratory. Different cell concentrations were derived from the bacterial growth culture by serial dilution method. The nutrients used for growth of culture are - Peptone: 5 g/lit., NaCl: 5 g/lit., Yeast extract: 3 g/lit.

2. RESEARCH FINDINGS

1. Effect of cell concentration on the strength

Effect of cell concentration of Bacillus subtilis JC3 on the strength of concrete is studied by preparing cement mortar specimens with different cell concentrations and tested for their compressive strengths. Maximum strength is observed for 10^5 cells/ml of mixing water so this is taken as optimum cell concentration to be used for further study. This improvement in compressive strength was mainly due to metabolic deposition of $CaCO_3$ in the voids /or pores within cement–sand matrix modifying the pore structure of bacteria induced cement mortar specimens. During bacterial growth, the calcium precipitation process occurs continuously, clogging the internal pores with calcium precipitate. Results are presented in Table 1.

This investigation was carried out primarily to understand the effect of bacterial cell concentration on the quantity of calcium carbonate precipitation. More

bacteria with enough nutrients will precipitate more calcite in the laboratory conditions but in the cement-sand environment, bacteria mineral precipitating ability depends on its compatibility with cement-sand matrix. Bacteria incorporated into cement-sand medium should not affect the physio-chemical properties of cement-sand. Hence cell concentration of bacteria plays a key role in optimizing the performance of cementitious materials. The appropriate bacterial cell concentration for maximum calcium carbonate precipitation can be established by determining the 28 day compressive strengths of various cement-mortar specimens induced with different bacterial cell concentrations. The sample whose 28 day compressive strength was highest determines the optimum cell concentration for high amount of crystalline calcite precipitation. Different cell concentrations were derived from the bacterial growth culture by serial dilution method.

2. Scanning Electron Microscopic (SEM) Investigations

Scanning Electron Microscope (SEM) analysis was made on the broken samples of size 5mmx5mm collected from the cement mortar cubes cured for 28 days. Improvement in hydrated structure of cement-sand mortar treated with Bacillus subtilis JC3 of different concentrations per ml of culture can be observed in a magnified view (2500x) of SEM micrographs as shown in Fig 1. The morphology of the newly formed crystals of rhombohedra shape suggests that the mineral may be $CaCO_3$ and its formation could be the result of the metabolic conversion of the nutrients by Bacillus subtilis.

3. X-Ray Powder Diffraction (XRD) Analysis

Mineralogical compositions of the deposited $CaCO_3$ crystals were investigated with X-ray powder diffraction analysis. Powder diffraction patterns are typically plotted as the intensity of the diffracted X-rays vs. the angle 2θ. The XRD Pattern was obtained by scanning from 2 to 80º 2θ using a vertical x-ray diffractometer. In the XRD patterns, the characteristic diffraction peaks (100% intensity) occurred, at 2θ= 18.25º with d value 3.342 (for quartz) in control cement mortar sample and, at 2θ= 26.82º with d value 3.035 (for Calcite) in bacteria incorporated sample. Crystal identification is accomplished by comparing the data (peaks and relative intensities) from samples with "standard" data provided by the International Center for Diffraction Data (ICDD). Fig 2 depicts the profiles of XRD patterns of bacteria incorporated and normal cement mortar samples. The areas under the peak are related to the amount of each mineral present in the sample. The widths of the peaks in a particular pattern provide an indication of the average crystallite size.

4. Thermo-gravimetric (TG) Analysis

Thermo-gravimetric Analysis (TGA) is a technique which measures a sample's weight as it is heated or cooled in a furnace. TGA thermal curve is drawn between temperature on x-axis and weight (mg) or weight percent (%) on y-axis. The descending TGA thermal curve indicates a weight loss occurred. Derivative thermo-gravimetric (DTG) Curves are drawn between the rate of mass change (%/^oC) against temperature on the *x* axis, when substance is heated at uniform rate, as shown in Fig 3. The sample size considered is 50 mg. During the Thermo-gravimetric analysis, the precipitated calcite material in concrete was exposed to temperatures ranging from 50 °C to 900°C at a rate of 10°C/min in an inert nitrogen atmosphere with a purge rate of 20 mL/minute. Through performance of the TGA analysis, the presence of $CaCO_3$ in the repair material is determined. When $CaCO_3$ crystals are present in the repair material, they will decompose into CaO and CO_2 upon heating ($CaCO_3 \rightarrow CaO + CO_2$). As $CaCO_3$ decomposes between the temperature range of 500–700°C a decrease in weight, caused by the release of

CO_2, is expected around that temperature interval for the samples treated with non-autoclaved, active bacteria. For the autoclaved bacteria the weight loss is rather small (2%) while for specimens with live bacteria a significant decrease in weight is observed (20%) as shown in Fig 3.

CONCLUSIONS

Based on the above investigations, the following conclusions are drawn:

1. The improvement in compressive strength is due to deposition on the microorganism cell surfaces and within the pores of cement–sand matrix, which plug the pores within the mortar. TG, SEM and XRD analyses reveal the growth of fibrous filler material within the pores due to the presence of such microorganisms. This growth is beneficial in the modification of the porosity and pore size distribution of cement mortar. Deposition of a layer of calcite in the pores of the specimens resulted in a decrease of permeability and enhances the strength and durability of concrete.
2. The SEM analysis revealed the dense growth of calcite crystals embedded with bacterial cells in bacteria incorporated specimen.
3. The XRD scanning image of powdered bacteria incorporated cement mortar sample confirms the presence of high amount of calcite mineral.
4. In the XRD pattern Fig 5.4 (a), of control cement mortar sample, the characteristic diffraction peak (100% intensity) occurred, at 2θ= 18.25º with reticular plane distance (d) value 3.342 (for quartz) which indicates presence of the relatively high amount of quartz mineral when compared to other minerals present in the sample. It can also be noted that the presence of calcite in control mortar sample is due to formation of hydrated C-S-H gel. In case of bacteria incorporated sample XRD spectra Fig 5.4 (b), the characteristic diffraction peak (100% intensity) occurred at 2θ= 26.82º with d value 3.035 (for Calcite) which confirms the presence of relatively high amount of calcite crystals when compared to other minerals present in the sample. This can be attributed to the copious deposition of CaCO3 in bacteria induced samples by Bacillus subtilis JC3 during its microbial activity. So the presence of CaCO3 was substantiated using X-Ray Diffraction (XRD) analysis. More number of calcite peaks suggests maximum calcite precipitation which would thereby reduce the pores in concrete.
5. TGA analysis performed on powdered bacteria incorporated cement mortar sample showed an extreme loss of weight at temperature range of 500–700°C confirming the presence of high amount of $CaCO_3$. It confirms the presence of CaCO3 in bacteria incorporated concrete specimens.

REFERENCES

1. Ramchandran S K, Ramakrishnan V, and Bang S S. South Dokata School of Mines and Technology, USA "*Remediation of Concrete using Microorganisms*" ACI Materials Jour**nal**, **98(**2001) pp 3-9
2. Zhong L, Islam M R. "*A New Microbial Process and its Impact on Fracture Remediation*", 70th Annual Technical Conf. and Exhibition of the Society of Petroleum Engineers, Dallas, Texas, Oct 22-25, 1995
3. Ghosh P, Mandal S, Chattopadhyay B D, and Pal S. "*Use of microorganisms to improve the strength of Cement-Sand Mortar*". Proc. of Int. Conf. on Advances in Conc. and C*onst.*, ICACC-2004,pp. 983-988
4. Henk M. Jonkers, Arjan Thijssen, Gerard Muyzer, Oguzhan Copuroglu and Erik Schlangen: "*Application of bacteria as self-healing agent for the development of sustainable Concrete*"**.** Ecological engineering 2010: 36(2); pp230-235

5. Stocks Fischer, S. Galinat, J K., and Bang, S S.: *Microbiological precipitation of $CaCO_3$*. Soil Biology and Biochemistry 1999; pp 31

Table 1 - Compressive Strengths (MPa) of cement mortar specimens induced with various *Bacillus subtilis* JC3 cell concentrations

Cell concentration/ml of mixing water	Average Compressive Strength (MPa) ± S.D	
	28 days	% Increase relative to control
Nil (Without Bacteria)	55.81±0.10	-
10^3	57.23±0.11	2.54
10^4	59.52±0.72	6.65
10^5	65.79±0.68	17.88
10^6	62.21±0.49	11.47
10^7	54.66±0.89	-2.06

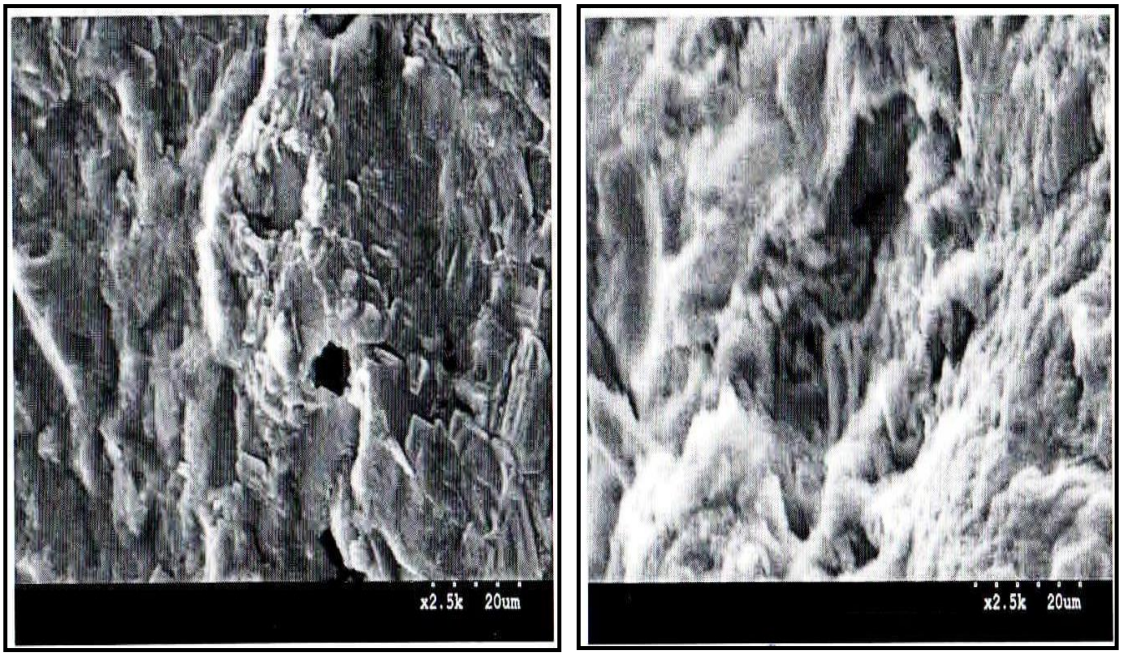

Cell Concentration –Nil (Control Specimen**)** Cell Concentration – 10^5/ml (Optimum)

Fig 1: Magnified SEM Micrographs (2500x magnification): Hydrated Structure of Cement-sand Mortar without Bacteria and with Bacteria incorporated in different concentrations

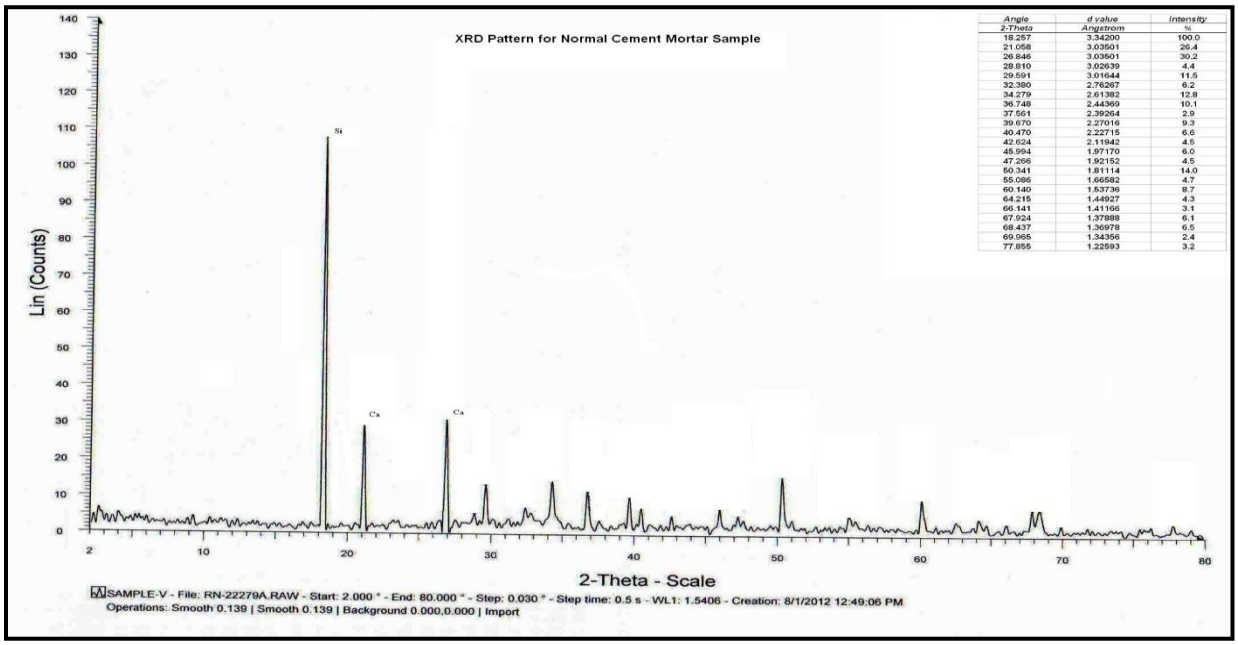

Angle 2-Theta	d value Angstrom	Intensity %
18.257	3.34200	100.0
21.058	3.03501	26.4
26.846	3.03601	30.2
28.810	3.02639	4.4
29.591	3.01644	11.5
32.380	2.76267	6.2
34.279	2.61382	12.8
36.748	2.44369	10.1
37.561	2.39264	2.9
39.670	2.27016	9.3
40.470	2.22715	6.6
42.624	2.11942	4.5
45.994	1.97170	6.0
47.266	1.92152	4.5
50.341	1.81114	14.0
55.086	1.66582	4.7
60.140	1.53736	8.7
64.215	1.44927	4.3
66.141	1.41166	3.1
67.924	1.37888	6.1
68.437	1.36978	6.5
69.965	1.34356	2.4
77.855	1.22593	3.2

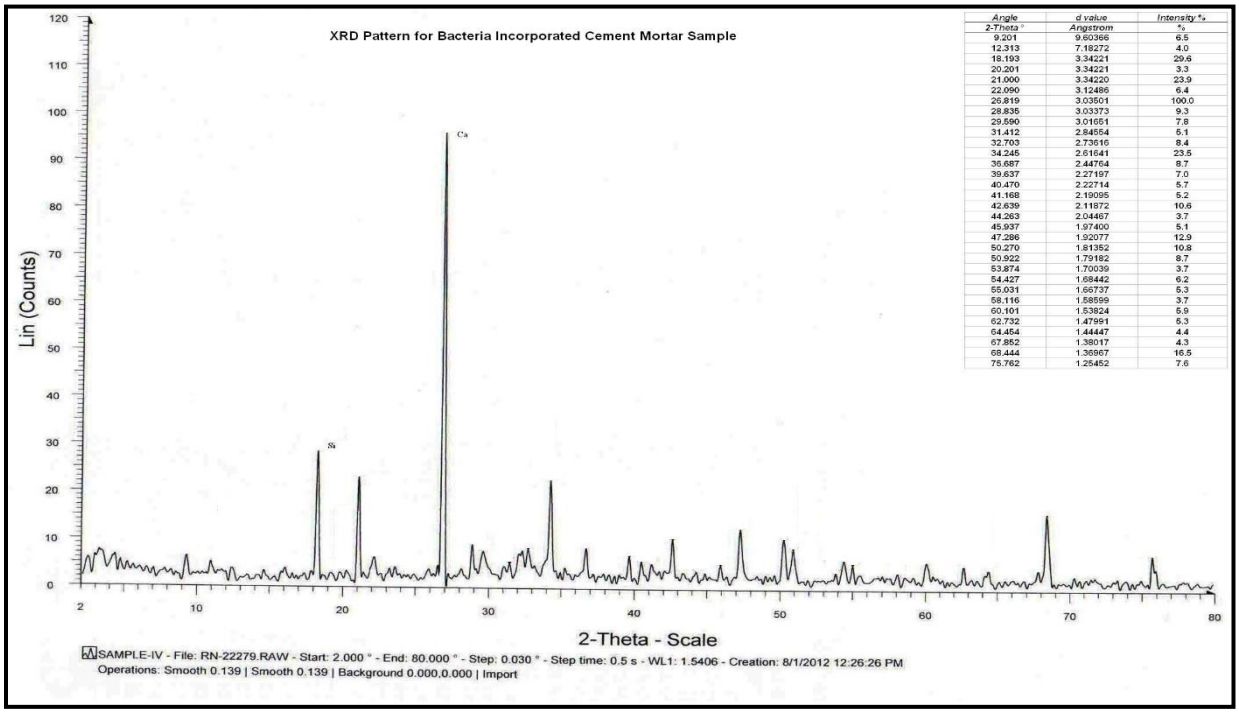

Angle 2-Theta °	d value Angstrom	Intensity %
9.201	9.60366	6.5
12.313	7.18272	4.0
18.193	3.34221	29.6
20.201	3.34221	3.3
21.000	3.34220	23.9
22.090	3.12486	6.4
26.819	3.03501	100.0
28.835	3.03373	9.3
29.590	3.01651	7.8
31.412	2.84554	5.1
32.703	2.73616	8.4
34.245	2.61641	23.5
36.687	2.44764	8.7
39.637	2.27197	7.0
40.470	2.22714	5.7
41.168	2.19095	5.2
42.639	2.11872	10.6
44.263	2.04467	3.7
45.937	1.97400	5.1
47.286	1.92077	12.9
50.270	1.81352	10.8
50.922	1.79182	8.7
53.874	1.70039	3.7
54.427	1.68442	6.2
55.031	1.66737	5.3
58.116	1.58599	3.7
60.101	1.53824	5.9
62.732	1.47991	5.3
64.454	1.44447	4.4
67.852	1.38017	4.3
68.444	1.36967	16.5
75.762	1.25452	7.6

Fig 2: Diffractogram of bacteria incorporated mortar and concrete specimens shows the abundant presence of Ca and precipitation was inferred to as calcite ($CaCO_3$) crystals

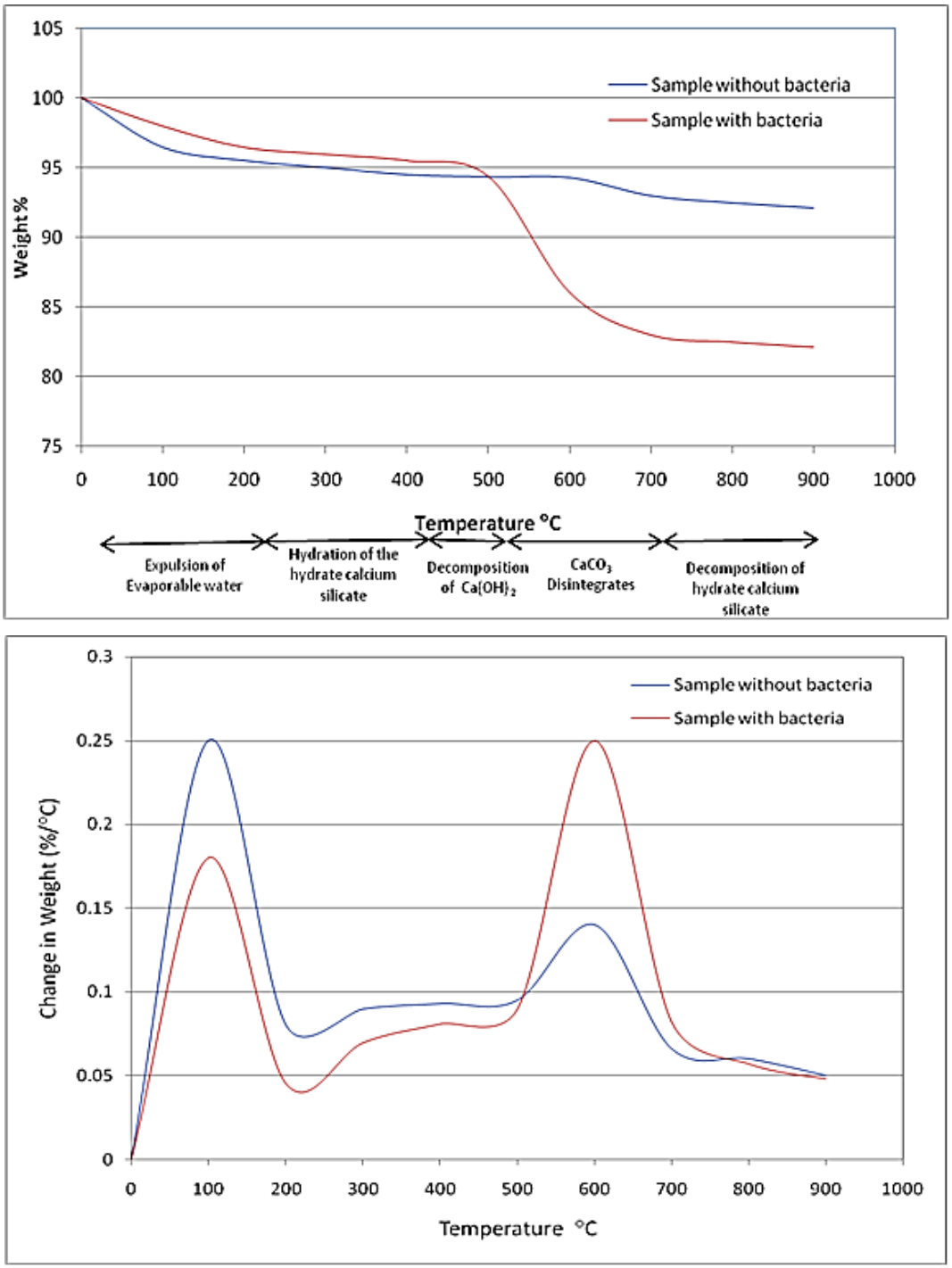

[1] Fig 3: TGA Results for cement mortar specimens with and without bacteria showing weight loss and Change in weight loss per ^{o}C

A Critical Approach for Energy Conservation in Irrigation Systems by Optimal Sizing of Pumps

[1] Basanagouda F Ronad, [2] Suresh H Janagmshetti
[1][2] Department of Electrical and Electronics Engg., BEC(A), Bagalkot

Abstract:-- **This paper presents achievement of energy conservation in irrigation systems by optimally sizing the pump and PVC pipe network. The proposed sizing technique employs irrigation water need, hydraulic head and pump operating hours with an optimal water flow at 1.5m/s. Based on crop water requirement and available operating hours, diameter of pipe and flow rate are assessed. The physical conditions of the agri-land are used utterly to determine hydraulic head. Pump capacity to discharge necessary water over the defined head at best efficiency is obtained from the hydraulic power equation of the pump. The presented method is employed to identify energy conservation potential at Malaprabha river bed, Karnataka, India. A critical survey of agri-lands is taken up and optimal sizes are suggested. It is found that, in a span of 1.5 km riverbed, approximately 40% of installations are in excess. Further, energy conserved, cost savings and possible reduction in CO2 emissions are determined. It is concluded that proposed method at larger scale, will achieve energy conservation in irrigation loads and drastically reduce burden on power grid without affecting the water supply reliability.**

Index Terms: Energy Conservation, Irrigation systems, Suction and Discharge head losses, Centrifugal pumps, Crop water

I. NOMENCLATURE

ET_{crop}	Crop water requirement (mm/day)
ET_o	Reference crop evapotranspiration (mm/day)
P	Mean daily percentage of annual day time hours
T_{mean}	Mean daily temperature (°C)
T_{max}	Average of maximum temperatures in month (°C)
T_{min}	Average of minimum temperatures in month (°C)
Q	Water flowrate (m^3/s or lit/hour)
V	Velocity of water flow in PVC pipes (m/s)
A	Cross sectional area of pipe (m^2)
d	Diameter of pipe (m)
l	Length of the pipe (m)
V_{be}	Velocity before expansion (m/s)
V_{ac}	Velocity after contraction (m/s)
h_f	Head lost due to friction (m)
h_e	Head lost due to diameter expansion (m)
h_c	Head lost due to diameter contraction (m)
h_b	Head lost due to bends (m)
h_{fi}	Head lost due to foot Valve and fittings (m)
H	Total hydraulic head (m)
η	Efficiency of the pump (%)
ρ	Density of water in (kg/m^2)
g	Acceleration due to gravity (m/s^2)
E_c	Energy conserved per day (kWh)
P_{ic}	Installed capacity in the field (hp or Watts)
P_{ac}	Assessed pump capacity (hp or Watts)
T_i	Operating hours of installed pump (Hours)

II. INTRODUCTION

India is a country with more than six lakh villages and 70% of population is involved in agriculture and associated activities. Agriculture is the backbone of Indian economy and contributes a major part in GDP. Farmers entirely dependent on variable rainfall and groundwater to fulfill irrigation need of the crops. It is estimated that, government subsidizes electricity for irrigation between Rs.30000 and 40000 corers each year. There are an estimated 21 million irrigation pumps in India out of which 12 million are on the electricity grid. Electricity consumption by irrigation pumpsets alone accounts between 20-25% of India's total electricity consumption, which has become burden on grid. Building further generating units and grid system, is too expensive. This created difficulty in load management and lead to load shedding. On other hand, to serve required crop water within available time,

 ISBN: 978-81-940803-3-6

farmers install excessive pump capacities and multiple pumps. This will cascade the excessive demand on the electric grid. This issue can be resolved by identifying the excessive installations and re-sizing them optimally. The optimized irrigation load will reduce burden on grid, achieve energy conservation and reduce the CO2 emissions [1]. Dr.Bansal had described the methodology to select rating of irrigation pumps. Sizing is carried based on discharge and head offered. The detailed methodology to assess the major and minor head losses is presented [2].

Dr.Guy Fipps discussed the assessment of hydraulic head and optimal irrigation pump rating. It is shown that for sustained operation, velocity of water in PVC pipes must be 5 foot/sec i.e. 1.52m/s. Further, potential damage to pipe network due to higher velocity is discussed [3]. Mathew Milnes presented assessment and significant causes of minor losses. Inference about improper sizing of pumps is discussed. It is proved that oversized pump results in excess water and undersized pump results in inadequate water output [4]. Literatures discussed the issues associated with design of irrigation pumps. The previous optimizing techniques of pumping systems, which have been the subject of numerous papers, mainly dealt with improvement of effectiveness of various system components, as well as their better mutual adjustment, with the aim of total cost reduction of the pumping system. However, re-sizing the pumps based on the exact crop water need for achievement of energy conservation has never been the topic of interest. The current scenario in Indian agricultural lands has a great deal of energy saving opportunities. In this regard, a critical method for sizing irrigation pumps based on exact water need and land structure is proposed. The proposed concept is employed in selected agriculture fields at Malaprabha riverbed, Karnataka, India, to assess the saving potential.

III. METHODOLOGY

The proposed method yield the optimal size of irrigation pump and the PVC pipe network without affecting the water supply reliability to the crops. The method incorporates crop water, local field conditions, availability of electricity supply and hydraulic head for sizing. The flowchart shown in Fig.1 presents the methodology employed in the present work.

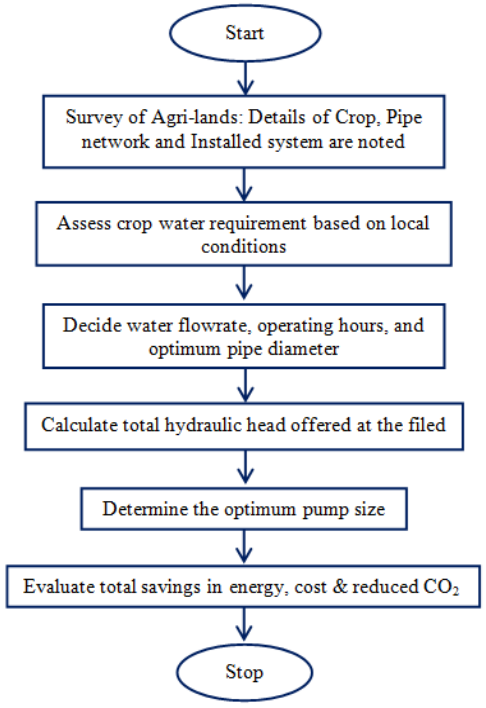

Fig.1: Flowchart representing the methodology

A. Irrigation Water Requirements of the Crops

Crop water requirement is the evapotranspiration due to environmental conditions. It depends on cultivation area, type of the soil and percolation property, season of the year, temperature, latitude of location and type of the crops grown. Thus, total crop water is assessed by evapotranspiration, which will yield optimum water need in mm/day with approximating climatic factors. The crop water requirement is given by (1) [5-6];

$$\mathrm{ET}_{\mathrm{crop}} = K_C \times ET_o \quad mm/day \qquad (1)$$

 ISBN: 978-81-940803-3-6

Reference crop evapotranspiration (ET0) depends on the local conditions of selected site and hence ET0 is assessed by mean daily temperature data using Blaney-Criddle method for selected site. The assessment of ET0 is presented by (2);

$$\mathrm{ET}_0 = p(0.46T_{mean} + 8) \quad mm/day \tag{2}$$

$$T_{mean} = \frac{T_{\max} + T_{\min}}{2} \quad {}^{\circ}C \tag{3}$$

Mean daily percentage of annual day time hours (p) varies from 0.24 to 0.30 throughout the year in the southern part of India. Crop factor (K_c) presents water requirement (ET_{crop}) of particular crop at varying growth stages. Four growth stages of crops are distinguished: initial stage, crop development stage, mid-season stage, late season stage. Major water consumption will be during mid-season stage. However, the length of the different crop stages will vary according to climatic conditions. With known values of crop factors and growth period, water requirements can be calculated for various crops. In the present methodology, sizing of the pumps is carried for maximum water requirement conditions i.e for the mid-season stage of any crop. Thus, the resulting pump will fit for all seasons and worst conditions. For the site at Malaprabha Riverbed (15.8351N-75.5394E), Karnataka, reference crop evapotranspiration were assessed for different months. It is observed that maximum value of ET0 is 6.20 mm/day. Further, crop water requirements for various crops for the selected site are evaluated. Table.1 presents the crops and water requirements of major crops grown in selected site.

Table.1.Crop factors at Mid-season stage & corresponding water requirements of major crops grown in North-Karnataka, India [5-6]

Crop	Crop Fact	Crop Water	Crop Water	Crop Water
	or (K_c)	**(mm/ day)**	**(m^3/Acre /day)**	**(lit/Hect./ day)**
Sugarcane-SG	1.15	7.13	28.8	71300
Cotton-CT	1.15	7.13	28.8	71300
Sorghum-SR	1.10	6.82	27.59	68200
Tomato-TM	1.15	7.13	28.8	71300
Onion-ON	1.00	6.20	25.08	62000
Maize-MZ	1.15	7.13	28.8	71300
Sunflower-SF	1.10	6.82	27.59	68200
Groundnut-GN	1.00	6.20	25.08	62000

B. Assessment of Flowrate and Diameter of PVC Pipe Network

Water flowrate is the amount of water discharged from the pump per second. Total water required per day has to be supplied within the span of electricity supply hours. Karnataka state government assures six hours of three phase quality power for irrigation purpose. To size pump optimally, water flowrate in liters/hour is accurately assessed based on supply hours. Required flowrate is given by (3);

$$Flowrate(Q) = \frac{Total\ water\ required\ per\ day\ in\ liters}{No.of\ hours\ of\ electricity} \quad lit/hour \tag{4}$$

Further, diameter of the pipe network is selected for water flow velocity of 1.5 m/s. For sustained operation without wear and tear and to prevent water hammer effect, velocity of water in PVC pipes is limited to 5-6 feet/sec i.e. 1.524 m/s. Water flowrate in m3¬/s in terms of velocity and pipe area is given by (4). Further, diameter of pipe with flowrate in lit/hour is assessed by (5);

$$Q_{Cubicmtr} = V \times A \quad m^3/S \tag{4}$$

$$d = \sqrt{Q_{lit/hr} \Big/ (4.248 \times 10^6)} \quad mm \tag{5}$$

C. Assessment of Hydraulic Head Offered to Pump

As water flows through pipe, it experiences resistance due to which part of the energy gets lost. Losses developed on motor depend on elevation of water level

to be lifted, bends, valves, friction, change in diameter and length of the pipe. Major loss of head is due to friction and is assessed from Darcy-Weisbach equation given by (6). Other losses are minor, as compared to friction and elevation. However, optimal sizing of pump necessitates them to be incorporated in the design procedure. These losses are assessed by (7)-(11). Major and minor losses together referred as dynamic head. Elevations at suction and discharge sides are termed as static head. Static head at suction side is variable in small reservoirs. On other hand, this head remain constant in riverbed pumps. Thus, total head offered to pump is sum of dynamic and static heads. This is presented by (12).

Head lost due to friction, $$h_f = \frac{4 f l V^2}{2gd} \quad m \tag{6}$$

Head lost due to expansion, $$h_e = \frac{(V_{be} - V_{ae})^2}{2g} \quad m \tag{7}$$

Head lost due to contraction, $$h_c = \frac{K V_{ac}^{\ 2}}{2g} \quad m \tag{8}$$

Head lost due to 90^o bend, $$h_b = 0.45 \frac{V^2}{g} \quad m \tag{9}$$

Head lost due to 45^obend, $$h_b = 0.25 \frac{V^2}{g} \quad m \tag{10}$$

Head lost due to foot Valve, $$h_{fi} = 0.75 \frac{V^2}{g} \quad m \tag{11}$$

Total Head(H), $$H = H_{static} + H_{dynamic} \quad m \tag{12}$$

D. Assessment of Pump Rating

HP rating of the pump is power required to lift water with desired flowrate against total head at the field. Pump capacity is assessed by hydraulic power equation, given by (13).

$$P_{in} = \frac{\rho \times g \times Q_{Cubicmtr} \times H}{\eta} \quad W \tag{13}$$

The pump rating is assessed at Best Efficiency Point (BEP), 70%. Cross verification is carried with selected diameter, pump rating in the performance sheet. The combination of power rating, head and flowrate must in line with best efficient condition of the pump. For given pump rating, optimum combinations of flowrate and head can be selected from manufacture data sheet. It is observed that an increased diameter of discharge terminal handles larger heads, for the same power rating.

E. Energy Conservation, Cost Savings and CO2 Reduction

Sizing is carried for six hours of operation per day. In practice, farmers operate the irrigation pumps during three phase supply for minimum six hours and against law, few more hours, using the condensers in one of the phases. This will create drastic change in the energy consumption pattern of the installed capacities with newly assessed pump ratings. Energy conserved per day by assessed pump over installed pump is given by (14). As the sizing is carried for mid-season stage of the crops, energy consumption during other periods will be much lower.

$$E_c = 0.745[(P_{ic} \times T_i) - (P_{ac} \times T_{6hours})] \quad kWh \tag{14}$$

In Karnataka state, electricity is being supplied freely for farmers and don't have metering provision for consumption monitoring. In such scenario, tariff structures can't be used to evaluate cost savings. This lead for assessment of generation cost savings with reduced consumption. With standard generation cost of 1.9 Rs/kWh is employed for analysis. Cost savings in the generation side by assessed pump per day during the mid-season stage is given by (15) [7].

$$Cost\ Savings = E_c \times Cost\ per\ kWh \quad Rs. \tag{15}$$

The reduced CO2 emissions are determined by standard emission protocol of India for CO2 emissions per kWh generation. It is estimated that, each unit of generation in India accounts for 0.909 kg of CO2¬ [8]. Thus,

reduction in emissions per day during mid-season stage is assesses by (16).

$$CO_2 \text{ emissions reduced} = E_c \times 0.909 \quad kg. \qquad (16)$$

IV. RESULTS AND DISCUSSIONS

A. Survey carried at Malaprabha riverbed

A critical survey is conducted with farmers and details of agriculture land and pumping units are collected. Installed pump capacity, length and diameter, fittings and bends in pipe network, crops grown, size of land, number of gaps in irrigation and number of hours of pump operation are noted. Walkthrough survey revealed that most of the installed ratings are oversized. Further, based on their water need and field conditions optimal pump rating is suggested for each case. The results depict the large energy conservation opportunity in irrigation systems for selected 30 agriculture lands. Existing total capacity of 250 Hp is optimally brought down to 129 Hp without affecting the water supply quantity.

The systems are designed for peak water requirement conditions i.e for the mid-session stage of the sugarcane crop. Thus the identified rating will be sufficient for all seasonal conditions. From 30 cases 121 Hp (48.4%) excessive installations are identified, resulting in 540 kWh units of energy conservation per day, savings in generation cost of Rs.1027 per day and reducing the CO2 emissions by 491 Kg/day. Few cases are identified, where lesser capacity is installed and crops running short of water. However, in total for 50 cases along 1.5km length of riverbed, 30% of excess installations are identified. With the proposed concept and sizing pumps optimally, significant energy can be saved without affecting the crop water requirements. Comparison of installed pump capacity and assessed pump capacity for 30 cases is shown in Fig.2. It is observed that most systems are oversized and are suggested with standard pump sizes of optimal capacity.

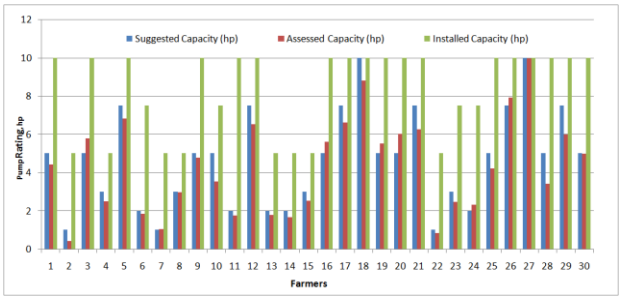

Fig.2: Comparison of Assessed and installed capacities

Fig.3 presents the comparison of energy consumed per day by existing pump capacity and optimum sized capacity with reference to excess capacity identified in each case. The assessment of energy conservation is carried for 6 hours of the electrical supply hour. Results revealed that, every installation possess the conservation potential irrespective of the installed sizes. Energy conservation increases with increase in excess capacity installations. With 1.9 Rs/kWh generation cost, the savings in cost are assessed.

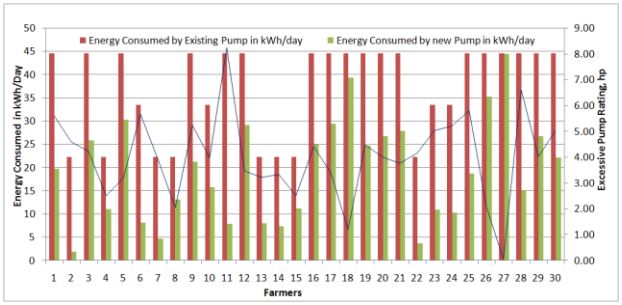

Fig.3: Comparison of energy consumed with excess pump capacities

 ISBN: 978-81-940803-3-6

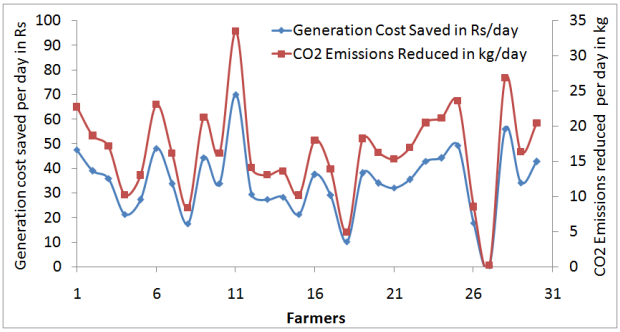

Fig.4: Comparison between cost saving and CO2 reductions

Fig.4 indicates the generation cost savings and reduction in CO2 emissions per day. It clearly presents the outcome benefits associated with cost savings from generation and potential to mitigate the CO2 emissions by the proposed concept of energy conservation.

CONCLUSIONS

Energy conservation opportunity in irrigation systems and solution is presented in the paper. Methodology for optimally sizing the pumps based on water need and local hydraulic conditions was proposed. Survey was conducted for 50 agriculture lands at Malaprabha riverbed and optimal sizing of pumps was carried for each case and suitable standard pump sizes were suggested. For 30 cases of the survey, optimal sizing of pumps indicated excess installations of 48.5%, 540 kWh of energy is conserved per day, saving Rs.1027 and reducing the CO2 emissions by 491 kg/day. Results proved that, significant energy can be conserved by optimally sizing the pumpsets. It was concluded that, implementation of the proposed scheme in large scale, will be a boon for the energy conservation and reduces the burden on national grid.

REFERENCES

Pradip Narale, Prof. Narendra Singh Rathore, Solar Water Pumping System For Agriculture, Department of Renewable Energy Engineering, Maharana Pratap University of Agriculture And Technology, Udaipur (Rajasthan), Energética India, AUG 15, pg 4-5.

Dr.R.K.Bansal, "Fluid Mechanics and Hydraulic Machines", Comprehensive Textbook, LAXMI Publications, Delhi, 2008.

Guy Fipps, "Calculating horsepower requirements and sizing irrigation supply pipelines", Texas Agricultural Extension Service, The Texas A&M University System, Mexico, December 2010.

Mathew Milnes, "The mathematics of pumping water", Department of civil Engineering, The Royal academy of Engineering, London, April 2011.

Dr. D.K. Subramanian and Dr. T.V. Ramachandra, "Aspects of Agriculture and Irrigation In Karnataka", Energy Research Group, Centre For Ecological Sciences, Indian Institute of Science, Bangalore 560 012, India

http://www.fao.org/docrep/s2022e/s2022e07.htm (Crop water requirements, 13th April 2016)

Matthew Brander, AmanSood, Charlotte Wylie, Amy Haughton, Jessica Love, "Electricity-specific emission factors for grid electricity", Ecometria, August 2011, emissionfactors.com

Allocation of Transmission Losses with the Optimal Place MENT of TCSC Using Grasshopper Optimization Algorithm in Deregulated Power System

[1] P.Jyoshna, [2] Dr.Ch.Chengaiah
[1] Research scholar, Department of Electrical and Electronics Engineering, Sri Venkateswara University, Tirupati, Andhra Pradesh, India.
[2] professor, Department of Electrical and Electronics Engineering, Sri Venkateswara University, Tirupati, Andhra Pradesh, India.

Abstract:-- **The transmission system plays an important role in delivering energy from the generating stations to load centres which are located remotely .As the power plants are interconnected via the transmission system network, this lowers the overall generation cost and improves the reliability of the system. The Introduction of Deregulation and its open access policy in electricity sector has brought completion in the market participants. In this paper Grasshopper Optimization Algorithm (GOA) are used for optimal location and setting of FACTS Device so that the real power loss is reduced. The GOA algorithm is tested to the real power loss reduction on IEEE 30 bus system to demonstrate its high efficiency with TCSC. After reducing the transmission loss, allocation of transmission loss can be done using postage Stamp method and power flow tracing method.**

Index Terms: Grasshopper Optimisation Algorithm (GOA), Real power loss minimization, Deregulation, Transmission loss.

I. NOMENCLATURE

Power system restructuring necessitates the need to explore the unused potential of existing transmission system capacity to overcome hurdles like environmental and capital investment costs. FACTS devices can reduce the system losses, increase power transfer capability and stability. As the expansion of transmission network involves several financial, social and technical problems efforts are made to optimally utilize the existing electric power systems effectively. Increased line flows and losses result in power system restructuring effectively. Here FACTS play a vital role in Transmission system.

FACTS is a conventional AC Transmission system, the ability of the power transfer is limited by the factors like thermal limit transient stability limit of the voltage and short circuit current and this limits define the maximum electric power which can be effectively transmitted through the transmission lines without causing any damage to the electrical equipment and the transmission line.

Generally this is achieved by the introduction of the variable impedance device like capacitor, inductor or regulating the reactive power flow in the system. For ideal transmission the active power should be equal to the apparent power. In other words power factor should be unity and the transmission line is considered to be loss less this is where the role of FACTS came in to picture One of the major issues in deregulated power system is transmission loss minimization and transmission loss allocation and cost allocation to the market participants. Roughly 3 to 6% of total generation cost is incurred by the transmission, which cost about some million dollars per year so the transmission loss has to be minimized by reducing the losses in an efficient manner. Allocation of transmission loss also became a contentious issue among the electricity producers and consumers. Since the generators and consumers are connected to the same network, action by one participant can have significant effect on others making it difficult to investigate the cost and each participant is responsible for it due to non - linear nature of line flows. Therefor it is necessary to

allocate the real power losses effectively without affecting the market participants.

A closed form of solution for transmission loss allocation and loss reduction does not exist due to the fact that transmission loss is a highly non-linear function of system states and it is a non-separable quantity. In absence of a closed form solution different utilities use different methods for transmission loss allocation and loss reduction. Most of these techniques involve mathematical operations and simple circuit laws.

The main objective of this work is to minimise the transmission losses by incorporating TCSC device using Grasshopper optimization Algorithm. After reducing the transmission losses, loss allocation can be done by postage Stamp method and power flow tracing algorithm for fair allocation of losses transparently without affecting the other market participants, based on these techniques the overall cost of generation can be reduced in Deregulated Power System.

In this work, the GOA are applied to optimal real power minimisation problem by finding the optimal location and setting of FACTS devices like TCSC for IEEE 14 bus systems. Finally, the validity analysis on GOA is added in this paper.

In subsequent sections modelling of TCSC Device can be done using Grasshopper optimization Algorithm (GOA) and Transmission loss allocation methods of postage stamp and power flow tracing method are discussed and finally conclusion is drawn for IEEE 30 Bus system.

II PROBLEM FORMULATION

The objective of this work is to reduce the real power loss. The minimisation involves number of equality and inequality constriants.

2.1 Objective function

The main objective of this work is to identify the optimal settings of reactive power control variables including the rating shunt of VAR compensating devices which reduce the real power loss and voltage deviation. Hence, the objective function can be expressed as

$$f = \min(P_{loss}) \quad (2.1)$$

The total real power loss of the system can be calculated as follows.

$$P_{loss} = \sum_{k=(i,j)}^{n} g_k(V_i^2 + V_j^2 - 2V_iV_j\cos(\delta_j - \delta_i) \quad (2.2)$$

Where, n is the total number of lines in the system; g_k is the conductance of the line 'k'; V_i and V_j are the magnitudes of the sending end and receiving end voltages of the line; δ_i and δ_j are angles of the end voltages.

2.2 Constraints

Various equality and inequality constraints present in the minimisation problem can be given below

2.2.1 Equality Constraints

The equality constraint for a given load at ith bus is given by following equations

$$P_{Gi} - P_{Di} - \sum_{j=1}^{nb} V_iV_jY_{ij}\cos(\theta_{ij} - \delta_j - \delta_i) = 0 \quad (2.3)$$

$$Q_{Gi} - Q_{Di} - \sum_{j=1}^{nb} V_iV_jY_{ij}\sin(\theta_{ij} - \delta_j - \delta_i) = 0 \quad (2.4)$$

Where P_{Gi} , Q_{Gi} are the active and reactive power of ith generator respectively, P_{Di}, Q_{Di} the active and reactive power of ith load bus, θ_{ij} the angel difference between ith & jth bus, nb number of buses.

2.2.2 Inequality Constraints

a. Reactive power limits

Generator voltage and reactive power of ith bus lies between their upper and lower limits as given below.

$$Q_{ci}^{min} \le Q_{ci} \le Q_{ci}^{max}; i \in nsvc \quad (2.5)$$

Q_{ci}^{min} , Q_{ci}^{max} are the minimum and maximum reactive power of the ith generator.

b. Voltage constraints

$$V_i^{min} \le V_i \le V_i^{max}; i \in nb \quad (2.6)$$

Where, V_i^{min} , V_i^{max} are the minimum and maximum limits of the ith unit.

c. Transmission line flow limit

$$\delta_i \le \delta_i^{max}; i \in ni \quad (2.7)$$

Where δ_i the apparent power flow of ith is is branch and δ_i^{max} is the maximum apparent power flow of ith branch.

d. Tap position Constraints

$$T_i^{min} \le T_i \le T_i^{max} \quad (2.8)$$

Where T_i^{min} , T_i^{max} are the minimum and maximum taps setting limits of ith transformer.

III Modelling of FACTS devices

3.1 Thyristor controlled series compensator(TCSC)

TCSC is a series compensator that can exhibit both capacitive and inductive characteristics to either decrease or increase the reactance of the line respectively. The increase in transfer capability of the transmission system by reducing the transfer reactance can be easily achieved by the smoothly variable series reactance characteristics of the TCSC. This improves the loadability of the system.

TCSC is modelled as shown in the fig.1. It can be placed at branches other than the transformer branches in the system by the following formulae the reactance values are updated in the system.

$$X_{new} = X_{line} + X_{TCSC} \quad (3.1)$$

$$X_{TCSC} = r_{TCSC} * X_{line} \quad (3.2)$$

Where X_{new} is the new reactance of the branch by adding X_{TCSC}, X_{line} is the old reactance of the branch, XTCSC is the variable reactance of the TCSC, r_{TCSC} is percentage compensation of reactance.

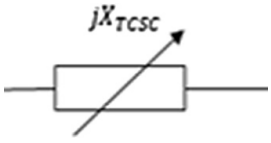

Fig.1 Model of TCSC

IV Optimization Algorithms

4.1 Grasshopper Optimisation Algorithm(GOA)

The GOA algorithm mimics the swarming behavior of grasshoppers in nature. Grasshopper, a pest insect, exhibits swarming behavior in finding their food source. These grasshoppers perform swarming behavior in both nymph and adulthood. In GOA, the position of the grasshoppers in the swarm represents a possible solution of a given optimization problem [16]. The position of the ith grasshopper is denoted as Xi and represented as given in (4.3)

$$Xi = Si + Gi + Ai \quad (4.3)$$

Where Si is the social interaction, Gi is the gravity force on ith grasshopper, and Ai shows the wind advection. The social interaction discussed as follows:

$$S_i = \sum_{j=1, j\neq i}^{N} S\left(d_{ij}\right) \widehat{d_{ij}} \quad (4.4)$$

Where d_{ij} is the distance between ith and jth grasshopper and it is calculated as $d_{ij}=\left|x_j - x_i\right|$, s is a function to define the strength of social forces as shown in (4.4), and $\widehat{d_{ij}} = \frac{x_j - x_i}{d_{ij}}$ is a unit vector from ith grasshopper to the jth grasshopper. The G component in (4.3) is calculated as follows:

$$G_i = -g\widehat{e_g} \quad (4.5)$$

Where g is the gravitational constant and $\widehat{e_g}$ shows a unity vector towards the Centre of earth. The A component in (4.3) is calculated as follows:

$$A_i = u\widehat{e_w} \quad (4.6)$$

Where u is a constant drift and $\widehat{e_w}$ is a unity vector in the direction of wind. By combining all the above terms we can form a mathematical model is as follows:

$$X_i^d = c\left(\sum_{\substack{j=1 \\ j\neq i}}^{N} c\frac{ub_d - lb_d}{2} s\left(\left|x_j^d - x_i^d\right|\right)\frac{x_j - x_i}{d_{ij}}\right) + \widehat{T_d} \quad (4.7)$$

here ubd is the upper bound in the d-th dimension, lbd is the lower bound in the d-th dimension $s(r) = f e^{-r/l} - e^{-r}$, $\widehat{T_d}$ is the value of d-th dimension in the target (best solution found so far), and c is a decreasing coefficient to shrink the comfort area, repulsion area, and attraction area. Note that S is almost similar to the S component in (4.3). However, we do not consider the gravity (no G component) and assume that the wind direction (A component) is always towards a

target ($\widehat{T_d}$). It should be noted that the inner c contributes to the reduction of repulsion/attraction forces between grasshoppers proportional to the number of iterations, while the outer c reduces the search coverage around the target as the iteration counter increases .The parameter c is updated with the following equation to reduce exploration and increase exploitation proportional to the number of iteration:

$$c = c_{max} - l\frac{c_{max}-c_{min}}{L} \quad (4.8)$$

Where c_{max} is the maximum value, c_{min} is the minimum value, l indicates the current iteration, and L is the maximum number of iterations.

V Transmission loss allocation methods:

5.1. Postage Stamp Method:

In this method the total loss is first divided into two groups that is generator losses and load losses and assumed to be 50% of losses are allocated to generator and 50% of losses are allocated to loads which is to be predefined, the losses then allocated to each generator and load in proportion to their generation and consumption. This method is simple and easy to understand it is transparent and no complex calculations involved. Though it is simple but it has certain disadvantages.

$$LP_{Gj} = \frac{TL}{2}\frac{PG_j}{PG} \quad (5.1)$$

$$LP_{Di} = \frac{TL}{2}\frac{PD_i}{PD} \quad (5.2)$$

Where, PGj, PDi– real power generation and load at buses i and j

PG, PD –Total power generation and load of this system

LPGj–Losses allocated to the generator i

LPDi–Losses allocated to the demand j

L–Total losses of the system

Algorithm for postage stamp method:

Select desire load and generation with ‘
IEEE-30 Bus system

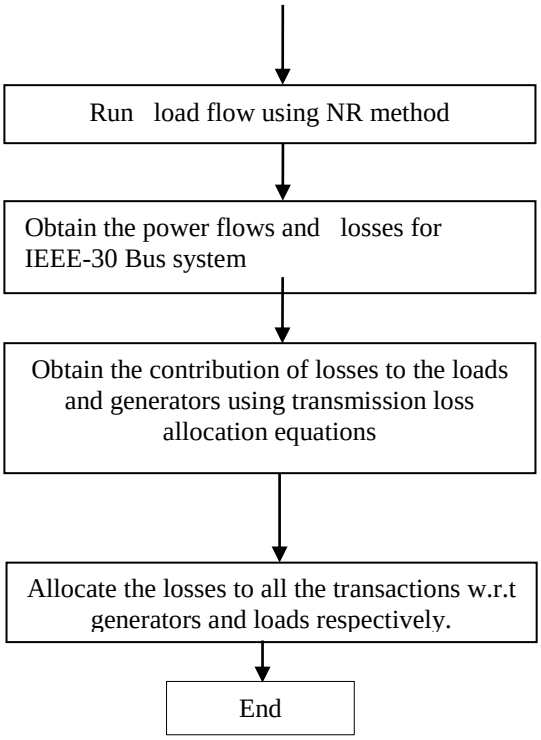

5.2. Power flow tracing (PFT) algorithm.

Power flow tracing algorithm works on the principle of Kirchhoff’s current law which requires the assumption of the proportional sharing of the network usage[1].With this principle losses are allocated proportionally by considering the network flow conditions. This method allows to allocate the transmission losses to individual loads and generators by analyzing the topology of the network flows. In this method the distribution factors can be determined by a simple inspection of network flows and in this method counter flows exist and negative generalized factors tended to correspond to zero to topological factors and would be given zero contributions. So the loss allocated to that particular transaction is zero. These are the advantages of this method.

Let us consider a network of ‘n’ nodes, b branches and P,Q,P_G,Q_G,P_D, and Q_D as nx1 vectors of nodal flows, nodal real and reactive power generations and nodal loads respectively and the branch flow matrix F (nxn)can be obtained from load flow solution. Here Kirchhoff’s current law is used to express branch flows as the sum of components supplied from individual generators or to loads[4].

$$P_{r\text{-}s}^{(gross)} = (P_{rs}/P_r)\Sigma[I_{u(r,k)}]P_{GK} \text{ for } s \epsilon \alpha_r^d \quad (5.3)$$

Where,

α_r^d= set of nodes supplied from node r
P_r = nodal power
K= Buses (generator bus)
P_{GK}= generating power at bus k
P_{sr}=branch power flow (r Є upstream, s Є down stream)
I_u= upstream distribution matrix

$$[I_u]_{rs} = \begin{cases} 1 & \text{for r=s} \\ -|P_{rs}|/P_r & \text{for s Є } \alpha_r^u \\ 0 & \text{otherwise} \end{cases}$$

Limits of Generation Reactive Power						
Bus	1	2	5	8	11	13
Q_G^{max}	0	50	40	40	24	24
Q_G^{min}	0	-40	-40	-10	-6	-6
Limits of Voltage and Tap settings						
V_G^{max}	V_G^{min}	V_{PQ}^{max}	V_{PQ}^{min}	T_k^{max}	T_k^{min}	
1.1	0.95	1.1	0.95	1.05	0.95	
Limits of FACTS devices						
TCSC	r^{max}	r^{min}				
	0.5	-0.5				

$$P_{r\text{-}s}^{(net)}=(P_{rs}/P_r)\Sigma[I_{d(r,k)}]P_{DK} \text{ for } s\text{Є}\alpha_r^u \quad (5.4)$$

Where,

P_{DK}= load at bus K.

K=buses (load bus).

P_{rs}=branch power flow (s Є upstream, r Є downstream).
α_r^u= set of nodes supplying node i.
I_d=downstream distribution matrix

$$[I_d]_{ij} = \begin{cases} 1 & \text{for i=j} \\ -|P_{sr}|/P_s & \text{for j Є } \alpha_r^d \\ 0 & \text{otherwise} \end{cases}$$

From the assumption of the power flow tracing algorithm 50% of total losses are allocated to the generation and 50% of total losses to the load demand. The final generation and demand per bus are computed as,

$$P'_{Gr}= (P_{r\text{-}s}^{net}+P_{Gr})/2 \quad (5.5)$$
$$P'_{Ds}= (P_{r\text{-}s}^{(gross)}+P_{Dr})/2 \quad (5.6)$$

Finally the real power losses allocated to each generator and demand are computed a

$$L'_{Gr}=P_{Gr}-P_{Gr}' \quad (5.7)$$
$$L'_{Ds}=P'_{Ds}-P_{Ds} \quad (5.8)$$

From the mathematical analysis, the proposed algorithms are tested for standard IEEE 30 Bus system with MATLAB/Simulink environment, which is discussed as case studies in the subsequent sections of this paper.

VI Results and Discussions

6.1Results for IEEE 30 bus system

The IEEE 30-bus system shown in Fig.6 consists of 41 branches, six generator-buses 1, 2, 5, 8, 11 and 13, and 4 branches 11, 12, 15 and 36 under load tap setting transformer branches. The bus 1 is selected as slack bus, the bus numbers 2, 5, 8, 11 and 13 as PV-buses. The others are PQ-buses. The system data, variable limits and the initial values of control variables were given in the Table. 1 below.

Table 2.Initial limits of IEEE 30 bus system control variables

Results of IEEE 30 bus system with TCSC

Control Variables	**GOA**
V1	1.1000
V2	1.0802
V5	1.0591
V8	1.0906
V11	1.0442
V13	1.0634
T6-9	0.9754
T6-10	1.0190
T4-12	0.9759
T28-27	0.95690
Optimal TCSC branch between the buses	16 – 17
r	-0.4233
Xnew	0.11089
Ploss	0.18572p.u.

Table–3 power flow profile for IEEE 30 Bus system

 ISBN: 978-81-940803-3-6

Table–4 Loss allocation to loads for IEEE-30 Bus

From bus	To bus	Without FACTS device	With FACTS device
			With TCSC
		Real power loss (MW)	Real power loss (MW)
1	2	6.072	5.566
1	3	3.727	3.525
2	4	1.229	1.121
3	4	1.03	0.946
2	5	3.130	2.902
2	6	2.352	2.189
4	6	0.752	0.712
5	7	0.113	0.105
6	7	0.331	0.305
6	8	0.102	0.098
6	9	0.000	0.00
6	10	0.000	0.00
9	11	0.000	0.00
9	10	0.000	0.00
4	12	0.000	0.00
12	13	0.000	0.00
12	14	0.055	0.045
12	15	0.149	0.129
12	16	0.036	0.037
14	15	0.003	0.006
16	17	0.014	0.026
15	18	0.030	0.027
18	19	0.004	0.007
19	20	0.023	0.03
19	20	0.099	0.120
10	17	0.034	0.05
10	17	0.188	0.207
10	22	0.028	0.02
21	23	0.002	0.004
15	23	0.013	0.036
22	24	0.044	0.032
23	24	0.002	0.004
24	25	0.054	0.029
25	26	0.042	0.039
25	27	0.037	0.041
28	27	0.000	0.00
27	29	0.083	0.076
27	30	0.156	0.143
29	30	0.032	0.03
8	28	0.002	0.00
6	28	0.065	0.066
Total losses		20.034	18.572

Table–5 Loss allocation to Loads for IEEE-30 Bus

Transmission loss – MW without FACTS Device		
Load No	**Postage Stamp Method**	**Power flow tracing Method**
2	0.7164	0.2978
3	0.0792	0.0484
4	0.2509	0.2015
5	3.11	3.1464
6	0.00	0.00
7	0.7527	0.9513
8	0.9905	1.0178
9	0.00	0.000
10	0.1915	0.1861
11	0.3302	0.3208
12	0.3698	0.2970
13	0.3302	0.2652
14	0.2047	0.1899
15	0.2707	0.2582
16	0.1156	0.1029
17	0.2971	0.3071
18	0.1056	0.1099
19	0.3136	0.3371
20	0.0726	0.1113
21	0.5778	0.6521
22	0.000	0.000
23	0.1056	0.1137
24	0.2872	0.3337
25	0.00	0.000
26	0.1156	0.0964
27	0.00	0.000
28	0.00	0.000
29	0.0792	0.1147
30	0.35	0.5573
Total	10.017	10.017

 ISBN: 978-81-940803-3-6

System with FACTS Device

Transmission loss – MW With FACTS Device		
Load No	**Postage Stamp Method**	**Power flow tracing Method**
2	0.6641	0.2735
3	0.0735	0.0446
4	0.2326	0.1851
5	2.8831	2.8994
6	0.00	0.00
7	0.6978	0.8742
8	0.9182	0.9376
9	0.00	0.000
10	0.1775	0.1711
11	0.3061	0.2951
12	0.3428	0.2729
13	0.3061	0.2436
14	0.1898	0.1737
15	0.2510	0.24
16	0.1071	0.0977
17	0.2755	0.3026
18	0.0979	0.1028
19	0.2908	0.3249
20	0.0673	0.1081
21	0.5356	0.6129
22	0.00	0.00
23	0.0979	0.1241
24	0.2663	0.3096
25	0.00	0.000
26	0.1071	0.1277
27	0.000	0.00
28	0.000	0.00
29	0.0735	0.0958
30	0.3244	0.489
Total	9.286	9.286

Table 6 Loss allocation to Generators for IEEE-30 Bus System without FACTS Device

Transmission loss – MW		
Generator No	**Postage Stamp Method**	**Power flow tracing Method**
1	8.778	9.289
2	1.238	0.726
Total	10.017	10.017

Table. 7 Loss allocation to Generators for IEEE-30 Bus System with FACTS Device

Transmission loss – MW with FACTS Device		
Generator No	**Postage Stamp Method**	**Power flow tracing Method**
1	8.1322	8.6006
2	1.1536	0.6854
Total	9.286	9.286

From the results of IEEE-30 bus system, it can be observed that, in Power flow tracing Method the network is taken in to consideration, allocation can be done. It allocates the losses of 9.286MW to the generators and loads equally.

From the results of IEEE 30 bus system it can be observed that, all the methods allot zero loss to the transfer bus which has zero injection power.

V.Conclusion:

In Postage Stamp method the structure of the network is not taken into consideration and it is based on the average cost, irrespective of the transmission distance and network structure of the system for a particular transaction. The transmission charges for two loads of same rate, out of which one is very near to generator and other is very far away from the generator and it is obvious that the transmission network use by the other loads is more than the first. In order to avoid the above dis-advantages power flow tracing method is used.

Power flow tracing Method takes the network in to consideration and allocates the real power losses proportionally to all the transactions. But here assumptions are made that the line inflows are equal to the line out flows. This method does not depend up on the choice of the slack bus and some market participants are getting extra burden for loss allocation with the equal division of losses to generators and loads. This method gives accurate results compared to the Postage stamp Method .

 ISBN: 978-81-940803-3-6

Future scope: Here in this paper only real power losses are considered for loss allocation. The above two methods can be extended to other Facts Devices using different optimization Algorithms and then the real power losses and then can be allocated the losses to the market participants for better voltage stability and cost allocation can also be done which is a major issue in today's competitive market.

References

[1] Janusz, Bialek, "Topological generation and Load Distribution factors for supplement charge allocation in transmission open access", *IEEE transactions on power systems*, vol.12, no.3, August 1997.

[2] "Power system restructuring and deregulation- trading, performance and information technology", Edited by Loi Lei Lai, john Wiley & sons Ltd, Chichester.

[3]A.Conejo,J.Arroyo,N.alguacil,andGuijarro,,"transmissio n loss allocation comparison of different practical algorithms", *IEEE transactions on power systems*, vol.17, no.3, pp.571-576, August 2002.

References

[1]. O.Alsac and B.Scott, "Optimal load flow with steady state security", IEEE transactions PAS-1973,pp.745-751.

[2]. J. A. Momoh, M. E. El-Hawary, and R. Adapa, "A review of selected optimal power flow literature to 1993 part I & II," *IEEE Trans. Power Syst.*, vol. 14, no. 1, pp. 96–111, Feb. 1999.

[3]. Naresh Acharya, N.Mithulanathan "Locating Series FACTS devices for congestion management in deregulated electricity markets" Electrical power system Research 77(2007) 352-360.

[4]. Iba K. Reactive power optimization by genetic algorithm. IEEE Trans Power Syst 1994;9(2):685–92.

[5]. Knnedey , J, Eberhart, R.: "Particle swarm optimization", IEEE International Conference of Neural Networks 4, 1995.

[6]. H. Yoshida et al., "A particle swarm optimization for reactive power and voltage control considering voltage security assessment," IEEE Trans. Power Syst., vol. 15, no. 4, pp. 1232–1239, Nov. 2001.

[7]. A. A. A. Esmin, G. Lambert-Torres, and A. C. Zambroni de Souza, "A hybrid particle swarm optimization applied to loss power minimization," IEEE Trans. Power Syst., vol. 20, no. 2, pp. 859–866, May 2005.

[8]. M. S. Kumari and M. Sydulu, "Improved particle swarm algorithm applied to optimal reactive power control," in Proc. IEEE Int. Conf. Industrial Technology, 2006, pp. 1873–1878.

[9]. M. Varadarajan and K. S. Swarup, "Differential evolutionary algorithm for optimal reactive power dispatch," Int. J. Elect. Power Energy Syst., 2008, to be published.

[10]. Chaochua Dai, Weirong Chen "Seeker Optimization Algorithm for optimal Reactive Power Dispatch" IEEE transactions on power systems, vol. 24, no. 3, august 2009.

[11]. Aniruddha Bhattachrya "Solution of optimal Reactive Power Flow using Biogeography-Based optimization" International Journal of Electrical and Computer Engineering, Vol:4, No:3, 2010.

[12]. Hamid Falaghi, Arsalan Najafi "Optimal Reactive Power Dispatch using Improved Differential Evolution Algorithm" Vol. 8, No. 1, March 2014.

[13]. S.Abdelkader,"A new method for transmission loss allocation considering the circulating currents between generators", *IEEE power systems conference 12th international Middle- East*, pp.282-286, March 2008

[14]. F.Galiana, A.Conejo, and I.Kockar, " Incremental transmission loss allocation under pool dispatch", *IEEE transactions on power systems*, vol.17,no.1,pp 26-32, February 2002

A New Innovative Prepaid Energy Meter Using Arduino and IOT

[1] N.Vineetha, [2] P. Bhavani, [3]B. Shahil, [4]K.N.V.S.R.S.Sastry,[5]N.Veeraiah
[1][2][3][4] B.Tech, Final year students of DVR & Dr.HS MIC college of Technology, Kanchikacherla, India.
[5] Asst.Professor, Dept.of ECE, MIC College of Technology

Abstract:-- **In present generation technology has been developed to a large extent. Smart phones play the major role in everyone's life. By using best technology I am designing a prepaid electricity bill using arduino and IOT module for domestic and commercial purpose. Generally the electricity reading is done by human beings. Humans are going to each and every house for electric reading. Sometimes it is not possible for them to go to some places because of bad weather conditions or floods etc. Sometimes the electric meter is not accessible for the human operator. So, by using this we can avoid such problems.**

Index Terms: Arduino Kit, IOT module, Energy Meter, Current sensor, etc

1. INTRODUCTION

Prepaid Electricity card is a good concept in which we can recharge the balance because like, we do recharge in our phones. In this project we are designing a system by using Arduino and IOT module. We can recharge the prepaid card by using the RFID card. In this project we are using an app called blink. If the balance is low or zero then it can automatically cutoff the power supply connection and intimates to the user by sending a message to their phone.

The system will read the recharge card and automatically sends the updates to the user like low balance alert, cutoff alert and recharge alert. We can recharge the prepaid card in various ranges like Rs.50, Rs.150 etc. According to the power consumption, the amount will be reduced. We are using a relay system which shutdown or disconnect the power supply when the recharge amount is over. Here we are using a buzzer which acts like alarm when it reaches to minimum balance.

Why Prepayment- From supplier point of view?

- Pay before use
- Keep customers on supply
- No bill production
- No bill distribution
- No need to chase payments
- Customer responsible for disconnection
- Social acceptability
- Load and demand side management

1.1Why prepayment – From customer point of view?

- >80% mobile phones used in India are prepaid Flexible payment solution
- Pay to suit your income status
- Daily, weekly, monthly budgeting
- Show true cost of consumption and money left
-

2. LITERATURE REVIEW

Electricity meter reading is done by human operator, this requires more number of time for billing. Due to the development of number residential buildings and commercial buildings the electricity meter task can be done by more number of human operators. It should be clear that such type of methods will take long time and doesn't complete the work within the time. In addition to this we can get large number of errors incorporated in the reading process and this type of system can't provide transparency.

3. COMPONENTS USED

- ARDUINO(ATMEGA328P-PU)
- ANALOGUE ENERGY METER
- OPTOCOUPLER(4n35)
- CURRENT SENSOR(ACS712)
- RELAY DRIVER(ULN2003)
- LCD 16*2

3.1 ARDUINO (ATMEGA 328P-PU):-

The ATMEGA328 is a single chip microcontroller created by "ATMEL" in the mega AVR family. It has a modified "HARDVARD" Architecture 8-bit RISC processor code.

Features:

- The ATMEL 8-bit AVR RISC based microcontroller combines 32KB and 1SP flash memory with read-write capabilities
- 1KB EEPROM
- 2KB SRAM
- 23 general purpose I/O lines
- 32 general purpose working registers
- 3 flexible timer/counters with modes internal and external interrupts
- serial programmable USART

- A byte-oriented 2 wire serial interference
- SP1 serial port
- 6-channel 10-bit A to D converter
- Programmable watchdog with internal oscillator and with 5 software selectable power saving modes
- The device operates between 1.8-5.5 Volts. The device achieves throughput approaching 1MIPS per MHZ.
- A common alternative to the ATMEGA328 is the "PICOPOWER".

Fig.1. Arduino (ATMEGA 328P-UP)

3.2 ANALOGUE ENERGY METER:-

Analogue or Analog meter is also known as electromechanical. The simple meter spins or moves forward when you are using electricity. The number of times the disc moves forward or backward determines how much electricity you are using to the electric grid.

Features:

- Cost-effective and flexible single-phase Energy Meter
- Detects signals and continues to measure accurately under at least 20 different tamper conditions
- Secure and reprogrammable Flash memory
- One-time, quick and accurate digital calibration
- Active power, voltage and current measurements are easily accessible
- USART interface
- Low-power AVR Microcontroller allows operation down to 1.8V

Fig.2. Analogue Energy Meter

3.3 Opto-coupler (4n35):-

An Opt coupler is a semi conductor device that uses a short optical transmission path to transfer an electrical signal between circuits or elements of a circuits, while keeping them electrically isolated from each other. Opt coupler prevent high voltages from effecting the system receiving the signal.

Opt coupler or Opt isolator means the control signal is used purely as a differential signal between Vcc and the control signal both sourced from the controlled circuit. Ground potential difference won't affect the operation.

Features:

- Isolation test voltage 5000 VRMS
- Interface with common logic families
- Input-output coupling capacitance<0.5pF
- Industry standard dual-in-line 6 pin package

Applications

- AC mains detection
- Reed relay driving
- Telephone ring detection
- Logic ground isolation

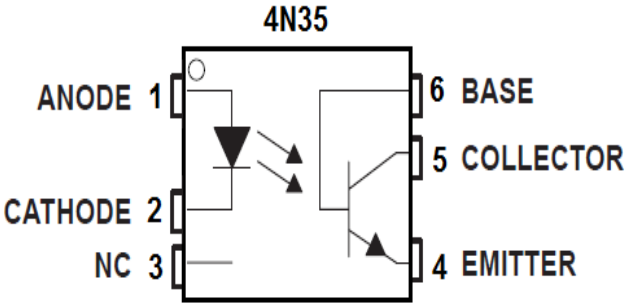

Fig.3. Opto-coupler (4n35)

3.4 Current Sensor (ACS712):-

A Current sensor is a device that detects electric current in a wire, and generates a signal is proportional to that current. The generated signal will be analog voltage or current or even a digital output. A current carrying wire produces a magnetic field. Current sensing resistors are used when the current is directly measured in the circuit.

Features and Benefits:

- Low-noise analog signal path
- Device bandwidth is set via the new filter pin
- 80 KHZ bandwidth
- Small footprint, low-profile SOIC8 package
- 66 to 185 mV/A output sensitivity
- Output voltage proportional to AC or DC currents
- Factory-trimmed for accuracy
- Nearly zero magnetic hysteresis

Fig.4 Current Sensor (ACS712)

3.5 Relay Driver (ULN2003):-

A Relay driver IC is an electro-magnetic switch that will be used whenever we want to use a low voltage circuit to switch a light bulb ON and OFF which is connected to 220V mains supply. The ULN2003 is an array of 7 NPN Darlington transistor capable of 500MA, 50V output. It features common-cathode fly back diodes for switching inductive loads. It can come in PDIP, SOIC, SOP (or) TSSOP packaging.

Features:

- 500-mA-Rated Collector current
- High-voltage outputs:50 V
- Output clamp diodes
- Relay drivers
- Stepper and DC Brushed Motor Drivers
- Lamp Drivers
- Display Drivers
- Line Drivers

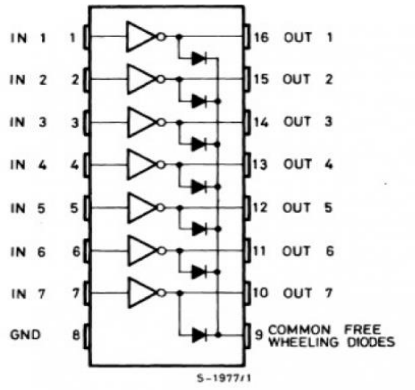

Fig.5. Relay Driver

3.6 LCD Display (16*2):-

LCD stands for LIQUID CRYSTAL DISPLAY.LCD is the technology used for displays in notebooks and other smaller computers like light emitting diode (LED) and gas-plasma technologies, LCD allows displays to be thinner than cathode ray tube (CRT) technology. A 16*2 LCD display is basic module and is commonly used in various devices and circuits. These modules are preferred over seven segments and other multi segments LED's. In 16*2 alphanumeric LCD there are 2 rows and 16 columns. There are 8 data lines from pin number 7 to pin number 14 in an LCD. In this LCD each character is displayed in 5*7 pixel matrix and it has two registers namely, command and data.

Fig.6. LCD Display

4. WORKING PRINCIPLE

Here we have interfaced electricity energy meter with arduino using the pulse LED.

When we switch on the system then it reads the previous values stored in the EEPROM and then it checks the available balance with the predefined value and work according to them. If available balance is greater than Rs 20 then arduino automatically turns on and provide power supply to the home. If the balance is less than Rs 20 then it sends the alert message to the user phone. If the balance is less than Rs 5 then the arduino turns off and the connection will lost and sends the message to user phone. We can get all the messages in a app called blynk.

We need to recharge the prepaid card by placing the card in front of the RFID reader then it scans the card and automatically recharges the amount. We are using a current sensor for calculating the total power consumption of the system.

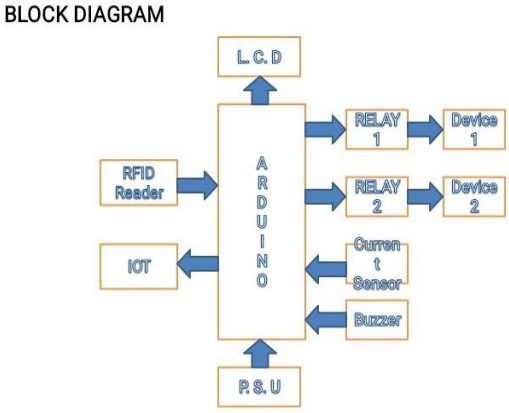

Fig.7 Block Diagram

Working Flow Chart:

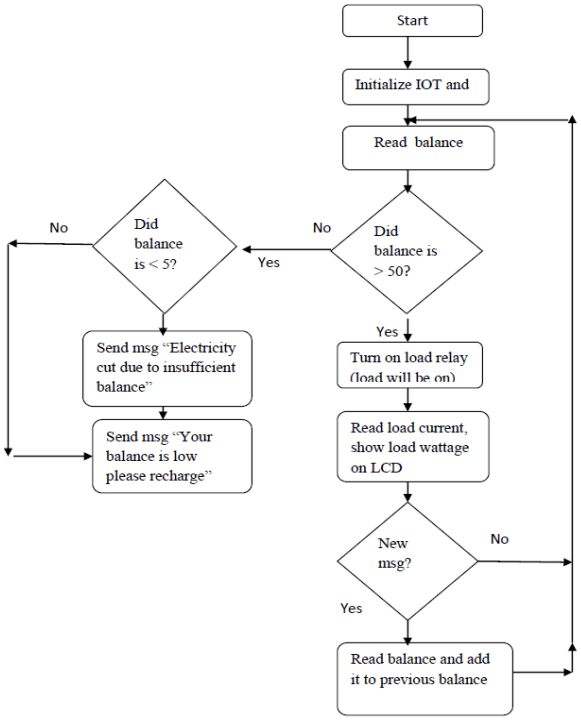

Fig.8 .Flow chart

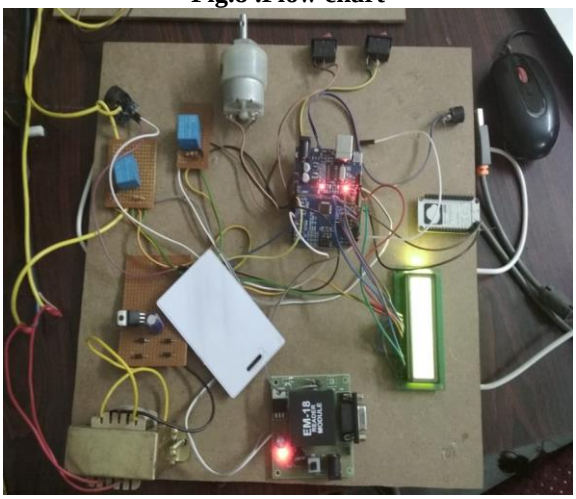

Fig.8. Energy Meter Using Arduino and IOT

5. RESULT

When the supply is provided to the meter, initially the LCD will turn on. We have set the recharge amount up to Rs 999. The costumers can recharge according to their requirement. Whenever they switch on the supply the power will consume and reading are updated in the app .If the customer wants to know how much amount used how much amount left then they can see the LCD display or they can check the app also. If the balance is low then the customer will get the alert message and the buzzer also sounds.

6. CONCLUSION

In present situation all customers are using manual communication. To reduce the manual efforts and human efforts we are implementing a automated system which monitors all the parameters and functionality between the customer and electricity board. Also, by implementing this system we can control the usage of electricity and avoid wastage of power. By using this system we can save the customer and human operator time and customers can easily monitor their usage of current. An attempt is made in which interfaced with static electronic energy meter is avoided where in complexity of the circuit is reduced and cost also gets reduced.

7. REFERENCES

[1] Sneha Salunkhe, Dr.(Mrs.) S. S. Lokhande "A Review: AUTOMATIC METER READING USING IMAGE PROCESSING" International Journal of Application or Innovation in Engineering & Management (IJAIEM) (Volume 5, Issue 6, June
2016 ISSN 2319 – 4847)

[2] Sachin Divate, Tanaji Dhikale, Trunal Dube, Milan Mitke "REMOTE WIRELESS AUTOMATIC METER READING SYSTEM" International Journal Of Emerging Technology and Advanced Engineering (ISSN 2250-2459, ISO 9001:2008 Certified Journal, Volume 3, Issue 4, April 2013)

[3] Tanvir Ahmed, Md Suzan Miah, Md. Manirul Islam and Md. Rakib Uddin "AUTOMATIC ELECTRIC METER READING SYSTEM: A COSTFEASIBLE ALTERNATIVE APPROACH IN METER READING FOR BANGLADESH PERSPECTIVE USING LOW-COST DIGITAL WATTMETER AND WIMAX TECHNOLOGY" International J. Eng. Tech 8(3):800-807, September 2011.

[4] Sai Kiran Ellenki, Srikanth Reddy G, Srikanth Ch.(2014) "An Advanced Smart Energy Metering System for Developing Countries" International Journal Of Scientific Research And Educational (||Volume| |2||Issue ||1|| Pages|242-258||2014|| ISSN (e):2321-7545).

Image Based Password Authentication Using Touch Screen and GSM Module

[1] K. Sumadhura, [2] R. Bhargavi, [3] R.L.N Bharath, [4]P. Phaneendhra Nath,[5]N.Veeraiah
[1][2][3][4] B.Tech, Final year students of DVR & Dr.HS MIC college of Technology, Kanchikacherla, India.
[5] Asst.Professor, Dept.of ECE, MIC College of Technology

Abstract:-- **Technology is playing a vital role in enhancing security. Without cameras, detectors and alarms world would be unable to identify threats and respond appropriately. An approach is to be made where an illiterate can also be benefited by the boons of technology with less cost and more user-friendliness. With this prototype, an interface is made where even an un-educated or a person of any age can use the application with ease. The inputs will be images where it is easy for any person to remember in a sequence. This can serve multiple areas like farms, cattle area, industries. The main aim of this paper is to enhance security to the root levels which is more efficient and low cost. Here in this paper, the password need not be a group of characters rather series of images can be used. With the use of graphical LCD and touch screen, this can be used effortlessly. The touch screen provides an easy interaction of the user with the application as it can be easily operated. Fastness has become a key role in every aspect, with the use of GSM module owner can get the information immediately if any broke out has been happened. A message will be sent to the owner when the door has been opened when a wrong password has been entered or when a fire broke out has occurred then the necessary precautions will be taken immediately. To accomplish this task an onboard computer is used which has input and output ports and is termed as the microcontroller. Advanced RISC Machine (ARM) is the heart of the application and controls all the processes.**

Index Terms: GLCD, Micro-Controller, Fire sensor, Touch screen, GSM module

1. INTRODUCTION

The motto of this paper is to provide security wherein every individual can be able to access it and should be benefited by the boons of the technology. Image based password authentication is a concept where passwords are in form of images. Person of any age can easily remember this password as images can be easily remembered than characters in form of string. Enhancing security can be done through this project as this can be used by any class of the society because of its low cost and accessibility. Using touch screen we can more easily access the project. GSM module will provide the information about the access of the door regularly so if there's any unauthorized person accessing the door then the information will immediately passed to the owner.

Comparing with the existing technology this will be more beneficial as it is more easily used because of touch screen which gives comfort of

Selecting the images easily, GLCD which gives the display of images without using much technology and it is low cost, GSM which instantly provides the information of the access of the door Buzzer is used to intimate surrounding places.

2. LITERATURE REVIEW:

In under developed areas there is no proper security system even there is a lot of advent in the technology nowadays. In especially cattle areas gates are made of small wooden pieces which can be easily damaged by the intruder. As technology is increasing day by day we even have to provide proper security even for these places. With less cost and more user-friendliness a system has to be developed where even an illiterate must find easy to use such an application

3. BLOCK DIAGRAM:

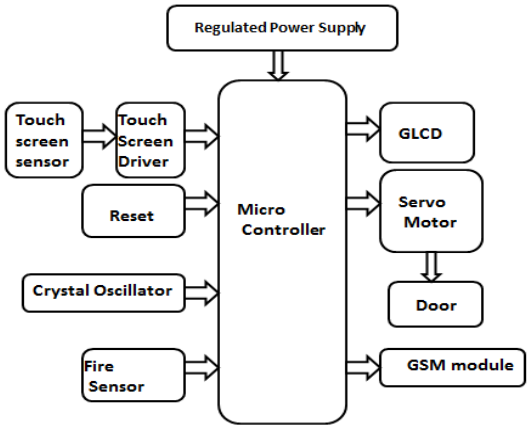

Fig1. Block Diagram of Image Based Password Authentication Using Touch Screen And GSM Module

4. HARDWARE DESCRIPTION:

1. Microcontroller
2. Touch screen Sensor
3. GLCD
4. GSM Module

1. Microcontroller

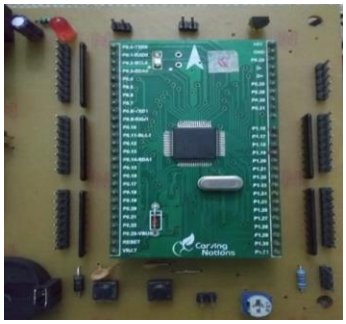

Fig2. ARM-7 Microcontroller

Microcontroller used in this paper is ARM7TDMI-S LPC2148 (Advanced RISC Machine). Some of the

Features Are:
•I6 bit/32 bit thumb micro-controller.
•Consists of 40 kB of on chip static RAM and 512 kB on chip flash memory.
•Two 10-bit ADC which provides 14 analog inputs.
•A 10-bit DAC which gives variable analog outputs.
•A RTC with 32 kHz clock input.
•Power saving mode

2. Touch Screen

Touch screen technology deals with the direct manipulation of gestures into digital data. In 1960s touch screen was first invented by E.A Johnson. The capacitive touch screen was first invented and later in 70's resistive touch screen was invented by Dr G. Samuel Hurst. Nowadays the touch screen has been widely used in every application to ease the complexity of giving the input. Various applications are ATM machines, Cell phones, Video games…etc. The popularity of cell-phone is due to the use of the touch screen as it gives an easy way to control the system. The demand for it is increasing rapidly day-by-day which allows any application to use it. Different types of touch screen technologies are:

1. Resistive
2. Surface acoustic wave
3. Capacitive
4. Surface capacitance
5. Projected capacitance
6. Infrared
7. Strain Gauge
8. Optical imaging.

Here in this paper, we are using a resistive touch screen as it is of low cost and can withstand in any harsh environment. Resistive touch screen consists of different layers such as:

1. Polyester Film
2. Transparent electrode film
3. Insulator
4. Spacer dot
5. Glass

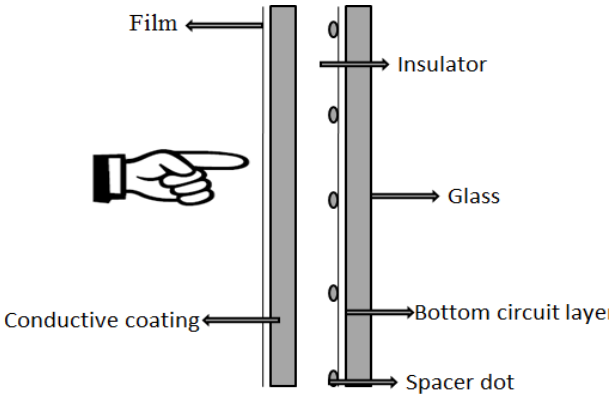

Fig3. Diagram of touch screen working

A little gap exists between glass screen and film screen using this panel is made. Film layer contains electrodes. Whenever the film screen is touched with a finger or any type of object bend occurs. When bending, the two electrode films connect, which generates a current flow. Resistive touch screen have many advantages like highly durableness, cost-effectiveness and in addition it is less sensitive to the scratches on the screen. A 4 wire resistive touch screen has uniformly coated with a resistive material and is separated by an air gap or an insulator. Electrodes are placed on the edges of the layer.

3. Graphical Liquid Crystal Display

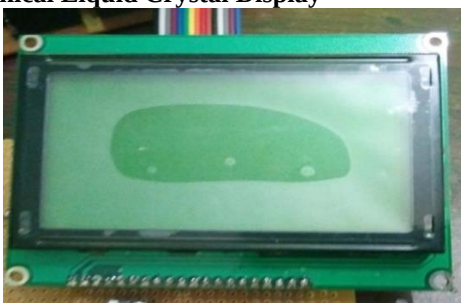

Fig4. GLCD

Here JHD12864E GLCD is used in this paper. It is a 128x64 display where it has 1024 pixels. 128x64 is divided into two parts equally and each is controlled by a separate controller. It has 128 columns and 64 rows. Each page has 8x8 bits which form 1 page.8 such pages makes one half and is controlled by a controller called controller selected.GLCD consists of 20 pins. Two power supply pins (VSS), Two Ground pins (GND), Two Controller Select

(CS0, CS1), Eight Data pins (D0-D7), Contrast adjust pin, Register Select pin (RS), Read/Write pin, Enable pin (En), Reset pin (RST), Output Voltage pin (Vout).The difference between an LCD and GLCD is that LCD can only display alphanumerical letters but can't display images and can display up to certain dimensions. Graphical Liquid Crystal Display (GLCD) is used to display customized characters and images. It finds many applications in video games, mobile phones, lifts.

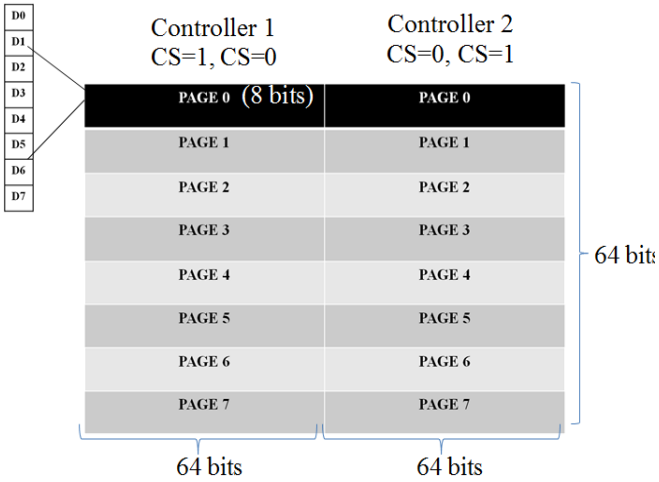

Fig5. Tabular Representation of GLCD Bits assignment

Each half of the display has vertical addresses of 64 pixels which are addressed from 0x40 to 0x7F and is represented as the Y-axis. Horizontal addresses are from 0xB8 to 0xBF and are represented as X-axis.
Left half of the display is controlled by chip select CS1=1, CS0=0.
Right half of the display is controlled by chip select CS1=0, CS=1.
X-axis addresses are used to select a page from page-0 to page-7.

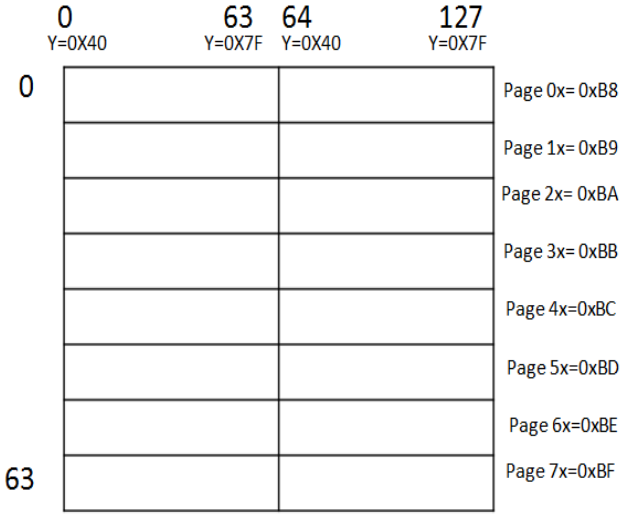

Fig6. Horizontal and Vertical addresses

4. Global System for Mobile Communication:

Fig7. GSM Module

GSM is a cellular network in which the mobile phones connect by searching a cell in the nearby vicinity. Global System for Mobile Communication (GSM) operates in 4 frequency ranges. Mostly it operates in 900MHz or 1800MHz bands. Country like America use 850MHz and 1900MHz as 900MHz and 1800MHz frequency bands were already allocated. The frequency bands of 400 and 450MHz were previously used by first generation is assigned in some of the countries. GSM-900 uses frequencies in the ranges of 890-915 MHz to send the information from the mobile station to the base station (uplink) and the downlink frequencies are in the ranges of 935-960 MHz (base station to mobile station) which provides 124 radio channels. GSM Module has been extended to cover a large frequency ranges which is denoted by "E-GSM" uses uplink frequencies of 880-915 MHz and downlink frequencies of 925-960 MHz, By adding 50 channels. TDMA allows 8-full rate or 16- half rate speech channels per radio frequency channel.

5. Buzzer:

Fig8. Buzzer

5. WORKING PRINCIPLE:

Here the microcontroller (ARM-7) will be the brain of the system in which it controls and coordinates all the commands. As GLCD can display images, the images to be chosen are displayed over which the user or owner will select the order of his password in which it has been already stored. When the password is chosen is right the door opens and we are using a dc motor for it. Immediately the message will be sent to the owner's number. If the

password is chosen to wrong the doors opens not and a message will be sent to the owner. When a fire broke out takes place the doors automatically opens and a message will be sent to the owner. The buzzer is an electronic signaling device used in automobiles, household applications, etc. Pressure variations occur whenever an electric potential is applied across piezo-electric material. When the voltage difference occurred in the push and pull of conductors take place internally. The sharp sound is generated by the continuous push and pull operation. The sound pitch is not dependent on the voltage level, so piezo-electric buzzer is independent on voltage ranges. It generates sound in the ranges of 2-4 KHz.

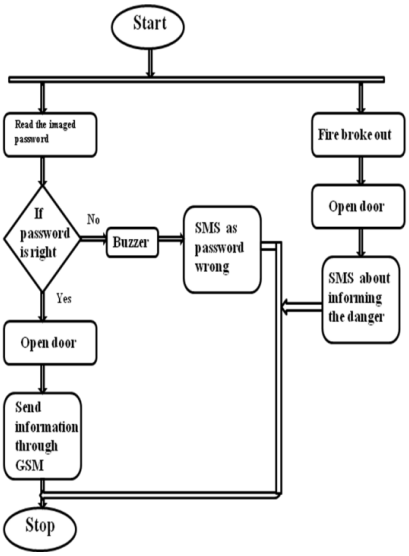

Fig9. Design Flow

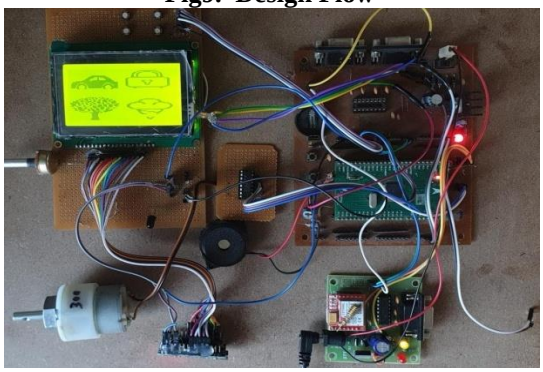

Fig10. Image based password authentication using touch screen and GSM

6. RESULT:

This project provides user a image based password where he can easily interact with the system using touch screen and the security is enhanced using GSM module.

7. CONCLUSION:

This paper "Image Based Password Authentication Using Touch screen and GSM" provides a user friendliness and low cost system which will enhance the security.

8. REFERENCES:

[1] G. E. Blonder, "Graphical passwords," in Lucent Technologies,Inc., Murray Hill, NJ,U.S. Patent,Ed. UnitedStates, 1996.

[2] ALSULAIMAN, F. A. & EL SADDIK, A., 2008, „Three-Dimensional Password for More Secure Authentication", IEEE Transactions on Instrumentation and Measurement, vol.57, pp.1929-1938.

[3] E.Shephard, "Recognition memory for words,sentences and pictures", Journal of Verbal Learning and Verbal Behaviour, 6,pp.156-163,1967.

[4] Sears, A.; Plaisant, C. & Shneiderman, B. (1992). "A new era for high precision touchscreens". In Hartson, R. & Hix, D. Advances
in Human-Computer Interaction. 3. Ablex, NJ. pp. 1–33.

[5] Walker, Geoff (August 2012). "A review of technologies for sensing contact location on the surface of a display". Journal of the Society for Information Display. 20 (8): 413–440. doi:10.1002/jsid.100.

Design of Efficient Single Precision Floating Point Multiplier using Urdhva Triyagbhyam Sutra of Vedic Mathematics

[1] Sai Venkatramana Prasada G S, [2] G Seshikala,[3] Niranjana S
[1] Department of Electronics and Communication, Srinivas University, Mangaluru, Karnataka, Research Scholar, School of Electronics and Communication, REVA University, Bengaluru
[2] Professor, School of E&C, Reva University, Bangalore, India, [3] Associate Professor-Senior Scale Manipal Institute of Technology, Manipal Academy of Higher Education, Karnataka, Manipal, India

***Abstract*:-- Multiplication of floating point(FP) numbers is greatly significant in many DSP applications. The performance of the DSP's is substantially decided by the speed of the multipliers used. This paper proposes the design and implementation of IEEE 754 standard single precision FP multiplier using Verilog, synthesized and simulated in Xilinx ISE10.1. Urdhva Triyagbhyam Sutra of Vedic mathematics is used for the unsigned mantissa calculation. The design implements floating point multiplication with sign bit and exponent calculations. The proposed design is achieved high speed with minimum delay of 3.997ns.**

Index Terms: Floating point numbers, Single precision, IEEE 754, Urdhva Triyagbhyam Sutra, Vedic mathematics.

1. INTRODUCTION

Multiplication of floating point binary numbers is the most important operation in DSP applications. IEEE 754 standard provides formats for the FP numbers. IEEE 754 standard format for single precision(32-bit) FP number consist of a Sign unit(1-bit), Exponent unit(8-bits) and Mantissa unit(8-bits) as shown in fig.1.

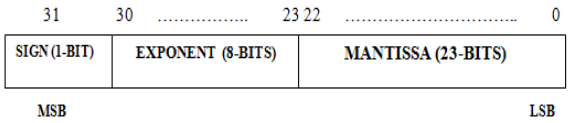

Fig.1: IEEE 754 Single Precision Format

MSB's of two 32-bit numbers are XORed to generate sign bit of the product. Exponent of the product is calculated by adding exponents of the inputs using Carry Look Ahead(CLA) adder and biasing to -127. Mantissa multiplication unit is designed using Urdhva Triyagbhyam Sutra of Vedic mathematics.

A. Urdhva Triyagbhyam Sutra

The exact meaning of Urdhva Tiryabyham sutra is "Vertically and Crosswise". Urdhva Tiryabyham Sutra can be applied to all the cases of multiplication. In this method, the partial products & their sum is obtained in parallel. The steps involved in 2x2 multiplication[14] using Urdhva Tiryabyham Sutra are shown in fig.2. The same procedure can be extended for 3x3 multiplication[3] as shown in fig.3.

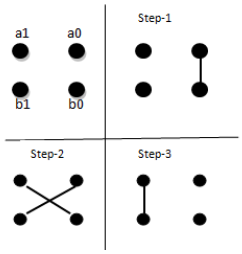

Fig.2. 2x2 Multiplication Using Urdhva Sutra

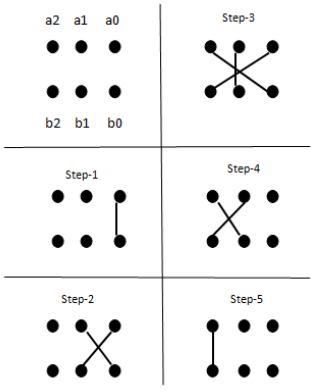

Fig.3. 3x3 Multiplication Using Urdhva Sutra

The 3x3 multiplier can be used for constructing higher order multipliers such as 6x6, 12x12 and 24x24 bit multiplication.

II. PREVIOUS WORKS

Swapnil Suresh Mohite, Sanket Sanjay Nimbalar, Madhav Makarand Bhathande, Rashmi Rahul Kulkarni presented the design of 32-bit FP multiplier using Urdhva Triyagbhyam sutra[1] which reduces the processing delay. Code was written in VHDL using Xilinx ISE series. Overall performance of designed multiplier depends upon the performance of mantissa multiplier unit. Mantissa multiplier was designed using Urdhva Triyagbhyam sutra. 3x3 multiplier was used as basic multiplier. 8-bit CLA is used for adding two 8-bit exponent. Output of the adder was biased to -127 to generate the exponent of output floating point number. The proposed multiplier circuit takes 71.239ns to perform multiplication of two 32-bit floating point binary numbers. This delay is significantly less than Booth multiplier.

Aniruddha kanhe, Shishir Kumar Das, Ankit Kumar Singh described the design and implementation of IEEE 754, 32-bit FP multiplier[3] using vedic mathematics. The Urdhva Triyagbhyam sutra was used for mantissa multiplication. Multiplication was achieved by adding the biased 8-bit exponent, multiplying the normalized 24-bit mantissa and resultant was converted in excess 127 bit format. The exponent calculation unit was implemented using 8-bit RCA. Sign bit was calculated by XORing the MSB's of the inputs. The multiplier was designed in Verilog HDL and simulated using Modelsim simulator. This design was synthesized using Xilinx ISE12.1 tool targeted on the Xilinx Vertex5. The design utilizes lesser number of LUT's, thereby reduces the power consumption.

Soumya Havaldar, K S Gurumurthy[4] proposed the design of multiplier for floating point numbers using vedic mathematics. This design also manages overflow, underflow and rounding. Design was coded in VHDL, simulated and synthesized using ISE14.6 tool targeting the Xilinx VertexVI FPGA. This work concludes that; the proposed design occupies less space and high operating speed due to vertical and crosswise calculation using Urdhva Triyagbhyam sutra.

Pooja Hatwalne, Ameya Deshmukh, Tanmay Paliwal, Krupal Lambat proposed a design and implementation of single precision FP multiplier using VHDL[5]. 24-bit multiplier using Urdhva Triyagbhyam sutra of vedic mathematics was designed for mantissa calculation. 8-bit CLA adder was used for exponent calculation. The design was synthesized and simulated in Xilinx ISE14.7 targeted on Spartan3 device. The proposed floating point multiplier showed optimized and better timing performance with total delay of 36.19ns.

III. SILULATION RESULTS

32-bit floating point multiplier design is implemented in VHDL and simulated using Xilinx ISE10.1. The unsigned mantissa multiplication is achieved by using Urdhva Triyagbhyam Sutra of Vedic mathematics. Fig.4-6 shows the RTL schematics of 32-bit floating point multiplier, mantissa unit and exponent calculation unit respectively.

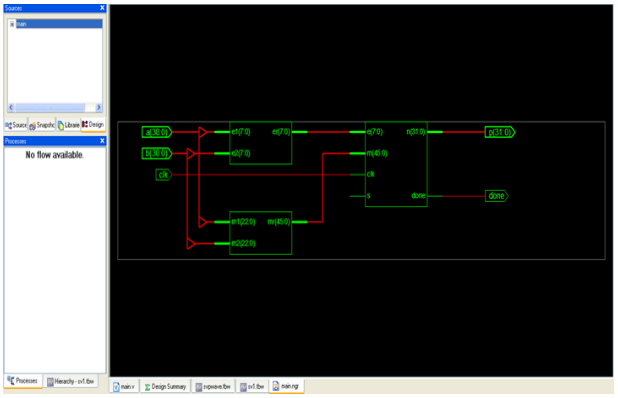

Fig.4: Schematic Of 32-Bit Floating Point Multiplier

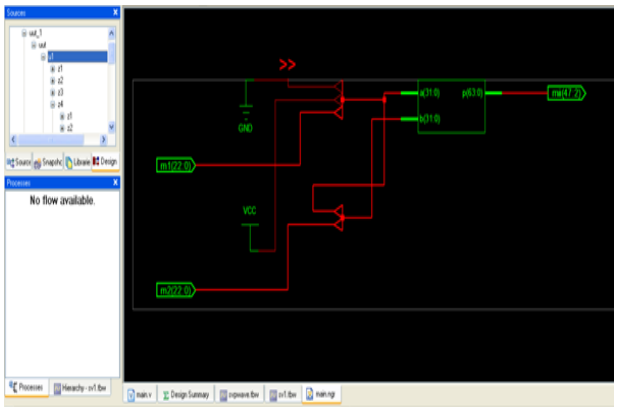

Fig.5: Schematic Of Mantissa Calculation

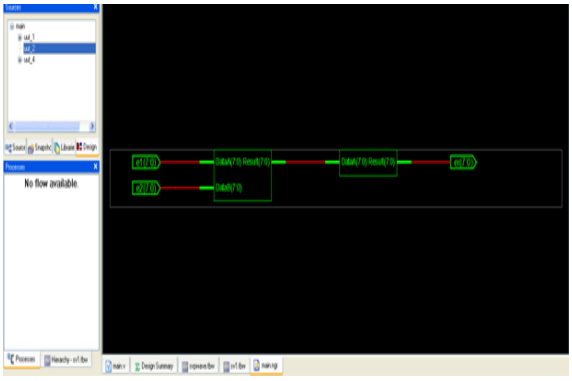

Fig.6: Schematic Of Exponent Calculation

 ISBN: 978-81-940803-3-6

Table 1: Performance Analysis

Parameters	Proposed Urdhva 32X32
NO. SLICES	298
NO. 4 IP LUT	579
NO.OF BONDED IOBs	96
COMBINATIONAL DELAY	3.997ns

Table 1 show the device utilization and combinational delay of the proposed design. Table 2 show the comparison of the proposed design with the designs of the literatures. The proposed design exhibits lesser device utilization and delay.

Table 2: Comparison of Performance Parameters

Paper	Number of Slices	LUT's	Bonded IOB's	Time delay(ns)
[1]	911	1580	96	71.293
[3]	-	966	99	5.246
[4]	-	705	96	21.823
[6]	-	672	96	4.94
[9]	1389	1545	129	13.141
[10]	2041	3317	206	89.374
[11]	-	1032	99	5.246
[12]	999	1819	-	14.17
Proposed design	**298**	**579**	**96**	**3.997**

CONCLUSION

The single precision FP multiplier using Urdhva Triyagbhyam Sutra is designed in VHDL, simulated using Xilinx ISE10.1 and parameters such as number of slices, 4 input LUT's and delay were analyzed and compared with the literatures. The proposed design utilizes lesser number of slices and LUT's thereby reduces the hardware requirement. High speed is also achieved by the use of Urdhva Triyagbhyam Sutra and CLA adder. This proposed work can be extended for the design of double precision(64-bit) FP multiplier using Vedic mathematics.

REFERENCES

[1] Swapnil Suresh Mohite, Sanket Sanjay Nimbalar, Madhav Makarand Bhathande, Rashmi Rahul Kulkarni, "32 bit Floating Point Vedic Multiplier", IOSR Journal of VLSI and Signal Processing(IOSR-JVSP), Volume 6, Issue 2, Ver. I, pp 16-20, Mar-Apr.2016.

[2] Sneha khobragade, Mayur Dhait, "Design of High Speed Single Precision Floating Point Multiplier Using Vedic Mathematics", International Journal of Innovative Research in Computer and Communication Engineering, Vol.3, Issue 7, pp 6875-6882, July 2015.

[3] Aniruddha kanhe, Shishir Kumar Das, Ankit Kumar Singh, "Design and Implementation of Floating Point Multiplier based on Vedic Multiplication Technique", IEEE International Conference on Communication, Information & Computing Technology(ICCICT), Mumbai, pp 1-4, Oct. 19-20,2012.

[4] Soumya Havaldar, K S Gurumurthy, "Design of Vedic IEEE 754 Floating Point Multiplier", IEEE International Conference On Recent Trends In Electronics Information Communication Technology, pp 1131-1135, May 20-21,2016.

[5] Pooja Hatwalne, Ameya Deshmukh, Tanmay Paliwal, Krupal Lambat, " Design and Implementation of Single Precision Floating Point Multiplier using VHDL on SPARTAN 3", International Journal of Latest Trends in Engineering and Technology, Vol.8, Issue 3, pp 263-269, May 2017.

[6] Sushma S Mahakalkar, Sanjay L Haridas, "Design of High Performance IEEE 754 Floating Point Multiplier Using Vedic Mathematics", IEEE International Conference on Computational Intelligence and Communication Networks, pp 985-988, 2014.

[7] Pratheeksha Rai, Shailendra Kumar, Prof. S H Saeed, "Design of Floating Point Multiplier Using Vedic Aphorisms", International Journal of Engineering Trends and Technology(IJETT), Vol.11, Number 3, pp 123-126, May 2014.

[8] Irine Padma B T, Suchitra K, " Pipelined Floating Point Multiplier Based on Vedic Multiplication Technique", International Journal of Innovative Research in Science, Engineering and Technology, Vol.3, Issue 5, pp 130-137, July 2014.

[9] Arish S, R K Sharma, " An Efficient Floating point Multiplier Design for High Speed Applications Using Karatsuba Algorithm and

Urdhva Triyagbhyam algorithm, IEEExplore, pp 303-308, July 2015.

[10] K Veeraraju, B Sujatha, "An Implementation of Single Precision Floating Point Vedic Multiplier Using Verilog", International Journal of Engineering Technology, Management and Applied Sciences, Vol.2, Issue 7, pp 128-134, December 2014.

[11] I V Vaibhav, K V Saicharan, B Sravanthi, D Srinivasulu, "VHDL Implementation of Floating Point Multiplier Using Vedic Mathematics", International Conference on Electrical, Electronics and Communications, pp 110-115, June 2014.

[12] Kusuma Keerti, "Design of High Performance Single Precision Floating Point Multiplier", ITSI Transaction on Electrical and Electronics Engineering(ITSI-TEEE), Vol.2, Issue 1, pp 36-40, 2014.

[13] Ajay A Raut, Dr. Pravin. K. Dahole, "Floating Point Multiplier for DSP Using Vertically and Crosswise Algorithm", IETE 46th Mid Term Symposium "Impact of Technology on Sill Development", International Journal of Electronics, Communication & Soft Computing Science and Engineering, pp 267-271, 2015.

[14] Shweta Agrawal , Vijay Kumar Magraiya, Abhay Khedkar "Implementation of Vedic Multiplier on Circuit Level", International Journal of Advanced Engineering Research and Science (IJAERS), Volume 1- No.6, pp 53-55, 2014.

A Comparision Analyis Of 2x1 Series Feed Array Antenna for Satellite Applications

[1] Devi Perla, [2]Rajya Lakshmi Valluri, [3]Harish Chunduri, [4] T.D.V.Gayathri
[1][2][3][4] Department of Electronics and Communication Engineering, ANITS, India

***Abstract*:-- This paper presents 2x1 series feed array antenna for satellite applications (8.1GHz-8.35GHz). Initially 2x1 series feed antenna is designed based on specifications, but this design didn't applicable for satellite applications. In order to applicable for desired frequency, slots are placed in the design. Various slots (I slot, Inverted U Slot and Plus Slot) are used to get desired specifications. Finally the designed antenna got better results for plus shaped slotted antenna which is resonating at 8.32GHz frequency with a return loss of -26.83dB, VSWR of 1.09 and gain of 7.27dB.This antenna is applicable for satellite applications.**

Index Terms: Array antenna; Series feed method; slotted design; Return loss; VSWR

INTRODUCTION

The antenna plays a key role in communication systems because based on the antenna performance only signal transmission depends. Now-a-days most of the modern communication system requires high gain, low cost, simple structure, low profile, compact size antennas. The microstrip antennas satisfies such requirement because it has low profileed., low cost. But the limitations of microstrip patch antenna are narrow frequency band, low gain.

In order to increase the gain and bandwidth of microstrip patch antenna, instead of one radiating element , two or more elements are used. All these radiating elements are internally connected and transmits signal in the desired direction. These antennas are called Microstrip patch array antennas. Based on then requirement, radiating elements can be placed in planar,linear or in circular manner. There are three different feeding methods such as series feed, corporate feed, corporate series feed method [1].

There are two ways to design array antenna. They are changing the feed position or placing slots on structure. In [2] a 2x2 array antenna used circular ring shaped slot on antenna elements in order to get broad band and circular polarization operation. In [3] a 4x1 square microstrip patch antenna is designed for wire less applications using series feed. In [4] series feed and parallel methods are used for designing array antenna for C-band applications. Gain enhancement antenna is described in [5], compared slot performance with a regular antenna structure. In [6], the patch array antenna performance interns of radiation pattern is improved by using taper structure. In [7] symmetric and asymmetric feed arrays are designed for radar applications and their performance is compared.

The Proposed 2x1 series feed array antenna is designed for satellite applications. A rectangular and slotted antennas are designed and their performance compared. The antenna is designed by using HFSS software.

ANTENNA DESIGN:

The 2x1 array antenna using series feed is designed in HFSS software is shown in Fig.1.The antenna structure consists of three layers i.e ground plane, substrate and patch elements. The FR4 substrate is used with dielectric constant of 4.4. The dimensions of the 2x1 series feed array antenna is shown in table.1.

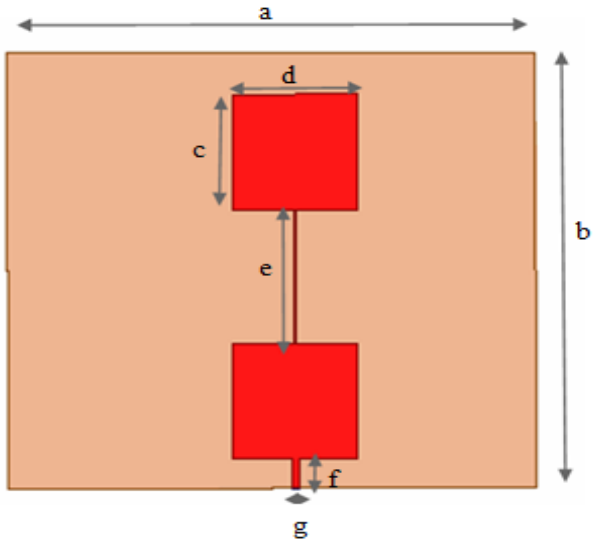

Fig.1:2x1 series feed array antenna

This 2x1 series feed antenna is resonating at a frequency of 8.46GHz with a return loss of -22.34dB and VSWR of 1.13 and gain of 7.3dB. The return loss plot is shown in Fig.2 and VSWR plot is shown in Fig.3.

Table.1: Dimensions of Series feed antenna

Parameter	Description	Value

A	Substrate width	34mm
B	Substrate length	30mm
C	Patch length	8mm
D	Patch width	8mm
E	Patch to Patch Distance	9.14mm
F	Feed line length	2mm
G	Feed line width	0.5mm

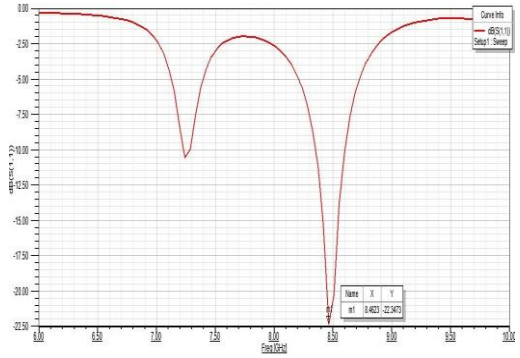

Fig.2: Return loss plot of 2x1 series feed

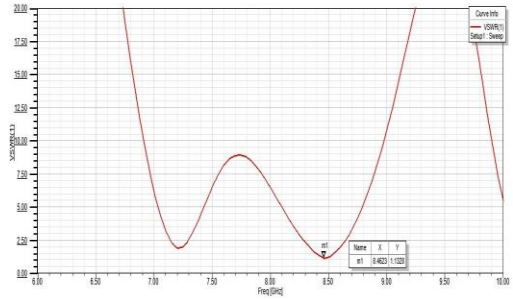

Fig.3: VSWR plot of 2x1 series feed

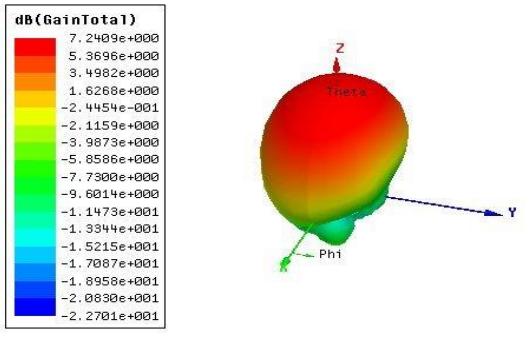

Fig:4. 3D gain plot of 2x1 series feed antenna

The proposed series feed antenna is not resonating in a desired frequency range. In order to resonate the design in specified frequency range (8.1GHz - 8.32GHz), different slots are placed in the array elements. The antenna is simulated for three different slots i.e I shape, inverted u and plus shaped slot.The Fig.5.shows slotted 2x1 series feed antenna.4

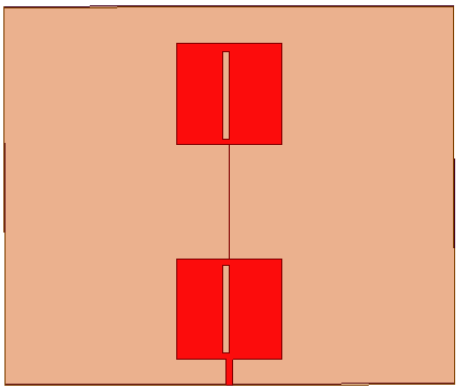

(a) I shaped slotted 2x1 series feed design

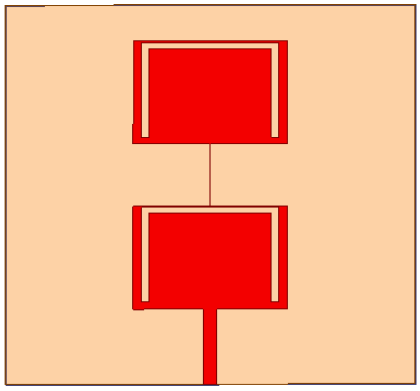

(b) Inverted U shaped slotted 2x1 series feed design

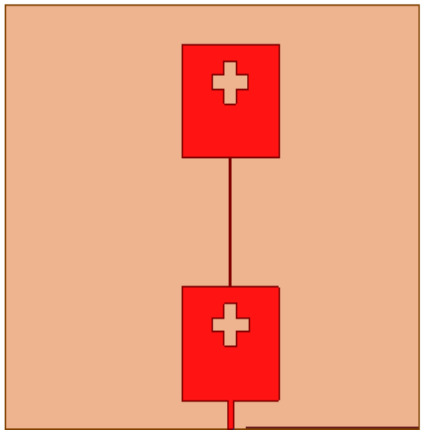

(C) Plus shaped slotted 2x1 series feed design

Fig.5: Slotted 2x1 array antenna designs

Initially, I shaped slot is placed in the antenna structure (shown in Fig.5(a)). In this case, the design is resonating at a frequency of 8.46GHz with a return loss of -22.85dB, VSWR of 1.15 and gain of 7.2dB. In this case also, the design is not resonating) in desired frequency range. So, Inverted U shaped slot and Plus shaped slots are placed on structure.

The inverted U shaped slotted 2x1 series feed antenna is shown in Fig.5(b), this design is resonating at a frequency of 9.42GHz with a return loss of -26.26dB, VSWR of 1.1and gain of 5.2 dB.
The Plus shaped slotted 2x1 series feed antenna is shown in Fig.5(c). This design is resonating at frequency of 8.32GHz with a return loss of -27.49dB, VSWR of 1.08 and gain of 7.27dB.
The Plus shaped slotted 2x1 series feed antenna is shown in Fig.5(c). This design is resonating at frequency of 8.32GHz with a return loss of -26.83dB, VSWR of 1.09 and gain of 7.27dB.

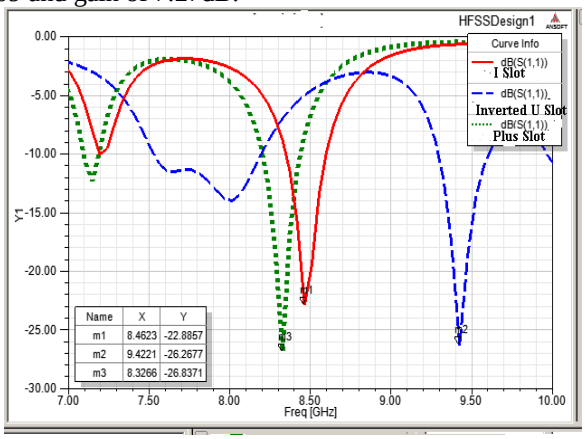

Fig.6. Return loss plot of slotted antennas

The Fig.6 shows the combined return loss plot of I, inverted U and Plus shaped designs and combined VSWR plots of slotted designs are shown in Fig.7.

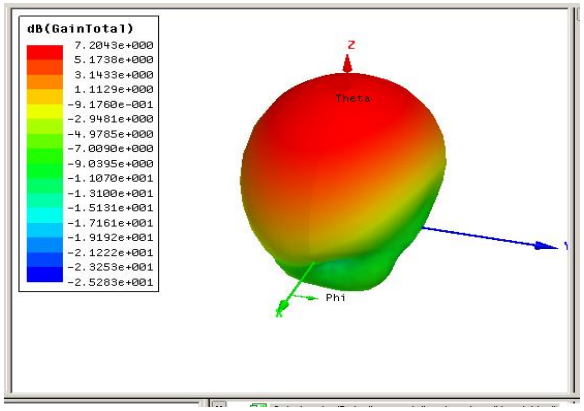

Fig.7. VSWR plot of slotted antennas

The Fig.8 (a) shows the gain plot of I slotted 2x1 series feed antenna and Fig.8(b) and (c) shows the gain plots of Inverted U and + shaped slotted antennas respectively

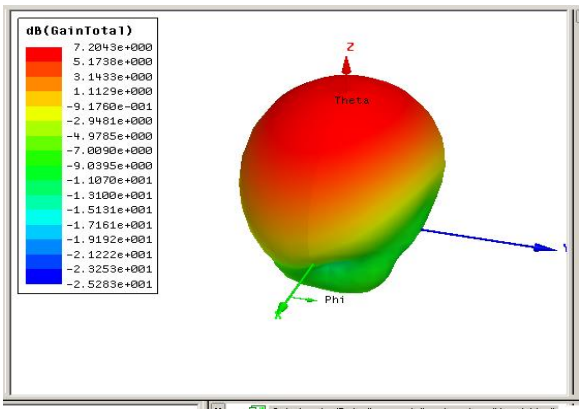

(a) I slot

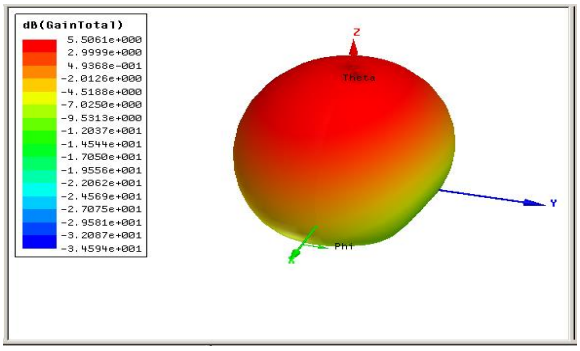

(b) Inverted U slot

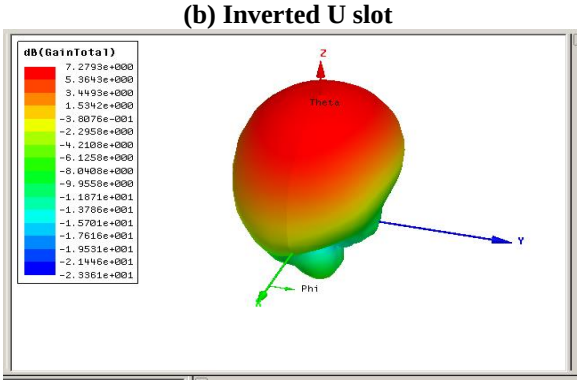

(c)Plus slot

Fig.8. 3D gain plots of slotted 2x1 series feed array antenna

The comparison results of slotted antennas are shown in Table.2. From these results, the 2x1 "I and inverted U" slotted designs are resonating at 8.46GHz and 9.42GHz.These designs are not suitable for satellite applications (8.1-8.35GHz). The Plus shaped slotted 2x1 design is resonating at 8.32GHz frequency. This antenna is suitable for satellite applications.

Table.2: Summary of results

Slot/ Paramet	Frequen-cy	Return Loss	VSWR	Gain

er				
I Slot	8.46GHz	-22.88 dB	1.15	7.2dB
Inverted U Slot	9.42GHz	-26.26 dB	1.1	5.2dB
+ Slot	8.32GHz	-26.83 dB	1.09	7.27 dB

CONCLUSION:

2x1 series feed antennas are designed and compared. The plus shaped slotted 2x1 series feed antenna is suitable for satellite application when compared to other designs. The + slot antenna is resonating at 8.32GHs with better return loss i.e -26.83dB and gain 7.27dB values. All antennas are suitable for X-band applications.

REFERENCES:

[1] Md. Tanvir Ishtaique-ul Huque1, Md. Kamal Hosain2, Md. Shihabul Islam3, and Md. Al-Amin Chowdhury," Design and Performance Analysis of Microstrip Array Antennas with Optimum Parameters for X-band Applications", IJACSA) International Journal of Advanced Computer Science and Applications, Vol. 2,Issue no. 4, 2011

[2] Tuan-Yung Han ,"Series-Fed Microstrip Array Antenna with Circular Polarization" International Journal of Antennas and Propagation, Volume 2012, Article ID 681431.

[3] Ashish Kumar, ridhi guptha. "Series microstrip patch antenna array for wireless communication", International Journal of Engineering Research & Technology (IJERT),Vol2, Issue3, March 2013.

[4] Kuldeep Kumar Singh, Dr. S.C. Gupta ,"Design and Simulation of Microstrip patch array antenna for C Band Application at IMT (4400-4900 MHz) advanced spectrum with Series feed and parallel feed", International Journal of Scientific & Engineering Research, Volume 4, Issue 12, December-2013

[5] M. Sathish*, V. Vignesh, S. Sivasubramanian and G. Vijaya Sripada ."Design, Analysis and Gain Enhancement of a Series-Feed Microstrip Patch Antenna Array for Wireless Applications", Journal of Chemical and Pharmaceutical Sciences JCHPS Special Issue 8: June 2017.

[6] Ragib Khan, D.C. Dubkariya, "Design of Series Feed Microstrip Antenna Array for Low Side Lobe Level", International Journal of Electronics & Communication Technology IJECT Vol. 6, Issue 3, July - Sept 2015.

[7] Ninu Sathianathan, Dr. Lethakumary B, Jobins ,"Asymmetric Series Feed Radar Antenna", IOSR Journal of Electronics and Communication Engineering (IOSR-JECE) e-ISSN: 2278-2834,p-ISSN: 2278-8735PP 72-78

Gas Turbine Blade Cooling of Flow Analysis by Using CFD

[1] Ramana Murthy Bagadi, [2]Grace SudeerKiran Ch,[3] IHari Babu
[1][2][3]Assistant Professor, Mechanical Engineering, Chaitanya Engineering College, Visakhapatnam

Abstract:-- **Gas Turbines are planned to persistently and productively produce valuable control from fuel vitality and are created into exceptionally dependable tall execution motors. Presently days in gas turbine the turbine edge worked at temperature limits 1550-2000 ˚c and gas turbine edges have been put to utilize in different areas like, control plants, marine businesses as well as for mechanical impetus. For tall warm proficiency progressed gas turbines utilize tall temperature at the passage of the turbine. Subsequently, for the reason of expanding warm effectiveness of the turbines, it is basic to plan compelling cooling plans. The current Turbine Chanel Temperature in progressed gas turbines is much higher than the dissolving point of the edge fabric. As a result a shifted run of cooling procedures are utilized to cool the edge to preserve typical operation of the turbine.**

An endeavor has been made to computationally analyze the impacts of one sort of cooling framework, i.e by utilizingholes (6) on the edgepivotally, wherein the cooling impacts of discussstream through a punctured turbine edgeentry has been mimicked utilizing ANSYS- FLUENT(CFD Fluent). The mass stream rates of discuss through the section were shifted to watch the variety of cooling impacts with mass stream rate and comes about were compared. The temperature contours of the Edge for diverse mass stream rates were watched. The patterns of diverse parameters like warmexchange,speed conveyance, weightconveyancewere famous. It wasamous that by keeping apertures on the edges surface increments the warm exchange rate and produces cooling impact than characteristic edge without apertures and increments the life of edges and hence gives higherWarm effectiveness and control output

Index Terms: Computational fluid dynamics (CFD), staggered holes, Heat transfer rate, CAD, Turbulent-Intensity model.

INTRODUCTION

Gas Turbine Basics: There are three fundamental parts of a gas turbine, to be specific: the compressor, the combustor and the turbine. The work of then attempt has been made to computationally analyze the impacts of one sort of cooling framework, i.e by utilizingapertures (6) on the edgepivotally, wherein the cooling impacts of discussstream through a punctured turbine edgeentry has been recreatedutilizing ANSYS- FLUENT(CFD Fluent). The mass stream rates of discuss through the section were shifted to watch the variety of cooling impacts with mass stream rate and comes about were compared. The temperature forms of the edge for distinctive mass stream rates were watched. The patterns of distinctive parameters like warm exchange, speed dissemination, weight dissemination were famous. It was famous that by keeping apertures on the edges surface increments the warm exchange rate and produces cooling impact than normal edge without apertures and increments the life of edges and hence gives higher warm proficiency and control yield

Confinements on Turbine Channel Temperature:

Due to the nature of its working, the control produced by a turbine increments with expanding the temperature at which the gas enters, called the turbine gulf temperature. An expanded control yield comes about in a better proficiency. In any case, the turbine channel temperature cannot be expanded self-assertively since of the limits forced due to the temperature at which the edge fabric soften

Require for cooling: As the edge fabric dissolves at a lower temperature than the working conditions of the turbine, a cooling strategy must be joined into the edge plan to guarantee the secure and smooth running of the turbine. It is critical, whereas concocting a cooling conspire, to have information approximately the boundary conditions of the edge amid turbine operation, so that expansive angles can be maintained a strategic distance from, Turbulent-Intensity demonstrate.

Turbine cooling basics: In spite of the fact that cooling is vital, it influences the gas turbine operation inadvertently:

1. The cooling air supplied to the blades and vanes is directly bled from the compressor. As a result the mass of air going into the combustor is decreased.
2. In order to incorporate the various structures like fins, cooling passages etc. The trailing edge thickness of the

blades must be increased which adversely affects the aerodynamic performance of the blades
Various parts of the turbine blade are cooled using various techniques. The front part, called the leading edge, is generally cooled by impingement cooling. The middle part is generally cooled by using snake-like passages endowed with ribs along with local film cooling. The back part, called the trailing edge, is generally cooled by impingement and film cooling.

Types of cooling:
There are two wide categories of cooling utilized in gas turbine blades:1. Internal Cooling 2.ExternalCooling In inside cooling, the cool compressed discuss streams inside inside the sections of the turbine edge and in this way warm exchange happens between the cold discuss within the entry and the adjoining hot surface of the blade. In outside cooling, the cool compressed discuss is catapulted from gaps on the surface of the edge or the vane and makes a lean film between the environment and the edge surface in this way anticipating contact between the hot air and the edge surface, enhancing warm exchange utilized for the cooling of the turbine edges for their long life. Edges of gas turbine can be cooled either inside or remotely.

LITERATURE REVIEW

K HariBrahmaiah – Examine the heat transfer analysis of gas turbine with four different models consisting of blade with and without holes and blades with varying number of holes (5,9,& 13) were analyzed. Transfer rate and temperature distribution, the blade with 13 holes is considered as optimum. Steady state thermal and structural analysis is carried out using ANSYS software with different blade materials of Chromium steel and Inconel-718. While comparing these materials Inconel-718 is better thermal properties and induced stresses are lesser than the Chromium steel.

R.D.V. Prasad- Examine steady state thermal & structural performances for N155 & Inconel-718 nickel Chromium alloys. Using finite element analysis four different models consisting of solid blade and blades with varying number of holes (5,9,& 13) were analyzed of cooling holes. The analysis is carried out using ANSYS software package. While comparing materials, it is found that Inconel-718 is better suited for high temperature the graphs drawn for temperature distribution, von-misses stresses and deflection, the blade with 13 holes is considered as optimum, the induced stresses are minimum and the temperature of the blade is close to the required value of 800 degrees Celsius.

GEOMETRY

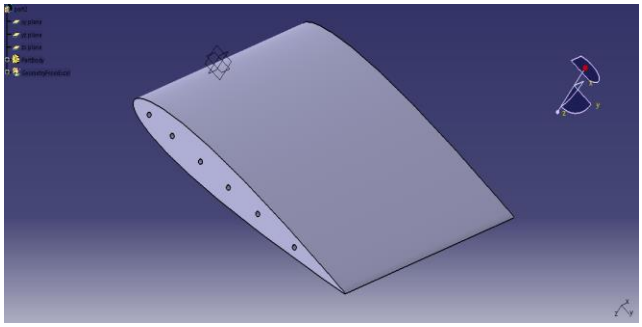

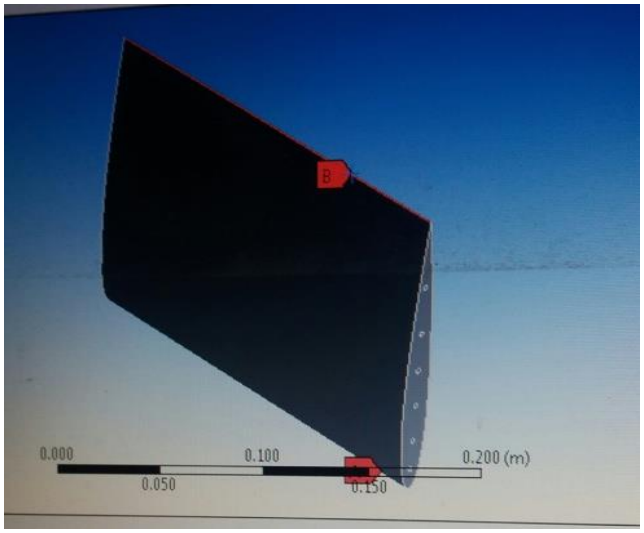

Geometry of turbine blade in catia v5

Chord	=	130mm
Length of extrusion	=	200mm
Thickness	=	100mm
Pitch of the blade	=	5.625deg
No of points	=	130

150240, No of nodes =166911

Setup
Boundary conditions: The boundary conditions utilized were as indicated. For the smooth channel as it were one mass stream rate of 0.01 kg/s was utilized in arrange to compare with the ribbed channel
Mass flow rate (m): 0.01 kg/s Convection Heat Transfer Coefficient (h) at outer surface of blade: 1000 W/m2-K Free-stream temperature of the surroundings (Tfree): 1700KTemperature of the air at the inlet(Tinlet): 300 K
Aerofoil shape design points:

X(mm)	Y(mm)	Z(mm)
129.3901	-12.5792	0
129.3156	-12.5612	0
129.0923	-12.5072	0
128.7206	-12.4174	0
128.2015	-12.2924	0
127.5361	-12.1327	0
126.726	-11.9391	0
125.7729	-11.7124	0
124.6791	-11.4537	0
123.447	-11.1643	0
122.0795	-10.8453	0
120.5797	-10.4981	0
118.951	-10.1243	0
117.1972	-9.72531	0
115.3223	-9.3028	0
113.3306	-8.85841	0
111.2268	-8.39389	0
109.0156	-7.91098	0
106.7021	-7.41148	0
104.2917	-6.89721	0
101.79	-6.37007	0
99.20268	-5.83195	0
96.53577	-5.28479	0
93.79543	-4.73059	0
90.98797	-4.17137	0
88.11988	-3.60922	0
85.19777	-3.04625	0
82.2284	-2.48464	0
79.21859	-1.92663	0
76.1753	-1.37449	0
73.10549	-0.83054	0
70.01629	-0.29713	0
66.91475	0.223343	0
63.80801	0.728487	0
60.70322	1.215896	0
57.6075	1.683183	0
54.52794	2.128003	0
51.47163	2.548053	0
48.44558	2.941112	0
45.45674	3.305087	0
42.51198	3.637979	0
39.61806	3.937949	0
36.78166	4.203333	0
34.00932	4.432663	0
31.30744	4.624657	0
28.68225	4.77828	0
26.13987	4.892724	0
23.6862	4.967394	0
21.32695	5.001974	0
19.06761	4.996369	0
16.91349	4.950696	0
14.86965	4.865318	0
12.94088	4.740757	0
11.13174	4.577765	0
9.446503	4.377188	0
7.889144	4.140046	0
6.463358	3.867399	0
5.17254	3.560414	0
4.019729	3.220255	0
3.007667	2.848089	0
2.138737	2.445041	0
1.414978	2.012175	0
0.838091	1.550462	0

Solution

SOLUTION

Sort of solver- Pressurebased. Physical show- Turbulent (k-e), vitality Equation Material property- Property of liquid such asair. Boundary condition- Weight, speed channel, speed outlet walletc. Solution strategy- Choosing the arrangement strategy such as energy condition, turbulent vitality equationetc. Solution initialization- Initialize the arrangement to urge the starting arrangement of theproblem. Run arrangement- Run the arrangement by giving no of cycle for arrangement ResultsAndConclusion

Turbine edge is carried out with differing models comprising of hub changing number of cooling gaps concurring to CFD examination of gas turbine edge:

• As we increases the no of holes the edge driving edge temperature will diminishes.

• Temperature will slightest for edge driving edge at 5 crevices bored

. • Normal edge temperature decreases by 3.98% when no of pivotalgapsshifted from 5 to 6.

• Warm trade coefficient of hot gas will increases with growing no of gaps.

• Within the greatest ebb and stream of the edge profile the temperature scattering is nearly uniform.

• Within the edge segment the temperature is directlydiminishing from tip to the root

. • Warm trade rate increases by 14.96% when no of gapsshifted from converge. In arrange to have a comprehensive understanding of the stream and to compare diverse stream scenarios, the results of the recreation have been displayed completely different groups. A number of drift charts were moreover drawn to appear the variety over the edge volume

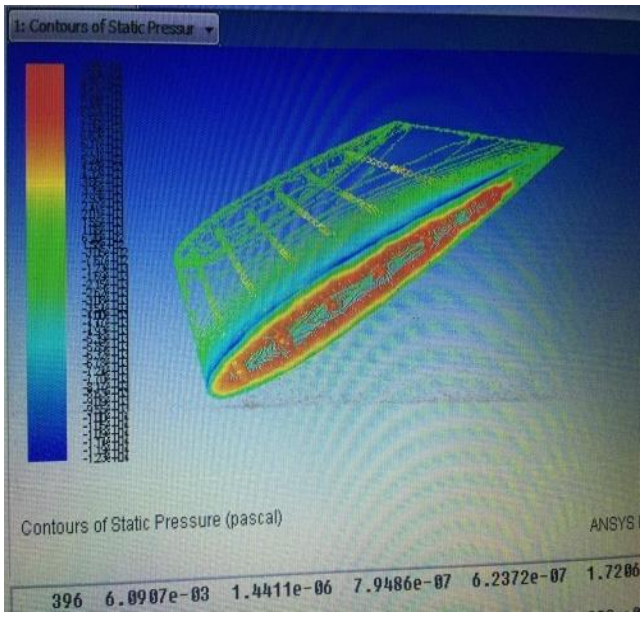

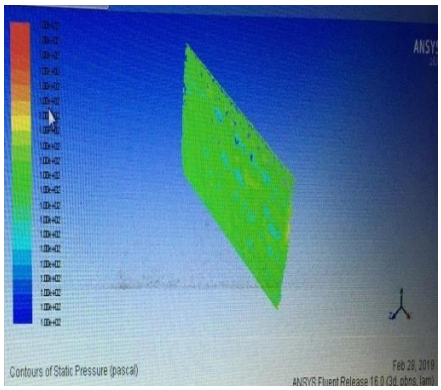

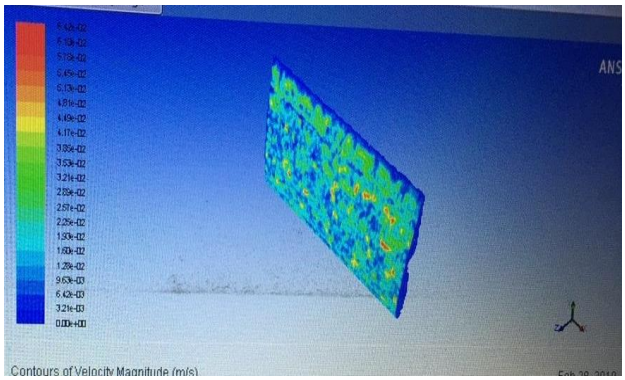

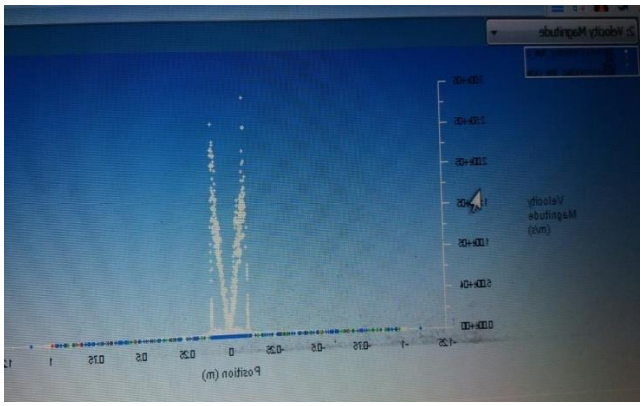

REFERENCES

1. Gupta, S., Chaube, A., &Verma, P. (2011). Survey on Warm Exchange Increase Methods: Application in Gas Turbine Edge Inner cooling .Universal Diary on Later Patterns in Designing & Technology,5(4).

2. Han, J. C., "Heat Transfer and Friction in Channels with Two Opposite Rib- Roughened Walls", ASME Journal of Heat Transfer,Vol. 106, Nov., pp 774-784, 1984

3. Han, J.C. and Park, J. S., "Developing heat transfer in rectangular channels with rib turbulators." Int. Journal of Heat and Mass Transfer, Vol. 31, No. 1, 183-195,1988.

Y.M. Zhang, W.Z. Gu, and J.C. Han, "Heat Transfer and Friction in Rectangular Channels With Ribbed or Ribbed-Grooved Walls," J. of Heat Transfer, 116, no.1:58- 65, 1994

4. Liou, T. M., Chang, Y. and Huang, D. W., , "Experimental and Computational Consider of Turbulent Streams in a Channel with Two Sets of Turbulence Promotersin Tandem", Diary of Turbomachinery, Vol. 112, pp 302-310, 1990.

5. Taslim, M. E., Li, T. and Kercher, D. M., "Experimental Warm Exchange and Grinding in Channels Roughed with Calculated, V-Shaped,and Discrete Ribs on TwoOpposite Walls", J. of Turbomachinery,Vol. 118, pp 20-28, 1996. 6. S. Acharya, V. Eliades and D.E. Nikitopoulos, "Heat Exchange Improvements in Pivoting Two-Pass Coolant Channels with Profiled Ribs: Portion 1 – Normal Results," ASME Paper No. 2000-GT-0227,2000

7. Johnson, B. V., Wagner, J. H., Steuber, G. D., &Yeh, F. C. (1994). Warm exchange in turning serpentine entries with chosen show introductions for smooth or skewed trip dividers. Diary of turbomachinery, 116(4),738-744.

8. Wright, L. M., Fu, W. L., & Han, J. C. (2004, January). Warm execution of calculated, V-shaped, and W-shaped rib turbulators in turning rectangular cooling channels (AR= 4: 1). In ASME Turbo Expo 2004: Control for Arrive, Ocean, and Air(pp. 885-894). American Society of MechanicalEngineers.

9. AlokChaube, P.K. Sahoo, S.C. Solanki , "Analysis of warm exchange augof Renewable vitality, 31, 317–331,2006.

Adaptive Gain Equalizer with Nonlinear Spectral Subtraction

[1] Raju Egala,[2] V Pavani, [3]P Saroja,[4]T Durga Prasad
[1][2][3] Assistant Professor, Department of ECE, Chaitanya Engineering College, Visakhapatnam, INDIA.
[4] Assistant Professor, Department of ECE, GITAM University, Visakhapatnam, INDIA.

Abstract:-- **In many application of noise cancellation, the adjustments in signal characteristics may want to be pretty fast. This needs the usage of adaptive algorithms, which has rapid converges. Due to computational simplicity and easy implementation Least Mean Squares (LMS) and Normalized Least Mean Squares (NLMS) Adaptive filters have been used in numerous signal processing applications. The Recursive Least Squares (RLS) algorithm has achieved itself as the "ultimate" adaptive filtering algorithm by exhibiting the excellent convergence behavior. Unfortunately, sensible implementations of the algorithm are regularly related with excessive computational complexity and/or poor numerical properties. The adaptive filtering was presented recently, have a good balance between complexity and the convergence speed. So let me describe a new technique to noise reduction in speech enhancement the use of fast affine projection (FAP) algorithm. This is adaptive filtering algorithm is new algorithm used to attenuating noise in speech indicators and also to superior noise reduction method for sturdy speech focus by the use of Adaptive Gain Equalizer with Nonlinear Spectral Subtraction methods we may achieve it.**

INTRODUCTION

An early and crucial technique for noise reduction was once to use the concept of the optimum wiener filter .There are two most regularly used algorithms for noise cancellation are normalized least mean squares (NLMS) and recursive least squares (RLS) algorithms. NLMS algorithm has low computational complexity among these two. On the contrary, the weakest factor of RLS algorithm is its excessive computational complexity in remedy it offers fast adaptation rate. The preference of the adaptive algorithm to be utilized is always a tradeoff between fast convergence and computational complexity. Due to the property of convergence of the FAP algorithm is most efficient then LMS, NLMS, and affine projection (AP) algorithms and same to that of the RLS algorithm. In this algorithm, one of the filter coefficient is updated one or greater at each time instant to achieve appropriate tradeoff between computational complexity and convergences rate. The proposed algorithm performance is studied through the energy conservation analysis used in adaptive filters and the general expressions for the steady-state mean rectangular error and transient overall performance evaluation have been derived in. we can say through this paper FAP algorithm is good in noise cancellation for speech enhancement. The results are evaluated with classical adaptive filter algorithm such as LMS, NLMS, AP and RLS algorithms. Simulation outcomes show the exact overall performance of the two algorithms. In the following we find additionally the highest quality parameter which is used in these algorithms. Today, an often used digital method for wonderful noise reduction for Robust Speech Recognition in speech conversation is spectral subtraction. This frequency area approach is based totally on Fast Fourier Transform and is a nonlinear, but straight ahead way of decreasing undesirable broadband noise acoustically added to the signal.

TABLE I. NOTATIONS

Symbol	Description
$\|.\|$	Norm of a scalar
$\|\|.\|\|^2$	Squared Euclidean norm of a vector
$(.)^T$	Transpose of a vector or a matrix
$(.)^{-1}$	Inverse of a scalar or a matrix
$<.,.>$	Inner Product of two vectors

II. BACKGROUND

In Fig. 1, we show the prototypical adaptive filter setup, where x(n),d(n) and e(n) are the input, the desired and the output error signals, respectively. The vector h(n) is the Mx1 column vector of filter coefficient at time , in such a way that the output of signal, y(n) , is proper estimate of the desired signal, d(n).

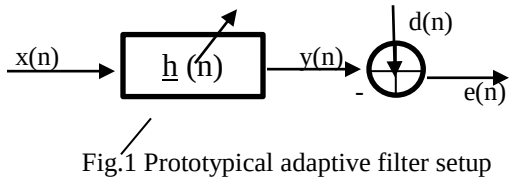

Fig.1 Prototypical adaptive filter setup

the filter vector update equation for the LMS algorithm is given by :

$$h(n+1)=h(n)+ Mx(n)e(n)$$

Where

$$\underline{x}(n) =[x(n),x(n-1)\ldots\ldots x(n-M+1)]^T$$

and is the step-size that determines the convergence speed and steady-state mean-square error (MSE). Also, the output error signal, is given by e(n)

$$e(n) =d(n)-\underline{h}^T(n)\,\underline{x}(n)\text{---------}1$$

To boost the convergence speed of the LMS algorithm, the NLMS and AP algorithms was proposed which can be stated as

$$\underline{h}(n+1) = \underline{h}(n) + \mu X^T(n)(\varepsilon I + X(n)X^T(n))^{-1}[\underline{d}(n) - X(n)\underline{h}(n)] \quad \text{--------}2$$

Where

$$X(n)= =[\underline{x}(n),\underline{x}(n-1)\ldots\ldots\underline{x}(n-K+1)]^T$$

And

$$\underline{d}(n) =[d(n),d(n-1)\ldots\ldots d(n-K+1)]^T$$

The update filter vector equation in RLS algorithm is:

$$\underline{h}(n+1)=\underline{h}(n)+C^{-1}(n)\underline{x}(n)e(n)\text{----------}3$$

C(n)=estimation of the autocorrelation matrix.

This is given by

$$C(n)= \sum_{i=0}^{n} \lambda^{n-i}\,\underline{x}(i)\underline{x}^T(i)\text{---------}4$$

where.

$0<<\lambda<1$

III. FAPA ALGORITHM

A Notation and problem description

With reference to Figure 1, the error signal, , e(n)can be expressed as:

$$e(n)=d(n)-\sum_{k=0}^{M-1} h_k(n)x(n-k)\text{----------}5$$

Considering the samples n-L+1,n-L+2…..n, where we focus on the situation where L>M, Eq.1 can be written as

(1) $\underline{e}(n)=\underline{d}(n)-X(n)\underline{h}(n)$

(2) $X(n)=[\underline{x}_o(n),\underline{x}_1(n)\ldots\ldots \underline{X}_{M-1}(n)]$

and columns furthermore defined through

$\underline{x}_j(n)=[x(n-j),x(n-j-1)\ldots.x(n-j-L+1)]^1$

The vector of desired samples are given by

$\underline{d}(n)=[d(n),d(n-1)\ldots\ldots.d(n-L+1)]^T$

and e(n) is defined similarly. The problem of adaptive filtering. Now formulated as venture of finding the update for h(n) , at each time instant *n* , such that the error is made as small as possible

Note that X(n)h(n) can be written as

$$X(n)h(n)= \sum_{k=0}^{M-1} h_k(n)x_k(n-k)\text{---------}6$$

i.e. as a weighted sum of the columns of X(n) with the elements of h(n) being the weighting factors. A greedy algorithm for successively constructing (better) approximations to a vector given the usage of linear mixtures of vectors from a given set is the BMP algorithm. Inspired by this algorithm, we devise a technique for recursively building an approximation to d(n) the use of linear combos of the columns of X(n) .

B. Algorithm development

Assuming that we have an approximation to d (n -1) at Time n-1 given through X(n -1) h (n-1) , the approximation error at time n is

$$e(n)= d(n)- X(n)h(n-1)\text{----------}8$$

In building a better approximation through the update of only one coefficient in h (n - 1), we would write the new error as

$$e_1(n)=\underline{d}(n)-(X(n)\underline{h}(n-1)+X(n)h(n))\text{---------}9$$

Note that j (n) is the index of the coefficient to be update in the zero'th P-iteration at time n , and u j is the M-vector with 1 in position j and 0 in all other positions. Intuitively, it would make feel to pick out j(n) as the index corresponding to that column of X(n) .The coefficient j(n) need to update. We pointed two methods to selecting j(n) : I) incrementing j(n) sequent through n Modulo M and II) deciding on j (n) in such a way as to Maximally reduce the residual of the corresponding update computation. Thus, in the FAPA, j(n) is determined as the index of the column of X(n) onto which e(n) has its most projection, -or in different phrases.

$$h_{j_0(n)}(n) = h_{j_0(n)}(n-1) + h_{j_0(n)}(n)\text{-----}10$$

where $h^{update}_{j_0(n)}(n)$ is the value of the projection of $\underline{e}_0(n)$ onto the unit vector with direction given by $\underline{x}_{j0(n)}(n)$,i.e.

$$h^{update}_{j_\circ(n)}(n) = \frac{<\underline{e}_\circ(n), \underline{x}_{j_\circ(n)}(n)>}{\left\|\underline{x}_{j_\circ(n)}(n)\right\|^2} \quad \text{-----11}$$

Thus,the zero'th P-iteration updates the filter vector as follows:

$$h^{(0)}(n)=\underline{h}(n-1)+h^{update}_{j_0(n)}(n)\underline{u}_{j_0(n)} \quad \text{----------12}$$

To have control on the convergence speed and stability of the algorithms, we introduce the step-size in the algorithm as following:

$$h^{(0)}(n)=\underline{h}(n-1)+\mu h^{update}_{j_0(n)}(n)\underline{u}_{j_0(n)} \quad \text{---------13}$$

Given this, the updated error expression can be written as

$e_1=d(n)-X(n)\,h^{(0)}(n)$----------14

If we choose do greater than one P-iteration at time n, the process described above beginning with finding the maximum projection of e (n) onto a column of X(n) can be repeated with $e_1(n)$ taking the position of e(n) This can be repeated as many instants as desired, say P times, leading to a sequence of coefficient updates:

$h_{j_0(n)}(n), h_{j_1(n)}(n) \ldots\ldots h_{j_{P-1}(n)}(n)$

Note that if P>2 it is completely possible that one specific coefficient is updated extra than as soon as at a given time n. The ensuing filter coefficient vector after P iterations at time n is denoted h(P -1)(n) , but where there is no chance of ambiguity we shall refer to this filter vector truly as h(n).

The technique discussed above is to making use the BMP algorithm to a dictionary of vectors given by means of the columns of X(n) for the purpose of constructing an approximation to d(n). The solely distinction is that we do this for each new time instant n while maintaining the results of the BMP from the previous time instant n -1 . It is observed that an almost equivalent, process to the one described above would result if we tried to find the least squares solution to the over determined set of equations (remember L >M):

X(n)h(n)= d(n)

In the given initial solution, say h (n), we permitted to adjust one vector element only.

$$j_\circ(n) = \arg\max_j \frac{1}{\left\|\underline{x}_j(n)\right\|}\left| <\underline{d}(n), \underline{x}_j(n)> - \sum_{k=\circ}^{M-1} h_k(n-1)<\underline{x}_k(n), \underline{x}_j(n)> \right|$$

and

$$h^{update}_{j_\circ(n)}(n) = \frac{1}{\left\|\underline{x}_{j_\circ(n)}(n)\right\|^2}\{<\underline{d}(n), \underline{x}_{j_\circ(n)}(n)> - \sum_{k=\circ}^{M-1} h_k(n-1)<\underline{x}_k(n), \underline{x}_{j_\circ(n)}(n)>\}$$

----------15 and 16

These are the pertinent equations if one coefficient update, i.e. one P-iteration is performed for each new signal sample. Note that having computed the terms of Eq. 15, very small additional work is involved in finding the update of Eq. 16. It is instructive to explicitly state these equations also for iteration no. i > 0 at time n :

$$j_i(n) = \arg\max_j \frac{1}{\left\|\underline{x}_j(n)\right\|}\left| <\underline{d}(n), \underline{x}_j(n)> - \sum_{k=\circ}^{M-1} h_k^{(i-1)}(n)<\underline{x}_k(n), \underline{x}_j(n)> \right|$$

and

$$h^{update}_{j_i(n)}(n) = \frac{1}{\left\|\underline{x}_{j_i(n)}(n)\right\|^2}\{<\underline{d}(n), \underline{x}_{j_i(n)}(n)> - \sum_{k=\circ}^{M-1} h_k^{(i-1)}(n)<\underline{x}_k(n), \underline{x}_{j_i(n)}(n)>\}$$

----------17 and 18

From these equations it is evident that some terms depend solely on n, i.e. they want to be computed once for each n and can consequence be used unchanged for all P-iterations at time n. Other terms depend on both n and the P-iteration index and ought to as a result be up to date for every P-iteration. Since, we must associate the update depending solely on n with generation no. 0, this is the computationally most costly update.

From the above section we can observe the prominent roles of inner products d(n),x(n) and x(n),xj(n) in computations. and these inner products are

$$\langle \underline{d}(n),\underline{x}_j(n)\rangle = \langle \underline{d}(n-1),\underline{x}_f(n-1)\rangle + d(n)x(n-j)-d(n-L)X(n-j-L)$$

and

$$\langle \underline{x}_k(n),\underline{x}_j(n)\rangle = \langle \underline{x}_k(n-1),\underline{x}_j(n-1)\rangle + x(n-k)x(n-j)-x(n-k-L)x(n-j-L)$$

We close this section by pointing out that efficient

Implementations of FEDS/FAP are available. With use of exponentially weighted and sliding window versions, implementations having a multiplicative complexity given by (5 +*P*) *M* can be devised. Multiplicative complexity of (3+ *P*) *M* are also possible by block exponentially weighted version.

IV. ADAPTIVE GAIN EQUALIZATION

The Adaptive Gain Equalization (AGE) approach for speech enhancement, introduced by Westerlund et al., [9] separates itself from the standard strategies of enhancing the SNR of a signal corrupted by using noise, via moving away from noise suppression and focusing in particular on speech boosting. Noise suppression traditionally, like spectral subtraction, appeared like subtracting an estimated noise bias from the signal corrupted with the aid of noise. Whereas speech boosting objectives to enhance the speech part of the signal with the aid of adding an estimate of the speech itself, for this reason boosting the speech part of the signal. The difference between noise suppression and speech boosting is introduced in Fig. 2(a) suggests a noise estimate being subtracted from a noise corrupted signal. While in Fig. 2. (b), an estimate of the speech signal is used to enhance the speech in the noise corrupted.

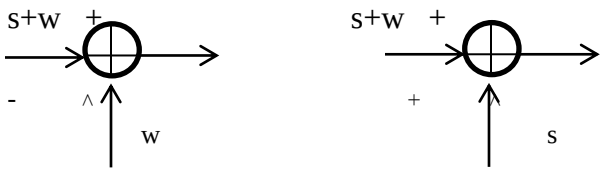

Noise Suppression Speech Boosting

Fig. 2 Difference between Noise Suppression and Speech Boosting.

V. CONCEPT OF ADAPTIVE GAIN EQUALIZATION

The concept of obtaining a speech bias estimate to perform speech boosting might also appear like a daunting task. But it does no longer need to be, the AGE technique of speech enhancement depends on a few primary ideas. The first of which is that a speech signal which is corrupted by using band limited noise can be divided into a range of subbands and every of these subbands can be individually and adaptively boosted in accordance to a SNR estimate in that particular subbands.

In each subband, a short term average is calculated simultaneously with an estimate of a slowly various noise flooring level. By the usage of the short term average and flooring estimate, a obtain feature is calculated per subband through dividing the short term average by the aid of the flooring estimate. This achieve function is increased with the corresponding signal in each subband to form an output per subband. The sum of the outputs from every subband forms the last output signal, which need to include a greater SNR when in contrast to the authentic noisy signal.

The proposed technique of the AGE acts as a speech booster, which is adaptively looking for a subband speech sign to boost. Fig.3 suggests this underlying notion in the back of the AGE. Outlining that speech energy is an exceedingly non stationary input amplitude excursion, if there is no such excursions no alteration to the subband will be performed, the AGE will remain idle, as a end result of the quotient between the short term magnitude average and the noise flooring estimate being unity, with them being about the same. If speech is current the short term magnitude average will change with the noise floor level approximately unchanged, therefore amplifying the

signal in the subband at hand due to the quotient becoming larger than unity.

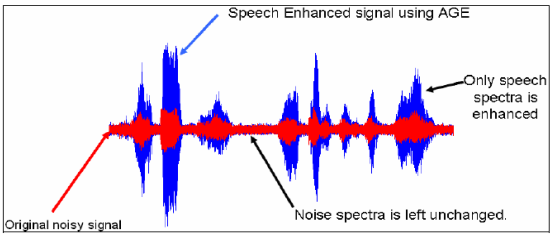

Fig. 3 Speech signal enhanced using AGE

VI. AN ILLUSTRATION OF THE ADAPTIVE GAIN EQUALIZER

The previous two section of the paper have outlined the fundamentals of the Adaptive Gain Equalizer is used in speech enhancement. To show the potential of using the AGE method a brief example will be demonstrated in this chapter. A speech signal which is corrupted by white noise is presented in Fig. 4.

The first step requires the signal to be filtered into number of subbands. In this example, number of subbands is chosen to be eight. The signal which is sampled at 16 KHz is filtered into eight subbands which are shown in the Fig. 5. From the Fig. 5, it is clear majority of speech is concentrated in first sub-

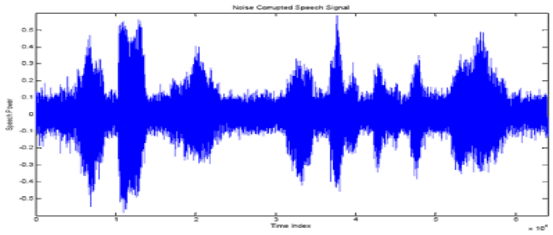

Fig. 4 Speech signal corrupted by white noise

bands, which is expected since human speech is generally assumed to be between 300 Hz and 3400 Hz and is expected to dominate in the subbands corresponding to this frequency range. Short term exponential magnitude average and noise floor is taken simultaneously and is shown in the Fig. 6. Using the short term exponential magnitude average and noise floor the gain is calculated, in this example the gain is limited to 5 dB and is displayed in Fig. 7. It is evident from Fig 7 that the AGE algorithm amplifies only the components of the signal which contain speech and remains idle when there is no speech component.

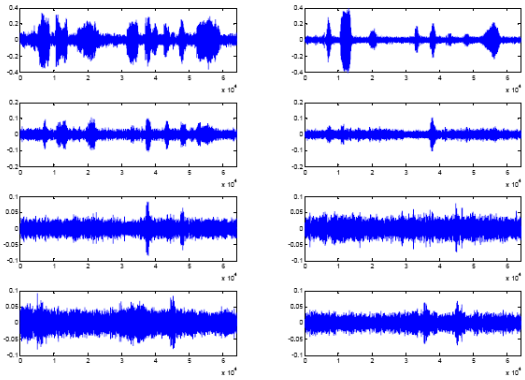

Fig.5 Speech signal corrupted by white noise and is filtered into eight subbands

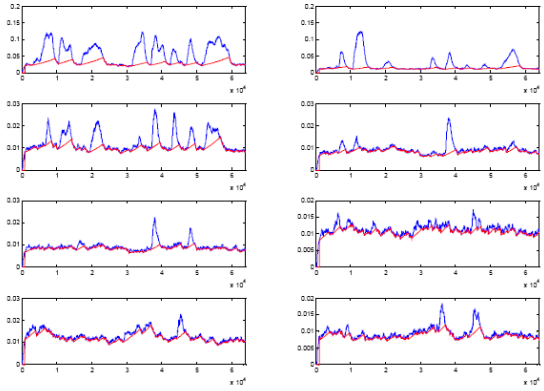

Fig. 6 Short term exponential magnitude average and noise floor per subband

The gain per subband is shown in Fig. 7 and is multiplied with its corresponding and then summed to form a speech enhanced signal and is shown in Fig. 8

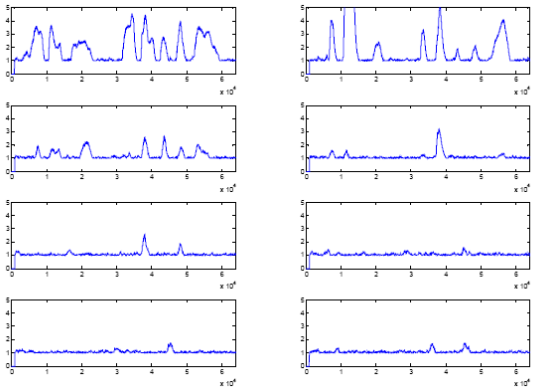

Fig. 7 Gain calculated per subband

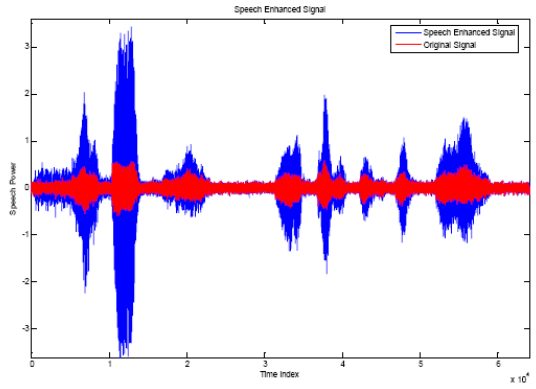

Fig. 8 Speech enhanced signal using 8 subbands.

VII. Nonlinear Spectral Subtraction

The basics of nonlinear spectral subtraction techniques (NSS) reside in the combination of two main ideas [10]:

• The noise-improvement model is used which is obtained in the course of a speech pause.

• The nonlinear subtraction is used when a frequency-dependent signal-to-noise ratio (SNR) is obtained. This means that in spectral subtraction a minimal subtraction factor is high SNR is used in turn.

VIII. Proposed Speech Enhancement Algorithm

AGE when coupled with Nonlinear Spectral Subtraction (AGE-NSS) performs better than AGE when SNR drops below -5db. The first step requires the signal to be filtered into number of subbands. In this paper, number of subbands is chosen to be eight. The signal which is sampled at 16 KHz is filtered into eight subbands. Nonlinear spectral subtraction is applied to each of the sub band. Short term exponential magnitude average and noise floor is taken simultaneously. Using the short term exponential magnitude average and noise floor the gain is calculated and it is multiplied with the spectra.

IX. Experimental Results

The order of the filter was once set to M=8. The parameter was once set to 0.002 in the LMS and 0.005 in the NLMS and AP algorithms. Fig. 4 shows the filtered output signal and the mean squared error (learning curve) in the LMS algorithm. The filtered signal SNR is calculated for this experiment. The SNR improvement (SNRI) is described as the original SNR subtracted from ultimate SNR. The SNRI in the LMS algorithm is 13.5905. Fig. 5, 6 indicates the effects for NLMS and AP algorithms. It is observed that the convergence speed in the NLMS and AP algorithms is faster than LMS algorithm. This reality can be observed in output of each filter and learning curve. For the NLMS and AP algorithms the SNRI are respectively 16.8679, 20.0307. In Figs. 7-8, we presented the results for FAP algorithm. The parameters was once set to L=25,P=8.

From result it is clear that FAP has faster convergence speed then LMS, NLMS and AP algorithms and comparable RLS algorithm.

TABLE II.SNR IMPROVEMENT IN DB

Algorithm	SNRI (db)
LMS	13.5905
NLMS	16.8679
APA	20.0307
FEDS	22.2623
FAPA	24.9078
RLS	29.7355

in the training phase, the uttered words are recorded the usage of 8-bit pulse code modulation (PCM) with a sampling rate of 8 KHz and saved as a wave file the usage of sound recorder software. The Automatic speech recognition systems work fairly properly under smooth stipulations but end up fragile in practical application involving real-world environments. Table shows the recognition performance achieved by the AGE and AGE-NSS were compared.

TABLE III. AVERAGE WORD ACCURACY

SNR in db	AGE	AGE-NSS	% of Improvement
5	41.5	50.75	18.23
0	35.5	41.25	13.94
-5	30.25	36.25	16.55
10	21.75	29.5	26.27
Average	32.25	39.4375	18.22

X. Conclusion

In this paper the adaptive noise cancellation set up imposed by FEDS and FAP algorithms. The results compared with the LMS, NLMS, AP and RLS algorithms, for attenuating noise in speech signals. From the simulation results it is observed that convergence rate of these algorithms is similar with the RLS algorithm. Also,

the most effective values of the FEDS and FAP algorithms were calculated by experiments. In these algorithms, the huge range of iterations to be performed at every new sample time is a user selected parameter giving rise to attractive and explicit tradeoffs between convergence/tracking properties and computational complexity.

We have proposed a method for combining the Adaptive Gain Equalizer method and Nonlinear Spectral Subtraction, so that improved speech recognition accuracy overall performance also obtained under these noise conditions. Comparative experimental outcomes are shown in the figure through Fig. 8. to Fig. 11 against AGE & AGE-NSS, the speech recognition accuracy for AGE-NSS performs better that AGE for all cases.

Results:

LMS algorithm:

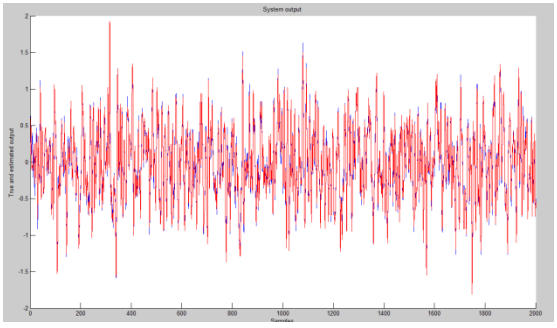

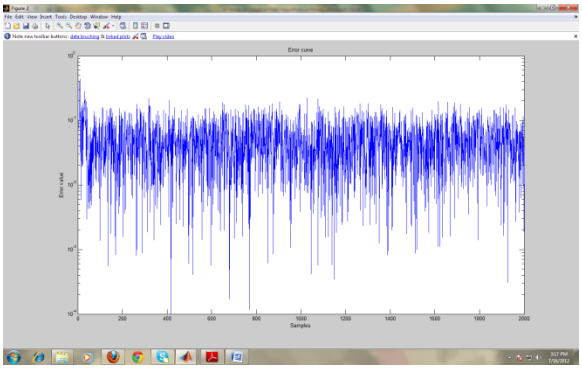

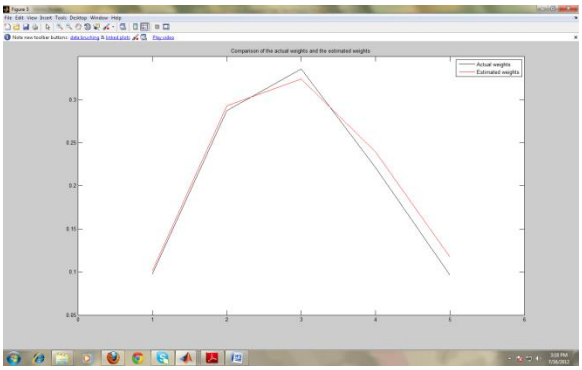

NLMS algorithm:

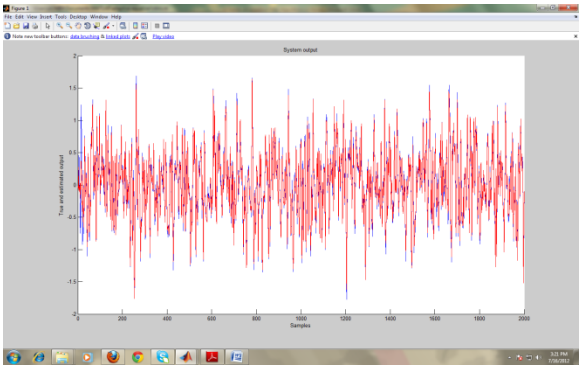

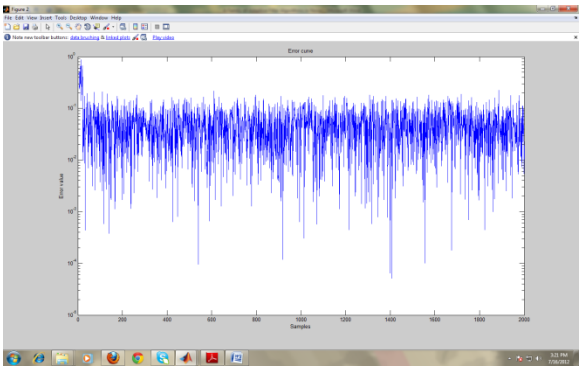

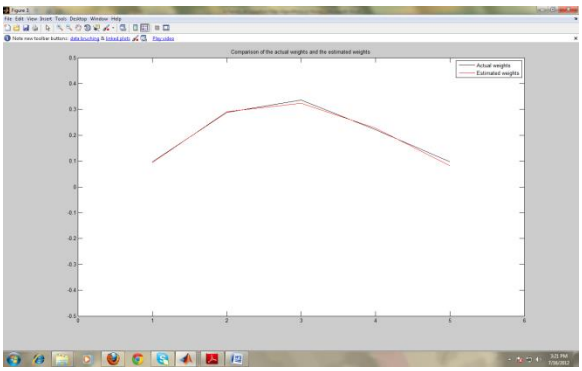

IIR-RLS algorithm:

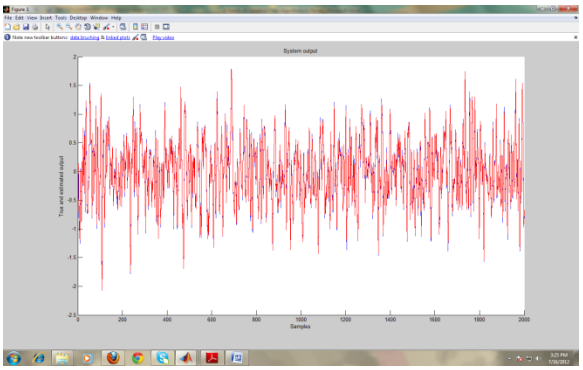
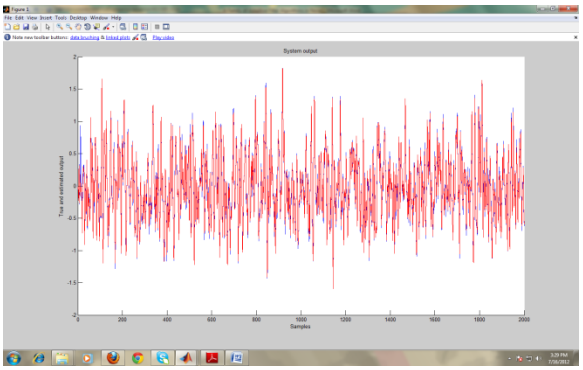
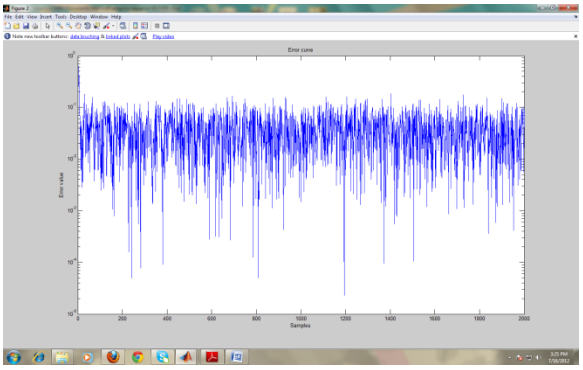
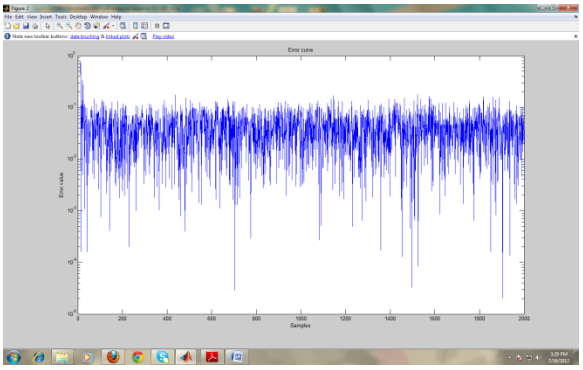
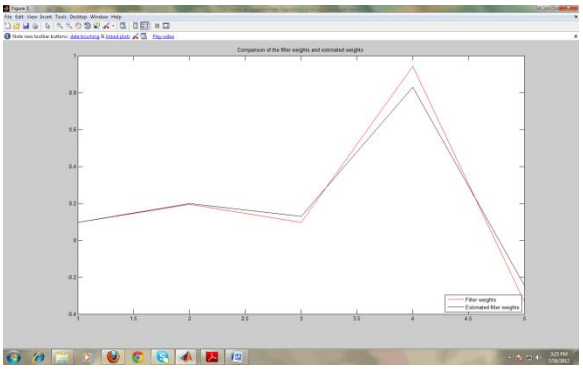
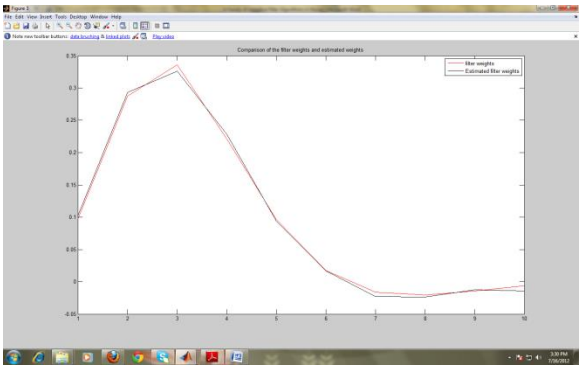
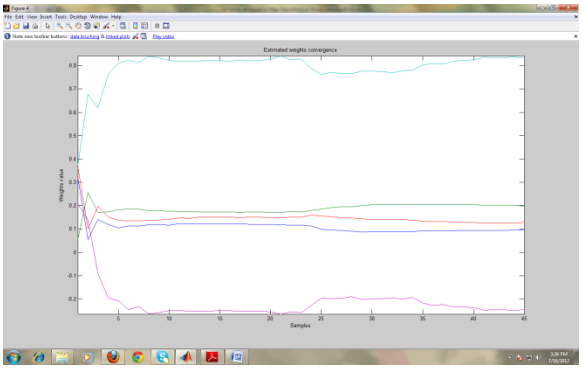
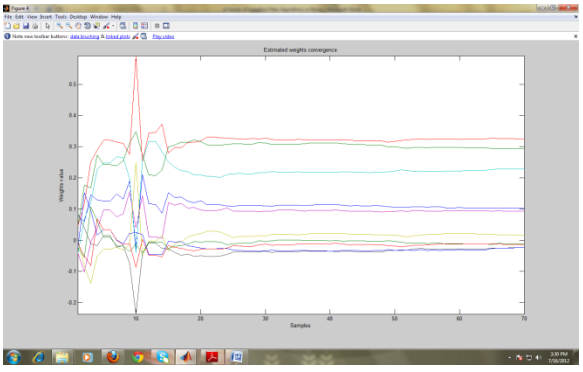

FIR-RLS algorithm:

Active Noise Control using the filtered-X LMS Algorithm

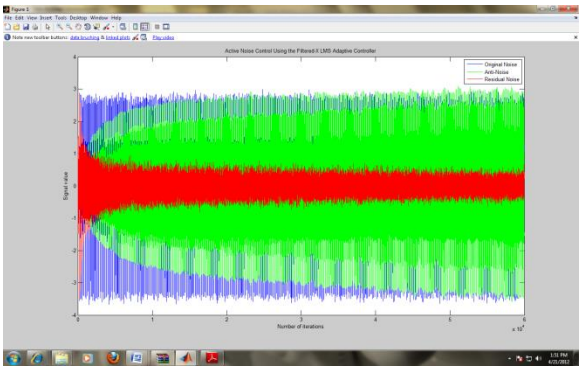

Adaptive Filters comparison

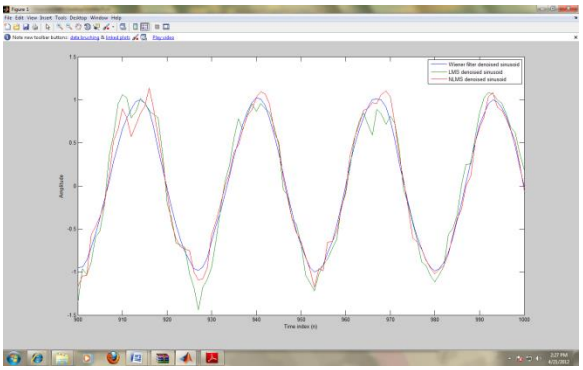

Kalman Recursive Least Squares Algorithm

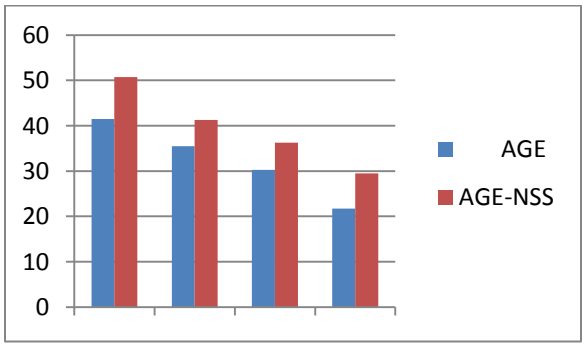

Fig. 8 Babble Noise added with speech signal

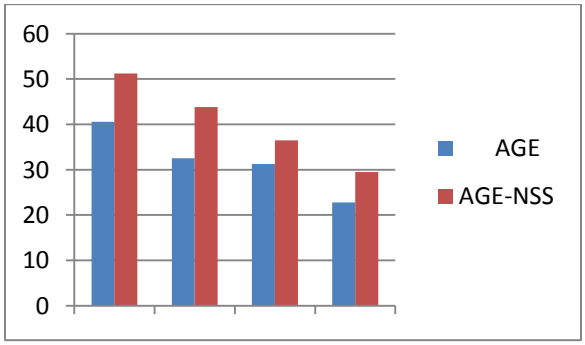

Fig. 9 Gun Noise added with speech signal

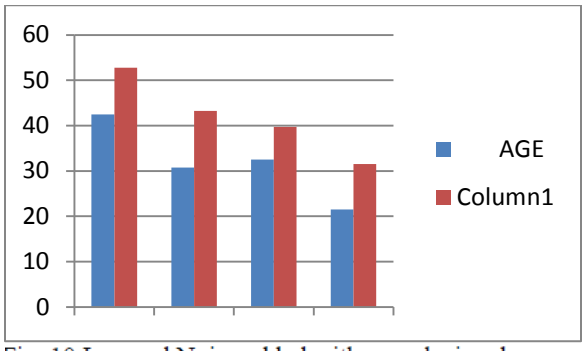

Fig. 10 Leopard Noise added with speech signal

REFERENCES

[1] W. Harrison, J. Lim, E. Singer, "A new application of adaptive noise cancellation," *IEEE Trans. Acoustic Speech Signal Processing*, vol.34, pp. 21-27, Jan 1986.

[2] B. Widrow, S. Steam, *Adaptive Signal Processing*. Englewood Cliffs, NJ: Prentice-Hall, 1985.

[3] G. Goodwin, k. Sin, *Adaptive Filtering Prediction and Control*. Englewood Cliffs, NJ: Prentice-Hall, 1985.

[4] J. R. Treichler, C. R. Johnson, M. G. Larimore, *Theory and Design of Adaptive Filters*, Wiley, 1987.

[5] S. I. A. Sugiyama, "An adaptive noise canceller with low signal distortion for speech codes" *IEEE Trans. Signal Processing*, vol. 47, pp. 665-674, Mar 1999.

[6] S. Haykin, *Adaptive Filter Theory*, 4 th ed, Prentice Hall, 2002.

[7] M. Honig, D, Messerschimitt, *Adaptive Filters: Structures, Algorithms and Applications*. Boston Kluwer Academic Publishers, 1984.

[8] F.Broujeny, *Adaptive Filters: Theory and Applications*, wiley, 2003.

[9] A. H. Sayed, *Fundamentals of Adaptive Filtering*, Wiley, 2003.

[10] P. S. R. Diniz, *Adaptive Filtering Algorithms and Practical Implementation*, 2 Editions, Kluwer, 2002.

[11] M. S. E. Abadi, J. H. Husøy, and A. M. Far, "Convergence analysis of two recently introduced adaptive filter algorithms (FEDS/RAMP)," *Iranian Journal of Electrical and Computer Engineering (IJECE)*, vol. 7, no. 1, winter-spring 2008.

[12] J. H. Husoy and M. S. E. Abadi, "Interpretation and convergence speed of two recently introduced adaptive filters (FEDS/RAMP)," in *Proc. Tencon, Chiang Mai, Thailand*, pp. 471-474, Nov 2004.

[13] M. S. E. Abadi and J. H. Husøy, "Channel equalization using recursive adaptive matching pursuit

algorithm," in *Proc. ICEE*, Zanjan, Iran, pp. 531-536, May 2005.
[14] J. H. Husoy and M. S. E. Abadi " A comparative study of some simplified RLS type algorithm" in *Proc. Intl. Symp on control, Communications and Signal Processing*, Hammamet, Tunisia, March 2004, pp. 705-708.
[15] M. S. E. Abadi, A. Mahloji Far, M. B. Menhaj, S. A. Hadei "A Fast Affine Projection Algorithm Based On Matching Pursuit with Partial Parameters Adjustment," *Amirkabir Journal of Science and Technology*. vol. 18. no. 67-A, 2008.
[16] H. C. Shin, A. H. Sayed "Transient behavior of affine projection algorithms" in *Proc. Int. Conf. Acoust. Speech, Signal Proc*, Hongkong, pp. 353-356, 2003.
[17] H. C. Shin, A. H. Sayed "Mean square performance of a family of affine projection algorithms" *IEEE Trans. Signal Processing*, vol. 52, pp. 90-102, 2004.
[18] J. H. Husoy, M. S. E. Abadi "Transient analysis of adaptive filters using a general framework" *Automatika, Journal for control, Mesurement, Electronics, computing and Communications*, vol. 45, pp. 121-127, 2004.
[19] T. Bose and G. F. Xu, "The Euclidean direction search algorithm in adaptive filtering" *IEICE Trans. Fundamentals*, vol. E85-A, no. 3, pp. 532-539, Mar. 2002.
[20] http://www.owlnet.rice.edu/~ryanking/elec431
[21] M.H. Hayes, Statistical Digital Signal Processing and Modelling, Wiley, 1996.
[22] B.Widrow and S.D. Stearns, Adaptive Signal Processing, New Jersey, Prentice-Hall, 1985.
[23] S. Haykin, Adaptive Filter Theory, New Jersey, Prentice-Hall, 1996.
[24] S.F.Boll, "Suppression of acoustic nose in speech using spectral subtraction", IEEE Trans. Acoust. Speech and Sig. Proc., vol. ASSP 27, pp. 113-120, April 1979.
[25] J.R. D. Jr., J.G.Proakis, and J.H.L Hansen, Discrete time processing of speech signals. Macmillan Publishing Company, 1993.
[26] Y.Kaneda and J.Ohga, "Adaptive microphone-array system for noise reduction", IEEE Trans. Acoust. Speech and Sig. Proc., vol.ASSP 34,no 6, pp. 1391-1400, December 1986.
[27] M.Dahl and I.Claesson, "Acoustic noise and echo canceling with microphone array", IEEE Trans. On Vehicular Technology, Vol.48, no.5, pp. 1518-1526, September 1999.
[28] B.D.Veen and K.M Buckley, "Beamforming: A versatile approach to spatial filtering", IEEE ASSP Magazine, 1988
[29] N. Westerland, M. Dahl., and I.Classeon, "Speech Enhancement Using An Adaptive gain Equalizer", in Proceedings of DSPCS, December 2003.
[30] J.Poruba, "Speech enhancement based on nonlinear spectral subtraction", Proceedings of the Fourth IEEE International Conference on Devices, Circuits and Systems, pp T031-1 - T031-4 April 2002.

Congestion Management Considering Economic and Efficient Generation Rescheduling

[1] N. Srilatha, [2]B. Priyanka Rathod, [3]G. Yesuratnam
[1][2][3] Osmania University, Hyderabad

Abstract:-- **Increasing interconnections and usage of power networks makes the system to work at almost full loading capacities. Any type of disturbance in such scenario results in congestion of the existing network. This condition, if not managed within required time may result in system collapse. This paper presents a simple and economic transmission line overload alleviation method that is very much required in day-to-day operation and control of power systems. This method of managing the congestion aims primarily at improving the voltage stability of the system while relieving the overload and does this economically to the possible extent. Relative Electrical Distances (RED) between the loads and generators is the criterion for relieving the overload in a transmission line, by rescheduling the generation. The process of rescheduling is done economically by making use of fuzzy logic considering the incremental fuel costs of the generators. This method is illustrated using IEEE 39-node New England system and a real-life system, 75-node North Indian power system**

Index Terms—Congestion management, Generation rescheduling, Voltage stability, Fuzzy Logic

INTRODUCTION

Congestion management is an important technical challenge in power system operation. The electric power market background makes the operation of system further complicated. The congestion management problem can be devised as the emerging problem that needs to be concentrated much in order to supply power to the consumers in most reliable manner. The economical operation of power system is also of much concern during this process.

Addressing of various power flow control issues is made more complex and difficult than ever before because of competition and leads to several techno economical disputes. Several algorithms based on conventional optimization techniques are reported in the literature [1-4] in this regard. When congestion occurs in a deregulated power system, generation has to be rescheduled to ensure system security. Zheng and Chowdhury [1] and Lobato et al. [2] have described optimization methods to analyze and solve the transmission overloads.

B.K. Panigrahi and V. Ravikumar Pandi [3] proposed a new optimization approach, to solve the congestion management using bacterial foraging (BF) optimization technique. The multi objective framework to minimize both generation cost and line overload index is given by Sinha A.K. et al. [4]. However, these conventional optimization techniques are generally time-consuming from a computation point of view, especially for large systems. Hence, these methods are not suitable for improving the system security under emergency operating conditions.

For on-line applications, there is a need for tools which can quickly detect potentially dangerous situations of congestion in transmission lines and voltage instability problems in order to provide guidance to the operators to steer the system away from cascade tripping and a possible voltage collapse. Hence, efforts to improve the speed and ability to handle stressed power systems have led to the development of artificial intelligent techniques like Fuzzy logic and Expert systems [5, 6], which may be appropriate for assisting dispatchers in Energy Control Centre. By using Operational Load Flow, Bansilal D. Thukaram and K. Parthasarathy [5] presented an expert system for alleviation of network over loads using phase shifting transformers and generation rescheduling. A. N. Udupa et al. [6] presented a fuzzy control approach for alleviation of network overloads using Generation Shift Sensitivity Factor (GSSF). These methods are well suited for vertically integrated power systems. Kothari et al. [7] presented reviews on congestion management issues in the deregulated electricity markets. Under emergency conditions the operator has to make quick decisions, with little concern for the theoretical optimality of the operating point. In this context, an efficient and simplified approach has been proposed based on RED concept in [8]. However, economics of generators is not considered here.

Congestion management is one of the major tasks performed by system operators (SOs) to ensure the operation of transmission system within operating limits. Generation rescheduling is one of the mostly used methods for the same purpose, it being simple and non-expensive.

This paper proposes congestion management technique utilizing RED concept and incremental fuel cost of rescheduling generators using Fuzzy logic. This results in minimum number of generators for rescheduling and less cost involved in the rescheduling process.

The scheme of work in the paper is organized as follows. The basis of generation rescheduling, Relative Electrical Distances (RED) concept is explained in section II. The task of congestion management is illustrated using three different approaches: I, II & III here. Management of congestion by rescheduling generation is implemented using only RED based method in Approach-I. Economics of rescheduling is not considered in this approach. In Approach-II, the economics of rescheduling the generators is considered by making use of their incremental fuel costs alone. So the effect of rescheduling only economically, neglecting the desirable proportions, is dealt in this approach. Approach-III, the proposed method, deals with rescheduling process using fuzzy logic, which considers both incremental fuel cost and desired proportion of generations, D_{LG}, as suggested by RED method. A comparison of all three approaches is presented for the considered test systems.

BASIS FOR GENERATION RESCHEDULING - RED

Consider a system where n is the total number of buses with 1,2,……g; g is the number of generator buses, and g+1,……n are remaining (n-g) buses.

For a given system we can write,

$$\begin{bmatrix} I_G \\ I_L \end{bmatrix} = \begin{bmatrix} Y_{GG} & Y_{GL} \\ Y_{LG} & Y_{LL} \end{bmatrix} \begin{bmatrix} V_G \\ V_L \end{bmatrix}$$

(1)

Where, I_G, I_L, and V_G, V_L represent complex current and voltage vectors at the generator nodes and load nodes. $[Y_{GG}]$, $[Y_{GL}]$, $[Y_{LL}]$, $[Y_{LG}]$ are corresponding partitioned portions of network Y-bus matrix. Rearranging (1) we get

$$\begin{bmatrix} V_L \\ I_G \end{bmatrix} = \begin{bmatrix} Z_{LL} & F_{LG} \\ K_{GL} & Y_{GG} \end{bmatrix} \begin{bmatrix} I_L \\ V_G \end{bmatrix}$$

(2)

Where, $F_{LG} = - [Y_{LL}] -1 [Y_{LG}]$.

The elements of $[F_{LG}]$ matrix are complex and its columns correspond to the generator bus numbers and rows correspond to the load bus numbers. Relative Electrical Distance (RED) is the relative location of load nodes with respect to generator nodes, and is obtained from $[F_{LG}]$ matrix.

$$[R_{LG}] = [A] - abs\{[F_{LG}]\}$$

(3)

Where, [A] is the matrix with (n-g) number of rows and g number of columns, with all elements equal to 1.

The desired proportions of generators for desired load sharing is also obtained from $[F_{LG}]$ matrix, and is given by

$$[D_{LG}] = abs\{[F_{LG}]\}$$

(4)

$[D_{LG}]$ matrix gives the information, for each load bus, about the amount of power that should be taken from each generator under normal and network contingencies, as far as the system performance is considered with respect to the voltage profiles, bus angles and voltage stability L-index. This matrix is used as the basis for the desired generation scheduling. If each consumer takes the power from each generator according to the $[D_{LG}]$ matrix the system will have minimum transmission loss, minimum angle separation between generator buses and minimum L-indices.

The methodology used for relieving congestion in case of any contingency can be explained as follows. For a particular operating condition, Congested transmission lines (over loaded lines) are identified and the contribution of each generator to the congested line is estimated [9]. Among all the generators, those which are contributing to the congested line(generators that have a share in the flow of overloaded line) are identified as Generation Decrease group (GD group).This is the group where generation decrease is recommended to relieve the overloaded line ;And the generators which are not contributing to the congested line (generators that do not have a share in the flow of overloaded line) are categorized under Generation Increase group (GI group). This is the group where generation increase is recommended.

At any instant of time, total generation change in GD group must be same as the total generation change in the GI group. The amount of generation change required to relieve the congestion of the mostly congested line is estimated. Then the total amount of required capacity change is shared by the generators of the GD group in proportion to the margins available on these generators. Here, the margins of the generators of GD group are estimated based on D_{LG} matrix. The same amount of generation change is to be met from the generators of GI group to avoid load shedding.

ECONOMIC GENERATION RESCHEDULING USING FUZZY LOGIC (PROPOSED APPROACH)

Generation rescheduling in this method is done economically using Incremental fuel costs and efficiently using D_{LG} values of RED method. Fuzzy Logic is used to obtain an optimal scheduling value, utilizing both the above-mentioned methods. Instead of selecting all the

generators of GI group for rescheduling, Fuzzy Inference System (FIS) helps in selecting only few generators, thereby, the time involved in changing the settings of generators is reduced in case of an emergency situation. The method is explained as follows.

Since these congestion management studies are first performed offline, all the contingencies are simulated at varying load conditions and the probable schedules of the generators are calculated beforehand, so that they might be of use under emergency operating conditions. If in any case, the then operating condition of system does not match with the conditions available offline, then algorithm may be followed.

Algorithm for proposed Approach

Step 1: The solution of the load flows of the system, or the status obtained from the state estimator gives the picture of the system regarding voltages and power flows. If any transmission line is overloaded, proceed to the next step, otherwise stop.

Step 2: Based on RED concept, form the F_{LG} and D_{LG} matrices. The elements of D_{LG} matrix corresponding to the overloaded line give the estimate of desired generation from all the generators. The line with highest overload is considered in case of multiple line overloads.

Step 3: Find the contribution of each generator towards this highly overloaded line.

Step 4: Split up the generators into two groups, GD group consisting of generators which actually contribute to the overloaded line, and GI group consisting of non-contributing generators.

Step 5: Estimate the margin available on each contributing generator using D_{LG} matrix.

Step 6: Estimate the required generation decrease ΔP^- to relieve the congestion using the actual contributions of generators in the congested line.

Step 7: The total power ΔP^- of all generators of GD group together constitute the rescheduling amount of power

Step 8: For distribution of the rescheduling amount of power among GI group of generators, D_{LG} coefficients and incremental fuel costs of generators of this group are given as inputs to the Fuzzy Inference System (FIS).

Step 9: These generators are assigned a priority by the FIS, based on which the rescheduling power is allotted. Generator with highest priority is first assigned additional power depending on the margin available on it.

Step 10: The remaining power is allotted to generator with next priority considering its margin. This results in allotting the reschedule amount of power to few generators only.

Step 11: After distributing total ΔP among few GI group generators, perform the operational load flow and check if congestion is relieved. If congestion still persists on the overloaded line or other lines, go back to step 2.

Fuzzy Inference System (FIS)

Fuzzy inference is the process of formulating the mapping from a given input to an output using fuzzy logic. The mapping then provides a basis from which decisions can be made, or patterns discerned. As the present approach concentrates both on RED concept and incremental fuel cost, both these factors are considered as inputs for FIS in order to reschedule the power generation among the non-contributing generators to the congested line.

The inputs required for the FIS are

1. Elements of D_{LG} matrix
2. Incremental fuel costs of the generators

Elements of D_{LG} matrix, referred to as D_{LG} coefficients of the generators indicate the Relative Electrical Distance of the generator with respect to the overloaded line, and hence provide an index of how much power it can contribute so that the system parameters like real power loss and voltage stability indices are improved. FIS is designed such that the order of rescheduling of generators is decided by a combination of D_{LG} coefficient of a generator and its incremental fuel cost. Hence, the output variable of FIS is priority of the generator; this priority is set to be high for a generator whose D_{LG} coefficient is high and incremental fuel cost is reasonably low. The priority of a generator ranges from 0 to 1, where 0 indicates the lowest priority and 1 indicates highest. The amount of power to be re-allotted to a particular generator will depend on its priority and the margin available on it to accommodate any additional generation (considering the reactive limits also). Thereby, only some generators of GI group are selected for rescheduling process and the remaining generators are left without disturbing their generation. As a result, the number of generators of GI group to be rescheduled is reduced and also the additional time and cost incurred for overload relieving is also reduced.

Membership Functions and Rule Base of FIS

First input variable, D_{LG} coefficient is categorized into five membership functions namely, Very Low Contribution (VLCn); Low Contribution (LCn); Medium Contribution (MCn); High Contribution (HCn) and Very High Contribution (VHCn). Similarly, the other input variable, Incremental fuel cost is also categorized into five membership functions namely, Very Low Cost (VL); Low Cost (L); Medium Cost (M); High Cost (H) and Very High Cost (VH). Similarly, Output of the FIS, Priority of the generator also consists of five membership functions, namely, Very Less Priority (P5); Less Priority (P4);

Medium Priority (P3); High Priority (H2) and Very High Priority (P1). All the membership functions, as shown in Fig.1 are considered to be triangular in nature in order to have an even distribution of variables throughout the range.

A fuzzy rule base is developed to select the generators to be rescheduled on a priority-based order as given in Table I. These rules can be explained as follows. P1 through P5 are the priorities assigned to the generators, where, P1 corresponds to highest priority with value of 1; and P5 corresponds to least priority with a value of 0.

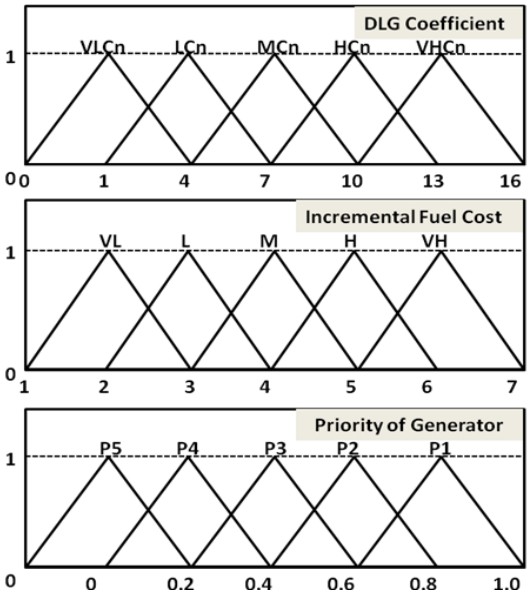

Fig.1. Membership functions of input and output variables

Fuzzy rules are similar to the general {If (..),then (..)} rules. One of the rules can be explained as follows.

"If D_{LG} coefficient of a generator is VHCn, and the Incremental Fuel cost is VL, then priority assigned is P1."

Similarly, 25 rules are framed in the proposed approach. The two inputs of FIS are combined using 'and' clause.

Table I. Fuzzy rule base

	Incremental Fuel cost					
D_{LG} Coefficient		**VL**	**L**	**M**	**H**	**VH**
	VLCn	P4	P4	P4	P5	P5
	LCn	P3	P3	P4	P4	P5
	MCn	P2	P2	P3	P4	P4
	HCn	P1	P2	P2	P3	P4
	VHCn	P1	P1	P2	P3	P4

CASE STUDIES

RED based congestion management method has been illustrated on IEEE 39-node New England System. The IEEE 39-node system is a simplified representation of the 345kV transmission system in the New England region having 10 generators and 29 load nodes as shown in Fig. 2.

The congestion in the system is simulated through a line outage which results in overloading of a nearby transmission line. This overload in the line is first relieved using Approach-I. For IEEE 39-node New England system, an example is illustrated to explain the congestion management procedure. As a consequence of line L10-13outage, the line L5-6 is overloaded, the flow being 726.1 MVA (flow limit is 500 MVA). From the contributions [10], it has been observed that flow in this overloaded line is actually contributed by generators G31 and G32 with percentages 55.8 and 44.2 respectively. Hence these two generators belong to GD group and remaining eight generators belong to GI group. Actual contributions of all the generators to the congested line as per D_{LG} matrix based on RED concept are indicated in Table II.

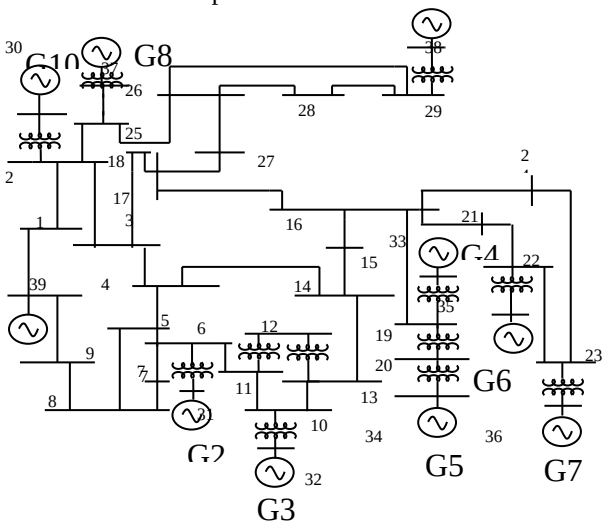

Fig 2. IEEE 39-node system

Margin available at G31 is (36.7-55.8) = -19.1%

Margin available at G32 is (29.1-44.2) = -15.1%.

The amount of generation decrease recommended at these two generators is in proportion to their margins. By changing the generation at G31, 128.3 MVA can be relived and at G32, 99.0 MVA in the overloaded line can be relived.

Amount of generation decrease suggested at

G31 is $\Delta P31- = 128.3/0.558 = 230.0$ MW.

G32 is $\Delta P32- = 99.0/0.442 = 224.0$ MW.

The total Generation decrease for the GD group is (230+224) =454 MW.

Generators in GI group are allotted with rescheduling power in the ratio of their D_{LG} values.

The Generation rescheduling is as follows:

ΔP30+=71 MW ΔP33+=47 MW ΔP34+=21 MW

ΔP35+=49 MW ΔP36+=27 MW ΔP37+=42 MW

ΔP38+=26 MW ΔP39+=173 MW

ΔP31-= 230 MW ΔP32-= 224 MW

The generation to be rescheduled is as follows in the case of Approach-II, where only incremental fuel costs of the generator are considered.

ΔP36+ = 140 MW ΔP39+ = 200 MW ΔP30+ = 114MW

ΔP31- = 230MW ΔP32- = 224MW

Table II. D_{LG} values of the overloaded line

G30	G31	G32	G33	G34	G35	G36	G37	G38	G39
6.5	**36.7**	**29.1**	**4.3**	**1.9**	**4.5**	**2.5**	**3.8**	**2.4**	**15.9**

In the proposed approach, priority of each generator is estimated as indicated in Table III from the output of the FIS. Based on the priority values, all the generators of GI group are ranked. The output of the FIS is the priority of the generators in the GI group ranging from 0 to 1, where 0 indicates the lowest priority and 1 indicates the highest.

The amount of generation decrease suggested at GD group generators (G31 and G32) is 230 MW and 224 MW respectively. Hence, the total amount of power to be rescheduled is 454 MW. All this power is to be allotted to the generators of GI group. Out of all the generators of GI group, G39 has the highest priority and the margin available on this generator is 200 MW. Out of 454 MW, 200 MW is allotted to G39. The generator of next highest priority is G30. Since the margin available is 250 MW, of the remaining power 250 MW is allotted to G30. Since some amount of power has to be allotted yet, the generator with next priority, G36 is allotted 4 MW. So with this proposed fuzzy logic approach the new generation scheduling is as follows

ΔP31- = 230 MW, ΔP32- = 224 MW

ΔP39+ = 200MW, ΔP30+ = 250 MW, ΔP36+ = 4MW

Table III. Priorities of GI group generators of IEEE 39-node system

GI group Generators	Priority (obtained using FIS)	Rank of Generator (Based on Priority)
G30	0.44	2
G33	0.228	4
G34	0.087	8
G35	0.196	6
G36	0.300	3
G37	0.199	5
G38	0.170	7
G39	0.700	1

Table IV. Performance parameters of IEEE 39-node system

System Performance parameter	Pre-Rescheduling Flow	Rescheduling based on RED (Approach-I)	Rescheduling based on Economy (Approach-II)	Rescheduling based on FLC (Approach-III)
Flow in congested line 5-6 (MVA)	726.1 (145%)	443.1 (89%)	443.9 (89%)	442.3 (88%)
Ploss (MW)	46.33	49.99	46.64	43.66
Vmin (pu)	0.982	0.982	0.982	0.982
Max (Li)	0.1108	0.1040	0.1038	0.1049
Σ L2	0.1457	0.1411	0.1404	0.1402
ve	0.0305	0.0295	0.0296	0.0311
No.of generators rescheduled	--	10	5	5
Cost of Rescheduling of GI group generators ($/h)	--	54.87	20.18	20.70

From the above Table, it is clear that generation rescheduling in all the three approaches leads to relieving congestion of the overloaded line. These results indicate that the voltage stability improvement is much better with first approach, however this approach is not acceptable as it is expensive. The second approach that is aimed at economic rescheduling of generators results in less cost of rescheduling as the number of generators considered has been reduced. The proposed Fuzzy logic-based approach provides the more optimal solution, the power losses are least, voltage stability improvement is observed and the cost of rescheduling is also almost as minimum as possible, similar to second approach.

From this analysis, it is obvious that the number of generator settings to be adjusted is reduced and the cost involved in doing so is also decreased inherently. The proposed approach not only improves the system security but also reduces the rescheduling cost of the generators of the GI group. Hence, this approach is most appropriate one for implementing in Energy Control Centre during emergencies.

The above results obtained from the proposed approach

are compared with the results in Reference [8]. The outage of line 4-14 is considered to observe the rescheduling effect of mitigating congestion in the line 5-6. The results [9] of comparison are listed in Table V. It can be observed that the main objective of reducing the congestion in the overloaded line is achieved along with the added advantage of reduced number of generators adjustment for rescheduling and reduced cost of rescheduling.

Table V. Comparison results of proposed approach with Reference [8]

Parameter	Reference [8]	Proposed Approach
Flow in line 5-6 after rescheduling	511.8 MVA (102.4%)	494.6 MVA (99%)
Number of Generators for rescheduling	10	4
Cost of Rescheduling	39.46 $/MWhr	11.40 $/MWhr
Power loss	58.0 MW	54.6 MW
Σ L^2	0.7259	0.7246
Ve	0.0331	0.0339

Similar analysis is also summarized for a real 75-node North Indian power system. 75-node Indian power system corresponds to Uttar Pradesh State Electricity Board (UPSEB) system, shown in Fig.3. It has 15 generators, 60 load points and 98 transmission lines (including 24 transformers).

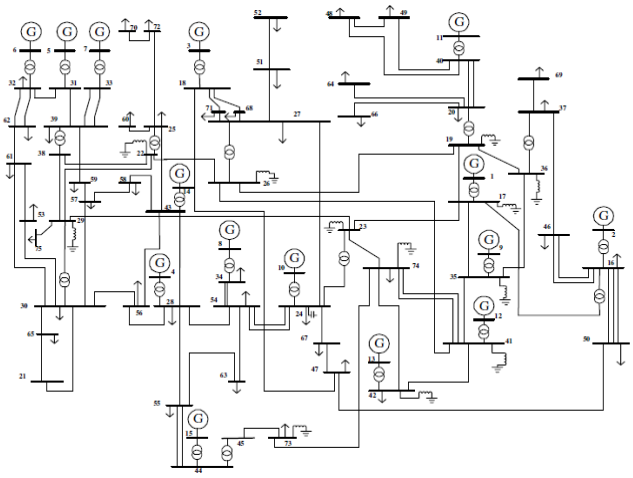

Fig.3. 75-node Indian Utility system

In order to illustrate the efficiency of the proposed method, the line connecting the buses 15 and 23 is considered for outage. This results in overloading of the line connecting 23 and 24 buses. The D_{LG} coefficients of all generators with respect to this overloaded line along with priority of all generators of GI group obtained using FIS are presented in Table VI . The results of rescheduling are illustrated in Table VII.

Table VI. D_{LG} values and Priorities of GI group generators of 75-node system

GI group Generators	D_{LG} values	Priority (obtained using FIS)	Rank of Generator (Based on Priority)
G2	10.7	0.221	12
G3	3.4	0.511	4
G4	9.2	0.343	6
G5	3.4	0.300	8
G6	2.7	0.225	11
G7	1.3	0.300	7
G8	1.5	0.260	10
G9	2.4	0.408	5
G10	7.2	0.525	2
G11	12.8	0.300	9
G14	2.4	0.554	1
G15	2.6	0.525	3

Table VII. Performance parameters of 24-node system

System Performance parameter	Pre Rescheduling	Rescheduling based on RED	Rescheduling based on Economy	Rescheduling based on FLC based economy
Flow in congested line (23-24) (MVA)	679.2 (133%)	582.4 (114%)	597.9 (117%)	567.1 (111%)
P loss (MW)	210.7	166.6	161.1	165.8
Vmin (pu)	0.918	0.936	0.937	0.937
Max (Li)	0.6716	0.5748	0.5489	0.5674
Σ L2	6.437	4.648	4.189	4.681
Ve	0.0655	0.0998	0.1093	0.1005
No. of generators rescheduled	--	15	8	8
Cost of Rescheduling of generators ($/h)	--	82.41	32.61	34.96

CONCLUSION

The objective of an energy control centre is to ensure secure and economic operation of power system. In this connection, three approaches for congestion relieving are discussed in this paper. Approach I based on RED concept

not only relieves the congestion but also improves the voltage security and reduces the system power loss. But, the incremental fuel cost incurred is very high in the approach. To overcome this, an Approach II based on incremental fuel cost of generators has been explained. This Approach II is acceptable from economics point of view, but in terms of voltage security and loss reduction this approach is not advisable. Hence, an Approach III, based on RED and economic operation, using fuzzy logic is proposed in this paper. This approach not only improves the voltage security and loss reduction but also the solution obtained is economical. Finally, an attempt has been made for curtailing the number of generators to be rescheduled for congestion relieving. The results obtained on the considered test systems and practical systems reveal that the proposed approach is most appropriate one for implementing in Energy Control Centre for security and economy-oriented power system operation under present day deregulated environment.

REFERENCES

[1] Yong Zheng and N. Chowdhury, "Expansion of Transmission systems in a Deregulated Environment", IEEE Canadian Conference on Electrical and Computer Engineering, Vol.4, May 2-5, 2004, pp.1943-1947.
[2] Lobato, L. Rouco, et al., "Preventive analysis and solution of overloads in the Spanish electricity market", Electric Power Systems Research, Vol.68, 2004, pp 185-192.
[3] B.K. Panigrahi, V. Ravikumar Pandi, "Congestion management using adaptive bacterial foraging algorithm", Electric Power Systems Research, 2009, Vol.50, pp. 1202-09
[4] Sinha A.K. et al., "Congestion management using multi objective particle swarm optimization" IEEE Trans. on Power Systems, 2007, Vol. 22(4), pp. 1726–34.
[5] Bansilal D. Thukaram, K. Parthasarathy, "An expert system for alleviation of network overloads," Electric Power Systems Research, Vol.40 (1997), pp. 143–153.
[6] A. N. Udupa, G. K. Purushothama, K. Parthasarathy and D.Thukaram "A Fuzzy control for network over load alleviation", Inter National Journal of Electrical Power and Energy Systems, Vol.23, 2001, pp.119-128.
[7] D.P. Kothari, et al. "Congestion Management on Power Systems – A Review", Electrical Power and Energy Research, Vol.70, 2015.
[8] Yesuratnam G., Thukaram D., "Congestion management in open access based on relative electrical distances using voltage stability criteria", Electric Power Systems Research, 2007, Vol. 77, pp. 1608–18.
[9] G. Yesuratnam, N. Srilatha, P. Lokender Reddy, "Congestion Management Technique Using Fuzzy Logic Based on Security and Economy Criteria" AIKED'12 Proceedings of the 11th WSEAS international conference on Artificial Intelligence, knowledge Engineering and Data Bases, pp. 157- 162, 2012.
[10] H. Ghasemi, C. Cañizares, and G. Savage, "Closed-Form Solution to Calculate Generator Contributions to Loads and Line Flows in an Open Access Market." IEEE PES General Meeting, Vol.2, 2003.

Comparing Radiation Characteristics of Fractal arrays with Random and Periodic Arrays

[1] N.Kalpana, [2]D.Rajitha, [3]K.Suresh, [4]Dr.M.Ramesh Patnaik, [5] T.Durga Prasad
[1][2][3] Dept.of ECE, Chaitanya Engineering College,VSP
[4] Dept. of Instrumentation Technology, AU College of Engineering(A),VSP
[5] Dept. of ECE, GITAM College of Engineering,VSP

Abstract:-- **In recent years, Antenna design has become one of the important considerations in communication technology. Different antenna designs serve different purposes basing on their performance characteristics, physical design constraints and radiation characteristics. This paper discusses the concept of fractal geometry and applies it to antenna theory. This paper aims to investigate how a random array antenna radiation characteristics can be improved by the choice of fractal geometry of Sierpinski gasket over random and periodic array antenna. Matlab code is used to generate antenna geometry and also its radiation pattern along with its array factor curves.**

I. INTRODUCTION

The diseased gene identifying based on a network of Wireless communication has been advancing day by day with ever increasing demand for wireless devices, but works have been still going on to achieve desired radiation characteristics for specific applications. Designing a low profile antenna i.e small in size with wide band or multiband application and less complex in design is one of the most important concern. Many attempts have been made to achieve multiband operation but in most of the cases size reduction may not be possible. This size reduction along with multiband operation can be achieved using fractal geometries as antenna designs. Antenna arrays provide high gain, diversity, beam steering and also Maximize SNR and cancel interference patterns when compared with single antennas. An array of antennas can be of antenna elements placed on a plane in either a periodic or random fashion. These two patterns of arrangement show different radiation properties. Side lobe reduction can be achieved by periodic arrangement of array elements but require more number of array elements. On the other hand, random arrays have higher side lobes, but require less number of array elements and are likely to work in case if one or two elements in array may fail hence they are more robust. This concept of antenna arrays can be extended to Fractal geometry to bridge the gap between random and periodic configurations in antenna arrays. This paper is organized as follows. In section II describes Basics of fractal Geometry followed by Linear arrays in section 3 and then comes section 4 which contains periodic arrays followed by random arrays in section 5. While the results are depicted in section 6, optimized array comparisons are shown in section 7 and followed by conclusions and references

II. FRACTAL BASICS

Fractal geometries can be defined as geometries a part of which exhibits same characteristics as that of whole structure. Fractal geometries are subset of Euclidean Geometry. Self-Similarity is a properties exhibited fractal geometries that play a crucial role in fractal based antenna designs. Self-similarity can be defined as at any magnification a part of structure always looks exactly similar to that of original structure. For example consider figure1 which is called Sierpinski carpet

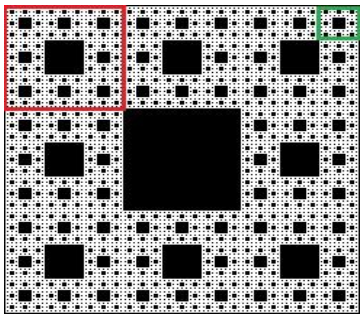

In above figure both large and small square boxes are exactly similar to that of whole structure even though they are at different magnification hence it is a self-similar structure. We can obtain a relation for fractal dimension if we know the scaling factor. Suppose if there are "N" such copies of original geometry scaled down by a fraction "F", then the dimension of the fractal is given by D , where

$$D = \frac{\log(N)}{\log(1/F)}$$

 ISBN: 978-81-940803-3-6

Examples of some fractals are Sierpinski gasket, von koch snowflake, Malinowski curve etc which are classified as deterministic. On the other hand there are another classification of fractals which represent naturally occurring objects like tress, mountains etc these fractals called as random fractals

Deterministic fractals

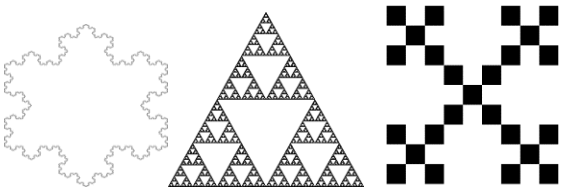

Random fractals

There may be many more fractal geometries in both deterministic and random fractals this paper limits the discussion to these fractals only. Fractal geometries can be generated using computer graphics with recursive algorithm. There are different procedures for both deterministic and random fractals. However this paper mainly focuses on Sierpinski triangle

Methods of generating Sierpinski gasket

A. Removing central part

Sierpinski triangle can be formed by removing the central part of base triangle. Initially we take a base triangle and join the mid points. Now the mid points are joined and 4 scaled versions of actual triangle are formed from which central triangle is removed. This completes one iteration and remaining 3 triangles resembles the scaled version of actual triangle. Same procedure is applied to those scaled triangle to as many required number of iterations. Usually equilateral triangle is taken but it is not mandatory. This method is difficult to implement using matlab. This is pictorially shown in figure 2

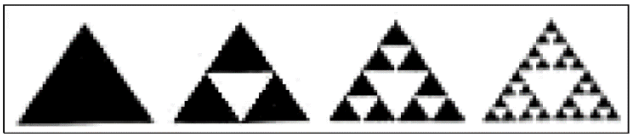

Figure2: Sierpinski gasket

More are the number of iterations lesser are the resonant frequencies but it is significant over first few iterations only later it diminishes after few iterations. Also the amount of scale that is required for each iteration diminishes as no of iterations increase. This equation gives the relation between resonant frequency of linear dipole versus normalized frequency of fractal antenna

$$f = fd\left[1-\exp\left(\frac{n-1}{n}\right)\frac{\ln D}{D}\right]$$

Where "f" is normalized resonant frequency of fractal antenna

And "fd" is the resonant frequency of linear dipole

Sierpinski Triangle for 4 iterations

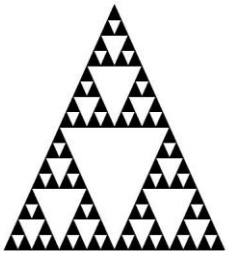

Sierpinski Triangle for 5 iterations

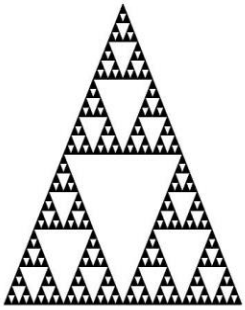

B. Using Iterated function system(IFS)

Fractal geometries can be generated using Iterated function system (IFS). Again Iterated function system is a composite of affine transformations and random point generation. Affine transformations for Sierpinski triangle are simpler and are generally expressed as matrices namely transitional and transformational matrix

Affine transformation :

$$W\begin{pmatrix} x \\ y \end{pmatrix} = \begin{pmatrix} a & b \\ c & d \end{pmatrix}\begin{pmatrix} x \\ y \end{pmatrix} + \begin{pmatrix} e \\ f \end{pmatrix}$$

Or

W(x,y) = (ax+by+e, cx+dy+f) where a,b,c,d,e,f are real Rotation and scaling are controlled by parameters "a,b,c,d" while "e,f" control linear translation

Now consider "A" be the original geometry and W1,W2,W3,....Wn be a set of linear transformations, then applying these set of transformations to original geometry A results in generation of new geometry by collecting results from $W(A) = \bigcup_{n=1}^{N} Wn(A)$

By repeatedly applying "W" to previous geometries new fractal geometry will be obtained

A1= W(A) , A2 =W(A1) .. Etc

while on the other hand random point generation algorithm generates Sierpinski triangle by specifying the number of points with which the fractal should be generated. This method makes use of matlab script that uses probability to randomly place points within a boundary which are specific to Sierpinski fractal. Matlab random number generator is used to create fractal aids in filling the ordered vs disordered gaps. This paper uses random point generation method to generate Sierpinski gasket

III. ANTENNA ARRAYS

Individual antenna elements when arranged in an array shows higher gain than any of the individual array elements. This happens because gain of individual elements adds up resulting in higher gain than any of its elements in an array. There are two different ways of arrangement in array, namely linear fashion and planar fashion. In constructing linear and planar arrays the radiation properties of distinct patterns must be analyzed in order to optimize the array for certain uses. The linear arrays are considered upon which "N" number of elements are placed in linear fashion along a particular axis while in planar array, all the array elements are arranged in a plane. Theoretically radiation pattern for an array antenna can be found from pattern multiplication theorem which states

Array pattern = (array element pattern) X (Array factor)

Normalized value of array factor is obtained as follows

$$(AF)n = \frac{1}{N}\frac{\sin(N\Psi/2)}{\sin(\Psi/2)}$$

Here, N is the number of elements and is defined as the array phase function and is a function of the element spacing, phase shift, frequency and elevation angle.

Figure3 and figure4 gives the radiation pattern for linear array antenna with 25 elements and 50 elements respectively

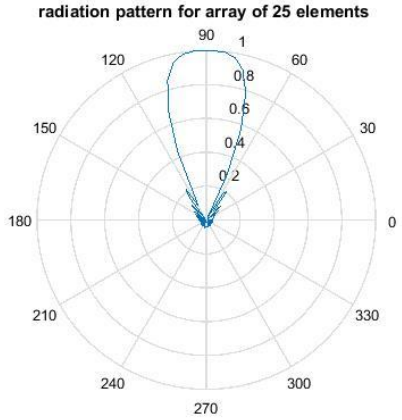

Figure 3 : linear array with 25 elements

$\frac{d}{\lambda} = 0.33$, for both arrangements

d/λ is the ratio of the distance between each element in wavelengths. The charge is kept equal for all elements to make the calculations simpler. As the elements are placed within 1 wavelength, there is constructive interference such that there is one main lobe and side lobe ratio decreases as more and more elements are placed in an array. But here the width of main lobe is observed to become narrower with increase in number of elements.

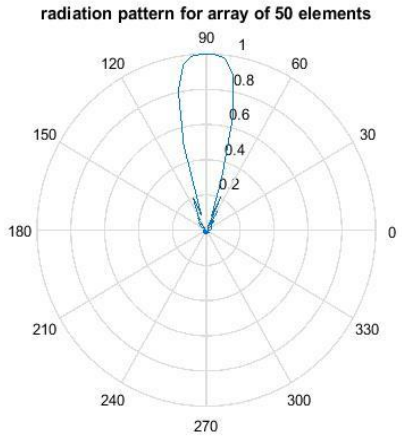

Figure4 : linear array with 50 elements

From the figures 3 and 4 we can say that side lobe are comparatively lower and main lobe is narrower in 50 element array compared to that of 25 element array. There is a trade of between gain and beam width in linear array arrangement.An optimized antenna will have no side lobes.

The side lobes would easily cause air traffic control to confuse a large airplane at the height of the side lobes with a small plane at the peak of the main beam. Another characteristic of an optimized beam involves a thin single main beam.

IV. PERIODIC ARRAYS

Planar arrays have all the antenna elements arranged on a plane in a grid. Side lobes are comparatively lesser in ratio to that of main lobe. This paper make use of matlab to generate periodic array consisting of 412 elements represented with "*" symbol in corresponding graphs. We have chosen the limits of axis as -0.5 to 1.0 since we have used matlab random point generator to generate random arrays and fractal arrays which defaultly takes axis from -0.5 to 1.0. These dimensions are chosen for scaling purposes, as our fractal array uses this size window. Matlab generated planar array of antenna is shown in figure 4A.The radiated field is shown in figure 4B in a gray-scaled color map where blue is the lowest point and Red is the highest point in radiation pattern.

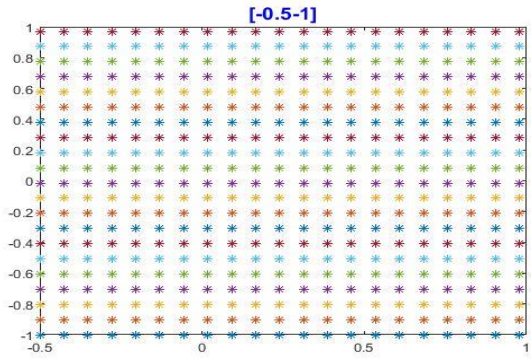

Figure 4A: Planar array with 412 elements having equal distances

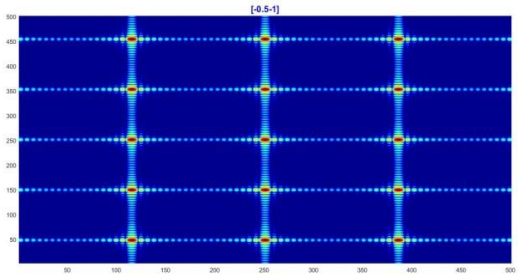

Figure 4B: Top view of radiation pattern for periodic array

V. RANDOM ARRAYS

The radiation characteristics of random arrays are more desirable. The random arrays have an advantage of exhibiting favorable radiation characteristics with less number of elements. In this type of array even if some elements fail the radiation characteristics are least affected. Using matlab random point generator, we plotted 412 random array elements. Figure 5A represents the random array of 412 elements. The radiation pattern of random array with 412 antenna elements is represented in figure 5B. One point to note in radiation pattern of random array is there is a 180-degree symmetry, which is more apparent about the main beam.

This paper bring the comparison between periodic arrays, Random arrays and attempt to show how the fractal arrays attempt to fill the void between the radiation characteristics of random array and periodic array. Fractal show that how the radiation characteristics of Random arrays can be achieved by using fractal geometries. In top view of radiation pattern Red indicate the highest point and blue indicate lowest point.

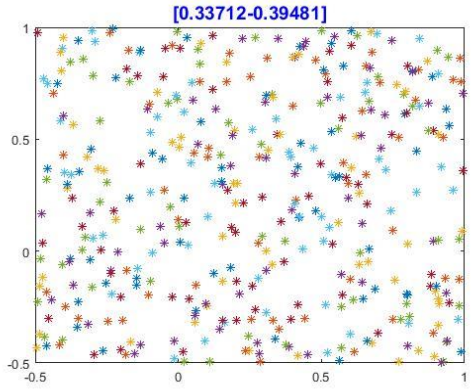

Figure 5A: Random array of 412 elements

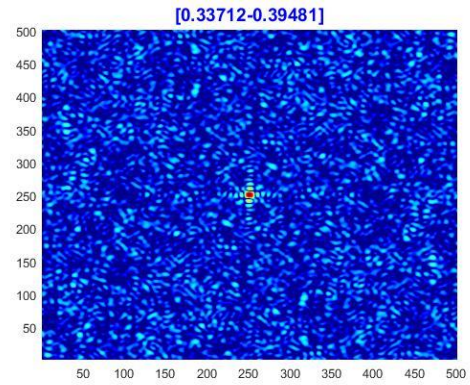

Figure 5B: Radiation pattern of Random array.

VI. SIERPINSKI FRACTAL

This paper makes use of Matlab code to generate Sierpinski triangle which essentially consists of 412 elements. The axis is defaultly fixed between -0.5 and 1.0 by random point generator in matlab. Figure 6A shows the fractal geometry of fractal array and figure 6B shows the

radiation pattern. The radiation pattern indicate that side lobes are lesser than that of in periodic array but larger than in random array. It can also be observed that if more number of elements are used in a fractal array, the side lobes are further reduced

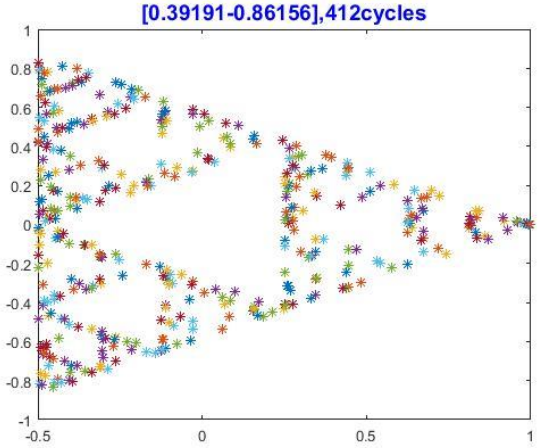

Figure 6A: Random-point-generated Sierpinski gasket.

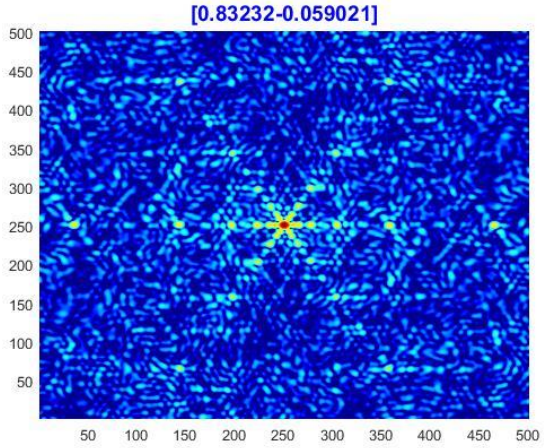

Figure 6B: Radiation from random-point-generated Sierpinski gasket.

VII. COMPARISON OF RADIATION PATTERN

In any antenna array it is always desired to have a low side lobe ratio. In figure 7C which represents the radiation pattern of periodic array the main lobe is in such a way that there is no chance of interference. Where as in figure 7A which represents the radiation pattern of random array has low side lobes unlike as in case of periodic array. Fractal array assumes the main lobe characteristics of periodic array and lower side lobe ratio like random array

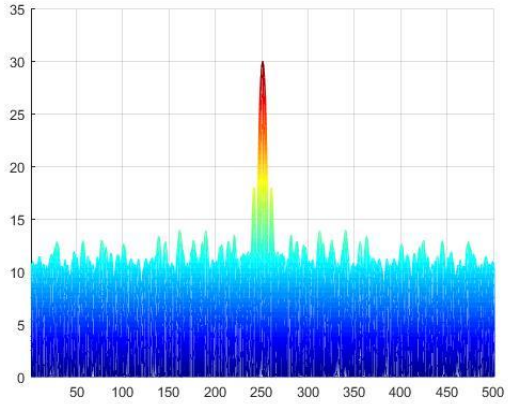

Figure 7A: Side view of radiation pattern of random array.

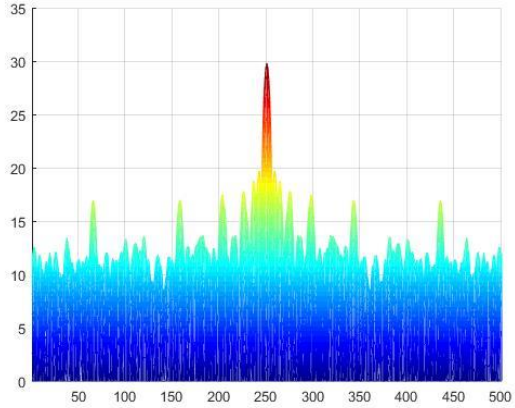

Figure 7B: Side view of radiation psttern of fractal array.

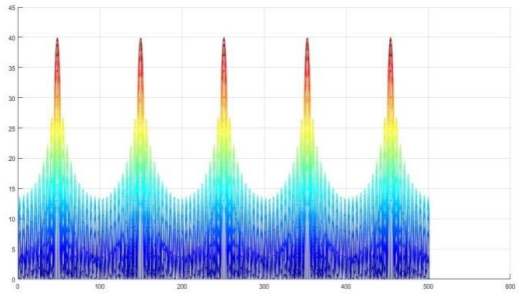

Figure 7C: Side view of radiation [pattern of periodic array

As the number of elements in an fractal array increases the side lobes are much reduced. Figure 7D represents the radiation pattern of fractal array with 700 array elements. But one point to be noted here is the main lobe degradation which is undesirable occurs with increase in number of elements. Hence we can say that side lobes in radiation

pattern of fractal antenna can be decreased at the cost of increase in main lobe degradation

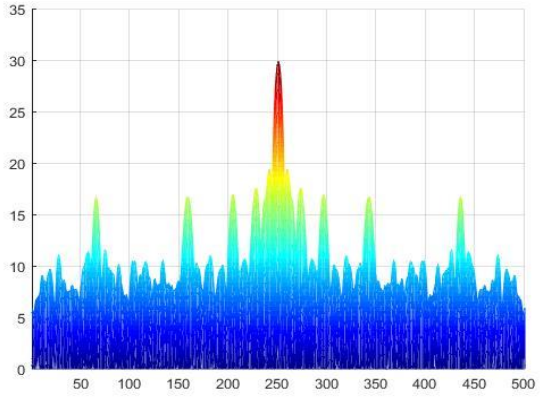

Figure 7D : Radiation pattern of fractal array with 800 elements

VIII. ADVANTAGES

1. Miniaturization of antenna size can be achieved while keeping high radiation efficiency using fractal antenna
2. Better impedance matching is possible using fractal antennas
3. Metamaterial applications like cloaks can be effectively done using fractal geometry
4. Shows consistency in performance over huge frequency range i.e (frequency independent)
5. Reduced mutual coupling in fractal array
6. Sierpinski gasket can be used as monopole and dipole elements whose peripherals are similar to cross section of monopole and dipole antenna

For linear dipole, the first resonance occur at $\lambda/2$ which may be higher for certain frequencies.For such frequencies height of antenna required will be higher which can obviously reduced by using Sierpinski triangle

IV. CONCLUSIONS

It can be observed that the random array performed better than the fractal array. According to previous work, there is an intersection point where the number of elements in a fractal array and random array cause for the one to be more effective as the other. As the array holds more elements, the random arrays perform better. Aside from the side lobe levels, the fractal did have overall a better main beam, regardless of the number of points. A draw back for random arrays with many elements at that, as the number of elements increases, main beam degradation is quite significant.

REFERENCES

[1] Mandelbrot, B.B .The Fractal Geometry of Nature. W. H. Freeman and Company, New York. 1983.
[2] Weeks. W. L. Antenna Engineering. McGraw Hill. London. 1968.
[3] Jaggard, D.L. Fractals in Engineering. From Theory to Industrial Applications. Springer.
[4] Jaggard, D.L., Jaggard A.D., Cantor Ring Arrays. In Microwave and Optical Technology Letters. Vol. 19 No. 2 October 5 1998.
[5] Jaggard, D.L., Jaggard A.D., Frangos V. P., Fractal Electrodynamics Surfaces and Super lattices. Jan. 1999.
[6] Jaggard, D.L., Jaggard A.D., Cantor Ring Diffractals. In Optics Communications. Elsevier. October 1998.
[7] Ulaby, Fawwaz. Fundamentals of Applied Electromagnetics. Prentice Hall, New Jersey.1999.
[8] Lee, S.W. Antenna Handbook, Theory, Applications, & Design. Reinhold Company. New York. 1998.
[9] Stutzman, W.L. Antenna Theory & Design. Wert company. Pennsylvania. 1995.
[10] Fractal antennas : design , characteristics and applications by NemanjaPoprsen, MicoGacanovic
[11] Fractal concepts for antenna design and analysis by K.J Vinoy
[12] https://www.nonstopsystems.com/radio/pdf-hell/article-hell-bernhard-antenna-msu-dnhoe.pdf

A Novel Multilevel Solar Inverter through Dispensed Maximum Power Point Tracking

[1] D.Rajani Kumar, [2] K. Sumalatha
[1] Assistant Professor, Department of EEE, Jayamukhi Institute of Technological Sciences
[2] Assistant Professor, Department of EEE, University college of engineering KU

Abstract:-- **The prospective paper presents a measured cascaded H-bridge multilevel photovoltaic (PV) inverter for single-or three-stage grid associated applications. The secluded cascaded multilevel topology improves the effectiveness and adaptability of PV systems. To acknowledge better use of PV modules and boost the solar energy extraction, an appropriated maximum power point tracking control plot endure connected to both single-and three-stage multilevel inverters, whichever permits free control of every dc-link voltage. For three-stage grid-associated applications, PV confounds might present unequal provided power, prompting uneven grid current. To comprehend this issue, a control conspire among modulation compensation endure likewise proposed. A test three-stage seven-level cascaded H-bridge inverter has been fabricated using nine H-bridge modules (three modules for exclusive stage). Every H- bridge module endure associated among a 185-W solar panel. Simulation results obtain exhibited to confirm the practicality of the prospective methodology.**

Keywords:- cascaded H-bridge inverter ,photovoltaic (PV) inverter nine H-bridge modules

1. INTRODUCTION

Solar Power Systems

A photovoltaic framework, also sun based PV control framework, or PV framework, endure a power conspire intended to supply usable sun powered power beyond methods for photovoltaic's. It comprises of a course of action of a few parts, including sun powered boards to ingest and change over daylight into power, a sun powered inverter to change the electric flow against DC to AC, equitable as mounting, cabling and other electrical accomplices to set up a working framework.

Entirely, a sun powered cluster equitable incorporates the group of sunlight based boards, the unmistakable piece of the PV framework, and does exclude the various equipment, frequently outlined as parity of plan (BOS). Besides, PV frameworks convert light specifically into power and shouldn't act mistaken for different advancements, for example, concentrated sun oriented power or sun oriented warm, utilized for warming and cooling. PV frameworks run against little, rooftop top mounted or assembling coordinated frameworks among limits against a couple to a few several kilowatts, to expansive utility-scale control stations of many megawatts. associated, while off-lattice or remain solitary frameworks represent a little bit of the market. Working quietly and among no moving parts or ecological emanations, PV frameworks have created against being specialty advertise applications into a develop innovation utilized for standard power age. A housetop conspire recovers the contributed vitality for its assembling and establishment inside 0.7 to 2 years and creates about 95percent of net clean sustainable power source over a 30-year administration lifetime.

Because of the exponential development of photovoltaic, costs for PV frameworks have quickly declined as of late. latest any case, they shift beyond market and the span of the framework. latest 2014, costs for private 5-kilowatt frameworks latest the United States were around $3.29 per watt,[4] while latest the exceptionally infiltrated German market, costs for housetop frameworks of up to 100 kW declined to €1.24 per watt.[5] Nowadays, sun powered PV modules represent not exactly 50% of the system's beyond and large cost leaving the rest to the rest of the BOS-segments and to delicate costs, which over incorporate client obtaining, allowing, review and interconnection, establishment work and financing costs. Notwithstanding, ready obtain two power change organizes latest this setup. Another fell inverter endure appeared latest Fig. 1(f), where exclusive PV board endure associated among its own dc/air conditioning inverter, and those inverters obtain again put latest arrangement to achieve a high-voltage level . This fell inverter would keep up the advantages of "one converter for every board, for example, better use per PV module, capacity of blending distinctive sources, and excess of the framework.

What's more, this dc/air conditioning fell inverter evacuates the requirement for the per-string dc transport and the focal dc/air conditioning inverter, which over further improves the general proficiency. The particular fell H-connect staggered inverter, which over requires a confined dc hotspot for every H-connect, endure one dc/air conditioning fell inverter topology.

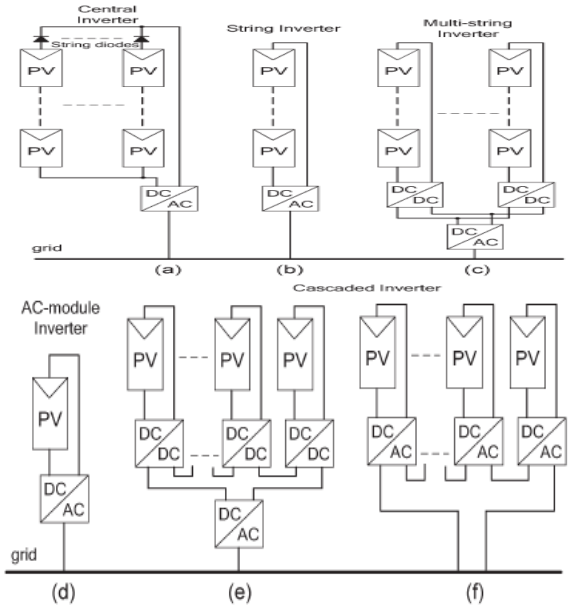

Fig. 1 Configurations of PV systems. (a) Central inverter. (b) String inverter. (c) Multi string inverter. (d) AC-module inverter. (e) Cascaded dc/dc converter. (f) Cascaded dc/ac inverter.

A measured fell H-connect staggered inverter topology for single-or three-stage lattice associated PV courses of action stopover realistic inside this paper. The board crisscross issues act routed to demonstrate the need of individual MPPT control, and an oversee conspire through disseminated MPPT oversee stopover at such point proposed. The circulated MPPT oversee plot protect act connected to both 1 and three-stage frameworks. Inside expansion, for the exhibited three-stage lattice associated PV framework, if exclusive PV module remains worked at its owing MPP, PV crisscrosses might acquaint anomalous power provided among the three-stage staggered inverter, prompting irregular infused matrix current. To adjust the 3-stage lattice current, tweak repayment remain besides added to the oversee framework.

II. SYSTEM DESCRIPTION

Particular fell H-connect staggered inverters for 1 and three-stage framework associated PV game plan obtain uncovered inside Fig. 2.

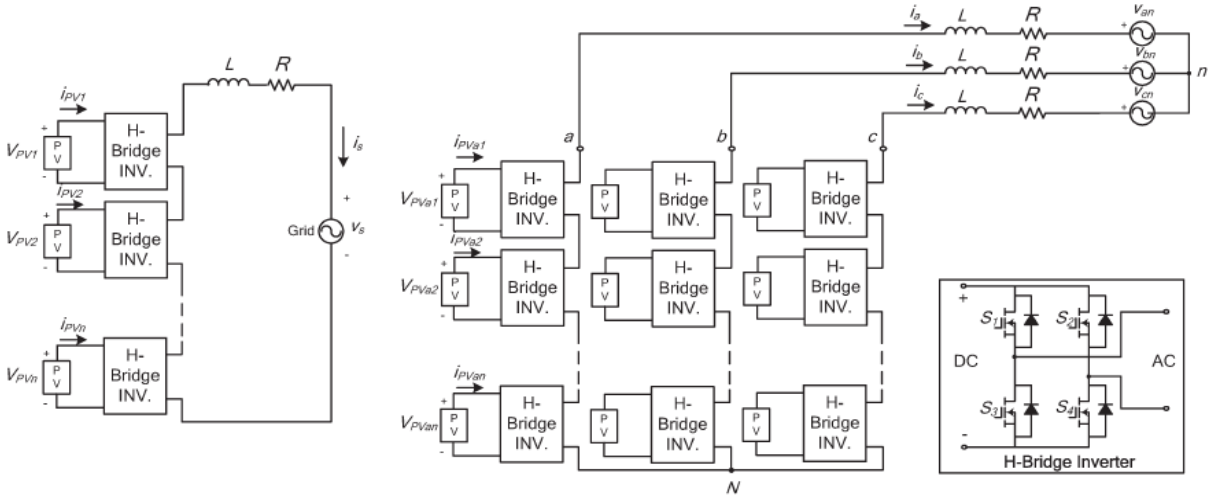

Fig. 2 Topology of the modular cascaded H-bridge multilevel inverter for grid-connected PV systems.

Each fragment comprises of n H-connect converters related inside arrangement, and the dc connection of exclusive H-connect save act nourished beyond a PV board or a short grouping of PV boards. The fell staggered inverter stopover irrelevant to the matrix through L channels, which over act utilized to lessen the exchanging music inside the current. Beyond various mixes of the four switches inside exclusive H-connect module, three yield

Vtg levels protect act created: −vdc, 0, or +vdc. A fell staggered inverter through n input sources desire give 2n + 1 levels to orchestrate the air conditioner yield waveform. This (2n + 1) level Vtg waveform empowers the decrease of sounds inside the incorporated current, lessening the span of the required yield channels.

III. PANEL MISMATCHES

Each portion comprises of n H-connect converters related inside arrangement, and the dc connection of exclusive H-connect safeguard act bolstered beyond a PV board or a short succession of PV boards. The fell staggered inverter

stopover irrelevant to the lattice through L channels, which over act utilized to diminish the exchanging sounds inside the current. Beyond various blends of the four switches inside exclusive H-connect module, three yield Vtg levels protect act produced: −vdc, 0, or +vdc. A fell staggered inverter through n input sources desire give 2n + 1 levels to combine the air conditioner yield waveform. This (2n + 1) level Vtg waveform empowers the decrease of music inside the combined current, diminishing the extent of the required yield channels.
Consider a working circumstance such exclusive board has an alternate light against the sun; board 1 has irradiance S = 1000 W/m2, and board 2 has S = 600 W/m2. On the off chance such equitable board 1 stopover followed and its MPPT coordinator decides the normal Vtg of the 2 boards, the power separated against board 1 would act 133 W, and the power against board 2 would act 70 W, as safeguard act seen inside Fig. 3.

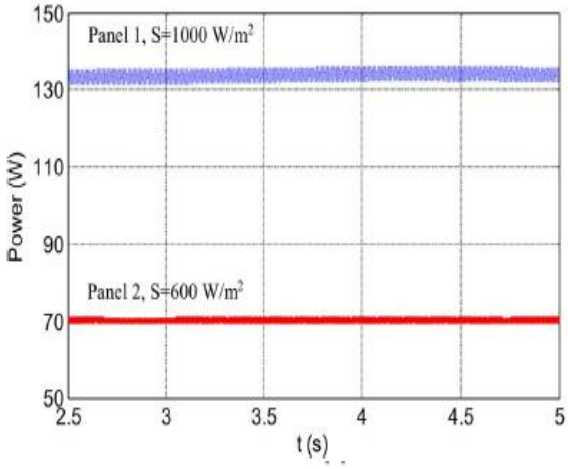

Fig. 3 Power extracted from 2 PV panels.

Without individual MPPT compose, everything impact collect starting the PV technique stopover 203 W. latest any case, Fig. 4 demonstrates the MPPs of the PV boards underneath the different irradiance. The best efficiency control guidelines inspiration act 185 and 108.5 W while the S esteems act 1000 and 600 W/m2, correspondingly, which over income to the all out power gather against the PV proposition would act 293.5 W if character MPPT protect act accomplish. These higher qualities stopover about 1.45 occasions of the 1 preceding. Latest this manner, personage MPPT manage inside exclusive PV segment wait required to intensify the proficiency of the PV association.

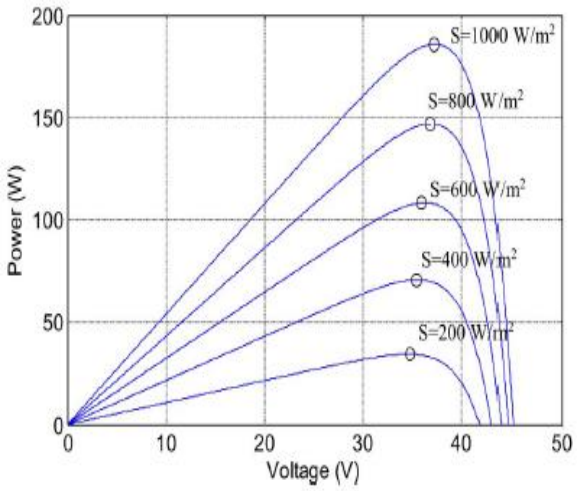

Fig. 4.P–V characteristic under the different irradiance

Inside a 3-stage framework associated PV framework, a PV crisscross might cause more issues. Aside initiating lessening the beyond and large effectiveness, this might even begin anomalous power provided to the three-stage lattice associated framework. On the off chance such ready act PV befuddles associating stage, the information impact of exclusive stage would act particular. Since the lattice Vtg stopover unbiased, this distinction inside information power desire make anomalous current the network, which over remains not permitted beyond matrix gauges.

IV. CONTROL SCHEME

A. Distributed MPPT manage

So as to annul the unfriendly impact of the jumbles and increment the productivity of the PV framework, the PV modules need to work at various voltages to improve the usage per PV module. The different dc interfaces inside the fell H-connect staggered inverter make autonomous Vtg oversee conceivable. To acknowledge individual MPPT oversee inside exclusive PV module, the oversee conspire prospective inside remain refreshed for this application. The conveyed MPPT chief of the 3-stage fell H-connect inverters remain appeared inside Fig. 5.

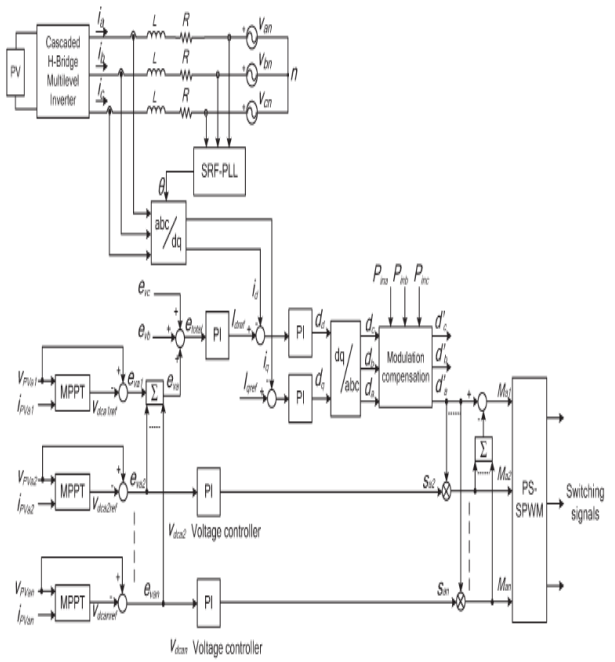

Fig. 5 manage scheme for three-phase modular cascaded H-bridge multilevel PV inverter.

Inside exclusive H-connect module, MPPT controllers remain added to create the dc-interface Vtg reference. Exclusive dc-interface Vtg remain contrasted among the relating Vtg reference, and the total of all blunders stopover controlled through an all out Vtg controller such decides the present introduction I_{dref} . The responsive current introduction I_{qref} save act set to zero, or if receptive power remuneration stopover required, I_{qref} protect latest addition act given beyond a receptive current number cruncher. The synchronous introduction outline stage bolted circle (PLL) has been utilized to discover the stage point of the matrix voltage.

The disseminated MPPT oversee conspire for the single-stage plot remain almost the equivalent. The all out Vtg controller gives the greatness of the dynamic current reference, and a PLL gives the recurrence and stage edge of the dynamic current reference. The present circle at such point gives the regulation list. To make exclusive PV module work at its owing MPP, take stage a for instance; the voltages vdca2 to vdc a act controlled separately through n − 1 circles.

A stage moved sinusoidal heartbeat width adjustment exchanging plan stopover at such point connected to deal among the exchanging gadgets of exclusive H-connect. It safeguard act seen such ready remain 1 H-connect module out of N modules chose balance index remain gotten beyond subtraction. For single-stage frameworks, N = n, and for 3-stage frameworks, N = 3n, where n remain the quantity of H-connect modules per juncture.

B. Modulation Compensation

As referenced before, a PV bungle might make more issues a three-stage particular fell H-connect staggered PV inverter. Through the individual MPPT oversee inside exclusive H-connect module; the info sunlight based intensity of exclusive stage would act extraordinary, which over acquaints strange current among the matrix. To illuminate the issue, a zero arrangement Vtg save act forced upon the stage legs inside request to influence the present streaming into exclusive stage.

In this way, the tweak pay obstruct, as appeared inside Fig. 6, remain added to the oversee plan of 3-stage particular fell staggered PV inverters. The key remain how to refresh the regulation catalog of exclusive stage without expanding the multifaceted nature of the oversee framework.

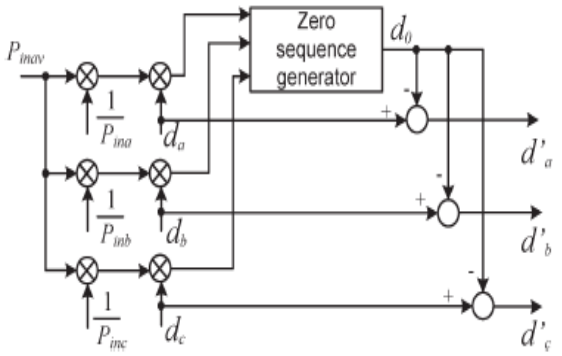

Fig. 6 Modulation compensation scheme

In the first place, the irregular power stopover weighted beyond proportion rj , which over stopover determined as

$$r_j = \frac{P_{inav}}{P_{inj}} \quad (1)$$

Where P_{inj} remain the information intensity of stage (j = a, b, c), and P_{inav} remain the normal info control. At such point, the infused zero arrangement adjustment files safeguard act produced as

$$d_0 = \frac{1}{2}[min(r_a.d_a, r_b.d_b, r_c.d_c) + max(r_a.d_a, r_b.d_b, r_c.d_c)] \quad (2)$$

Where dj remain the adjustment catalog of stage (j = a, b, c) and stopover dictated beyond the present circle controller. The tweak index of exclusive stage remain refreshed by

$$d_j' = d_j - d_0 \quad (3)$$

Just straightforward figurings act required inside the plan, which over won't expand the intricacy of the oversee conspire. A model remain exhibited to demonstrate the

tweak pay conspire all the more unmistakably. Accept such the information intensity of exclusive stage stopover unequal

$P_{ina} = 0.8 \quad P_{inb} = 1 \quad P_{inc} = 1$ (4)

By infusing a zero succession balance registry at t = 1 s, the fair-minded balance catalog desire act refreshed, as appeared inside Fig. 7. It protect act seen that, through the remuneration, the refreshed tweak catalog stopover strange relative to the power, whichever implies such the yield Vtg (vjN) of the three-stage inverter stopover uneven, however this creates the ideal impartial network current.

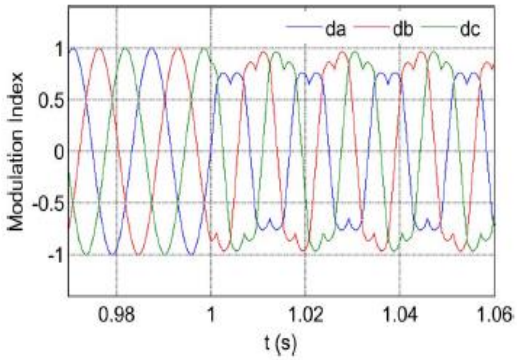

Fig. 7 Modulation indices before and after modulation compensation

V. SIMULATION RESULTS

Reproduction tests act completed to approve the prospective thoughts. A particular fell staggered inverter model has been worked inside the research center. The MOSFET IRFSL4127 stays chose as inverter switches working at 1.5 kHz. Three-stage seven-level fell H-connect inverters stopover mimicked and tried. Exclusive H-connect has its owing 185-W PV board associated as an autonomous source. The inverters stopover associated among the lattice through a transformer and the stage Vtg of the auxiliary oblique remain 60 Vrms. The plan parameters obtain appeared Table I.

TABLE I
SCHEME PARAMETERS

Parameters	Value
DC-link capacitor	3600 µF
Connection inductor *L*	2.5 mH
Grid resistor *R*	0.1 ohm
Grid rated phase voltage	60 Vrms
Switching frequency	1.5 kHz

A. Simulation Results

To check the prospective oversee plot, the three-stage matrix associated PV inverter stopover reproduced inside 2 disparate conditions. Initially, all PV boards act worked under a similar irradiance S = 1000 W/m2 and temperature T = 25 ◦C. At t = 0.8 s, the sun based irradiance on the first and 2 boards of fragment a reductions to 600 W/m2, and such for alternate boards remains the equivalent. The dc-interface voltages of stage a act appeared inside Fig. 8.

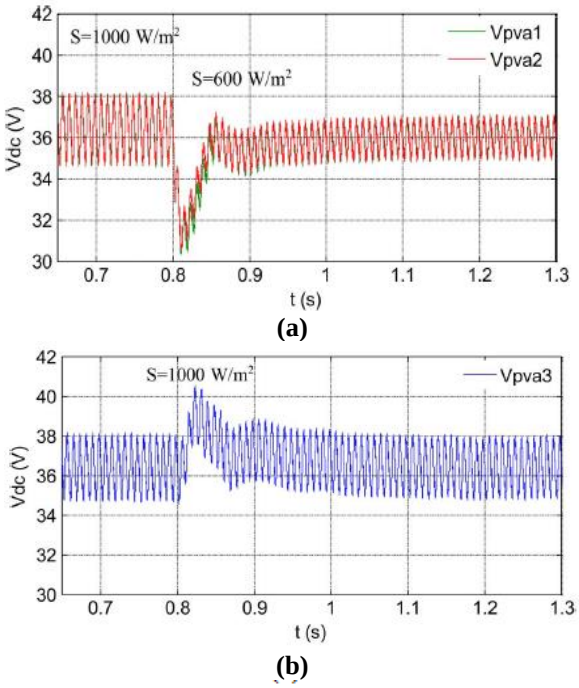

Fig. 8 DC-link voltages of phase a through distributed MPPT (T = 25 ◦C). (a) DC-link Vtg of modules 1 and 2. (b) DC-link Vtg of module 3

The PV contemporary waveforms of segment a act proven inside Fig. 9. After t = 0.Eight s, the currents of the first and 2d PV panels act an awful lot smaller because of the low irradiance, and the lower ripple of the dc-hyperlink Vtg maintain act discovered inside Fig. 8(a).

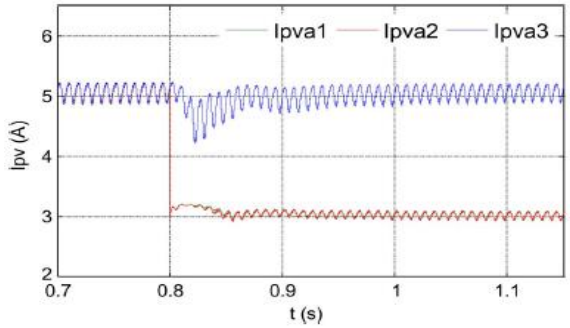

Fig. 9 PV currents of phase a through distributed MPPT (T = 25 ◦C).

The dc-interface voltages of stage b act appeared inside Fig. 10. All stage b boards track the MPP Vtg of 36.4 V, which over demonstrates such they act not impacted beyond different stages. Through the circulated MPPT control, the dc-connect Vtg of exclusive H-connect protect act controlled autonomously. Inside different words, the associated PV board of exclusive H-connect save act worked at its owing MPP Vtg and won't act affected beyond the boards associated among other H-spans.

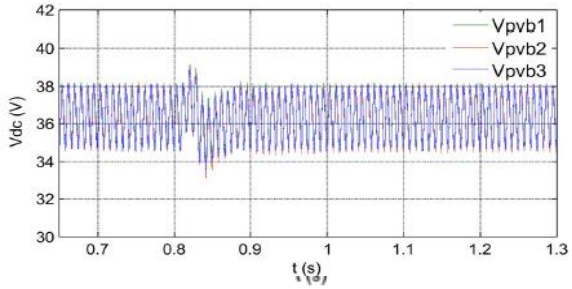

Fig. 10 DC-link voltages of phase b through distributed MPPT (T = 25 ◦C).

Thus, more solar energy maintains act extracted, and the performance of the overall PV scheme could act increased. Fig. 11 shows the power extracted against every segment. At the beginning, all panels act operated beneath irradiance S = a thousand W/m2 and exclusive section remain producing a maximum power of 555 W. After t = zero.8 s, the power harvested against phase a decreases to 400 W, and those against the alternative 2 levels stopover the same.

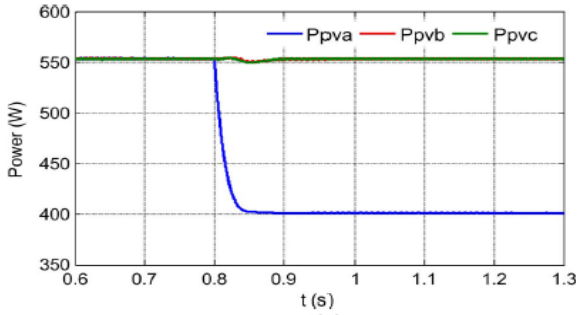

Fig. 11.Power extracted from PV panels through distributed MPPT.

Clearly, the power provided to the three-stage matrix associated inverter stopover unequal. Act such as it may, beyond applying the regulation remuneration plot, the power infused to the matrix stopover still adjusted, as appeared inside Fig. 12. Inside expansion, beyond looking at the all out power removed against the PV boards through the all out power infused to the matrix, it safeguard act seen such ready remain no additional power misfortune brought about beyond the adjustment remuneration conspire.

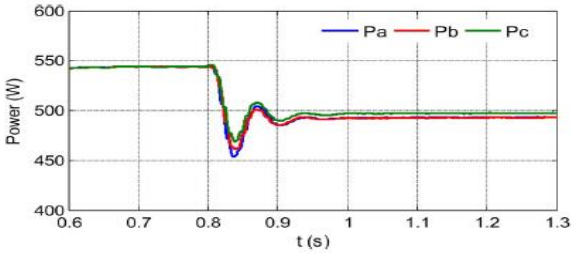

Fig. 12 Power injected to the grid through modulation compensation.

Fig. Thirteen shows the output voltages (vjN) of the 3-phase inverter. Due to the injected 0 collection thing, they act peculiar after t = 0.Eight s, which over assist to equilibrium the grid cutting-edge shown inside Fig. 14.

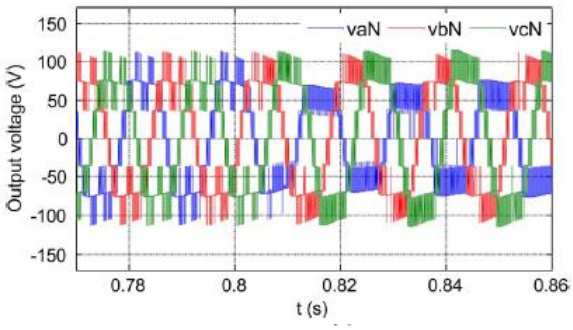

Fig. 13 Three-phase inverter output Vtg waveforms through modulation compensation.

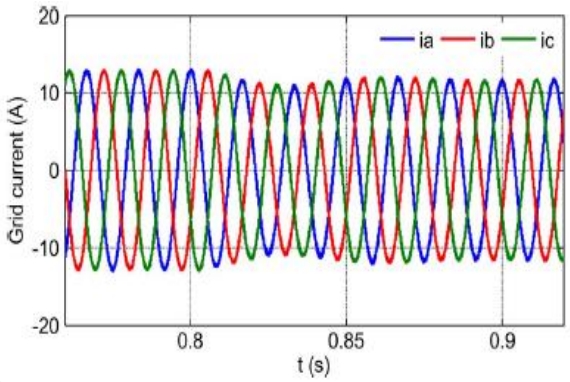

Fig. 14.Three-phase grid current waveforms through modulation compensation

VI. CONCLUSION

In this paper, a particular cascaded H-bridge multilevel inverter for grid-associated PV applications has been displayed. The multilevel inverter topology desire improve the usage of associated PV modules if the voltages of the different dc links obtain controlled autonomously. Hence, a

conveyed MPPT control conspires for both single-and three-stage PV systems has been connected to expand the general effectiveness of PV systems. For the three-stage grid-associated PV system, PV befuddles might present unequal provided power, bringing about uneven infused grid current. Modulation compensation conspire, which over expand the unpredictability of the control scheme or cause additional power misfortune, endure added to adjust the grid current. A measured 3-stage seven-level cascaded H-bridge inverter has been worked latest the lab and tried among PV panels under various fractional shading conditions. among the prospective control conspire, exclusive PV module receptacle act worked at its own MPP to augment the solar energy extraction, and the three-stage grid current endure offset even among the unbalanced provided solar power.

REFERENCES

[1] J. M. Carrasco et al., "Power-electronic. systems for.the.grid.integration.of.renewable.energy.sources: A.survey," IEEE Trans. Ind. Electron., vol. 53, no. 4, pp. 1002–1016, Jun. 2006.

[2] S. B. Kjaer, J. K. Pedersen, and F. Blaabjerg, "A.review.of.single-phase.grid.connected.inverters for.photovoltaic.modules," IEEE Trans. Ind. Appl., vol. 41, no. 5, pp. 1292–1306, Sep./Oct. 2005.

[3] M. Meinhardt and G. Cramer, "Past, present and future.of.grid.connected.photovoltaic-and.hybrid power-systems," in Proc. IEEE PES Summer Meet., 2000, vol. 2, pp. 1283–1288.

[4] M. Calais, J. Myrzik, T. Spooner, and V. G. Agelidis,"Inverter.for.singlephase.grid.connected.photovoltaic.systems—An.overview," in Proc. IEEE PESC, 2002, vol. 2, pp. 1995–2000.

[5] J.M. A.MyrzikandM. Calais, "String.and.module integrated.inverters.for.single-phase.grid.connected photovoltaic. systems—A.review," in Proc. IEEE Bologna Power Tech Conf., 2003, vol. 2, pp. 1–8.